ARMY RESEARCH LABORATORY

Advanced Gun System (AGS) Dynamic Characterization: Modal Test and Analysis, High-Frequency Analysis

by Morris Berman,
Ting Li, and Abraham Frydman

ARL-TR-2138 December 1999

The findings in this report are not to be construed as an official Department of the Army position unless so designated by other authorized documents.

Citation of manufacturer's or trade names does not constitute an official endorsement or approval of the use thereof.

Destroy this report when it is no longer needed. Do not return it to the originator.

ERRATA SHEET

re: ARL-TR-2138 "Advanced Gun System (AGS) Dynamic Characterization: Modal Test and Analysis, High-Frequency Analysis," December 1999, by Morris Berman, Ting Li, and Abraham Frydman

Request the following pen-and-ink change be made to subject report:

Page 81, block 4, change "model" to "modal."

Abstract

Dynamic characterization tests were performed on the Advanced Gun System (AGS) vehicle. The tests were designed to provide modeling information for high-frequency shock prediction codes, as well as finite element codes. These data obtained were also used to validate the modeling codes. The vehicle was analyzed in a full-up condition with the turret attached. A model analysis was performed to a maximum frequency of 100 Hz. The high-frequency characterization was performed up to 10 kHz.

Methodologies to extract damping estimate up to 10 kHz were developed and implemented. Damping estimates up to 10 kHz were extracted from the structural data obtained during this test.

Table of Contents

INTENTIONALLY LEFT BLANK.

List of Figures

List of Tables

INTENTIONALLY LEFT BLANK.

1. Introduction

A series of dynamic characterization tests was performed on the Advanced Gun System (AGS) vehicle. These tests were designed to provide the experimental validation of new high-frequency shock prediction codes, as well as a conventional finite element model. After validation, ballistic shock predictions based on these codes were to be compared against live-fire test results to assess the code's predictive capability.

The testing was performed at the Aberdeen Test Center (ATC). Unlike previous similar tests (Bradley Fighting Vehicle [BFV] [1], M113 armored personnel carrier [APC] [2], heavy composite hull [3]), testing and instrumentation were performed exclusively by ATC and U.S. Army Research Laboratory (ARL) employees. The Army was able to rent a large portion of the test instrumentation, which significantly reduced the equipment cost. A summary of the modal analysis theory can be found in ARL-MR-246 [2].

Army research has found that critical components in armored vehicles can be damaged by high-frequency ballistic shock waves resulting from nonperforating impacts or blast effects. To enhance the survivability of new vehicles, the Army has set the upper frequency range for ballistic shock hardness at 10 kHz, based on measurements in live-fire tests.

Prediction of the levels of the high-frequency ballistic shock(s) under battlefield threat conditions is needed to establish hardness requirements for the design and test qualification of components in new vehicles. Prior to live-fire testing, pretest predictions are also needed to increase confidence in the vehicle's survivability under the test conditions.

The 10-kHz frequency range of the shock is well beyond the practical limits of standard prediction techniques such as the finite element method (FEM), which is typically limited to 500 Hz for large and complex structures such as armored vehicles. Consequently, new, practical, and experimentally verifiable techniques that can perform predictions at these high frequencies are sought. The MANTA code, developed by Teledyne Brown Engineering, is potentially one

such analytical tool. The code has been successfully verified on tests of surrogate armored vehicle structures. The AGS vehicle represents the first test/model correlation of the code for a fully configured armored vehicle.

Certain operations of the MANTA Code require experimentally obtained structural parameters such as frequency-dependent damping and frequency response functions (FRF). Analytical predictions are very sensitive to damping value, but it is difficult to experimentally extract damping value with high accuracy, especially higher frequency damping. Therefore, the AGS posttest analysis concentrated on new or improved techniques to obtain more accurate damping estimates.

1.1 AGS Configuration. The limited quantity of time over which the vehicle was available permitted testing of only a single vehicle configuration. The primary impetus for this series of tests was to verify ballistic shock predictions against a live-fire test. Therefore, the configuration with the most applicability to the live-fire test was utilized for the modal test.

The AGS vehicle tested was number PV6. The vehicle was in operational condition and dressed in armor level II. Since the objective of the test was to measure the hull response, the external bolt-on armor had to be removed so that sensors could be mounted to the hull itself. In an effort to linearize the structure, the tracks and coaxial machine gun were also removed from the vehicle. All of the nonattached internal accessories, as well as the commander's machine gun mount, were removed. The wind sensor was folded down and secured with tape. Two mock rounds were in the autoloader throughout the test: one high-explosive antitank (HEAT) round and one kinetic energy (KE) round. Figure 1 is a photograph of the test setup. The fan in the lower left corner was used for cooling the shaker.

1.2 Vehicle Support System. There were two primary objectives that the vehicle support structure had to satisfy. First, the support had to have as minimal an effect on the structural dynamics of the hull as possible. Second, the test boundary conditions must be easy to model

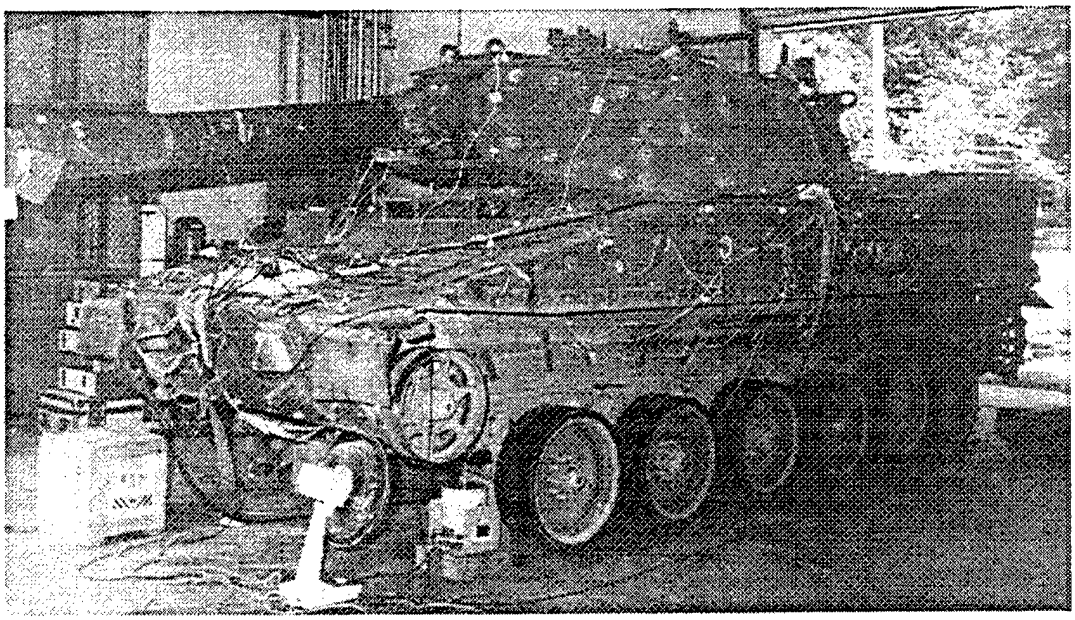

Figure 1. Modal Test Setup.

numerically. This can be a difficult task since a true free-free or fixed-fixed condition is very difficult to realize in an experimental setup.

If the vehicle can be suspended on a very soft suspension, such that the six rigid-body modes are well below the first flexible mode, then the hull can be considered to be in a free-free boundary condition. To this end, the vehicle was placed on top of five Firestone airmount airbags. Two airbags were placed under the front corners of the vehicle. Three airbags were required under the rear of the vehicle due to the weight of the engine and its associated components. Each bag was kept inflated to 60 psi for the duration of the test. A specification sheet for the airbags appears in Appendix A. The suspension can easily be modeled as a set of springs with their spring rates given by the known airbag pressure and the specification sheet.

2. Modal Test and Analysis

2.1 Excitation System. Four MB Dynamic Modal 50 shakers were used to excite the AGS vehicle. Each shaker is rated at 50 lb of force with the use of forced cooling and 25 lb of force

utilizing natural convection cooling. Due to time constraints, only a single excitation configuration was tested. The two front shakers were placed just behind the lowest glacis panel on the floor of the vehicle at the left and right sides. The two rear shakers were also placed on the floor of the vehicle just forward of the final drive sprockets along the edge of the floor.

The excitation forces were measured with PCB Model 208A02 force transducers. The shakers were attached to the vehicle with a small-diameter stinger. The stinger arrangement significantly reduces the magnitude of nonaxial forces that are transmitted through the force transducer. The force transducers were then screwed into metal plates that were cemented with dental adhesive onto the underside of the vehicle. At each force input location, a driving-point accelerometer was also attached.

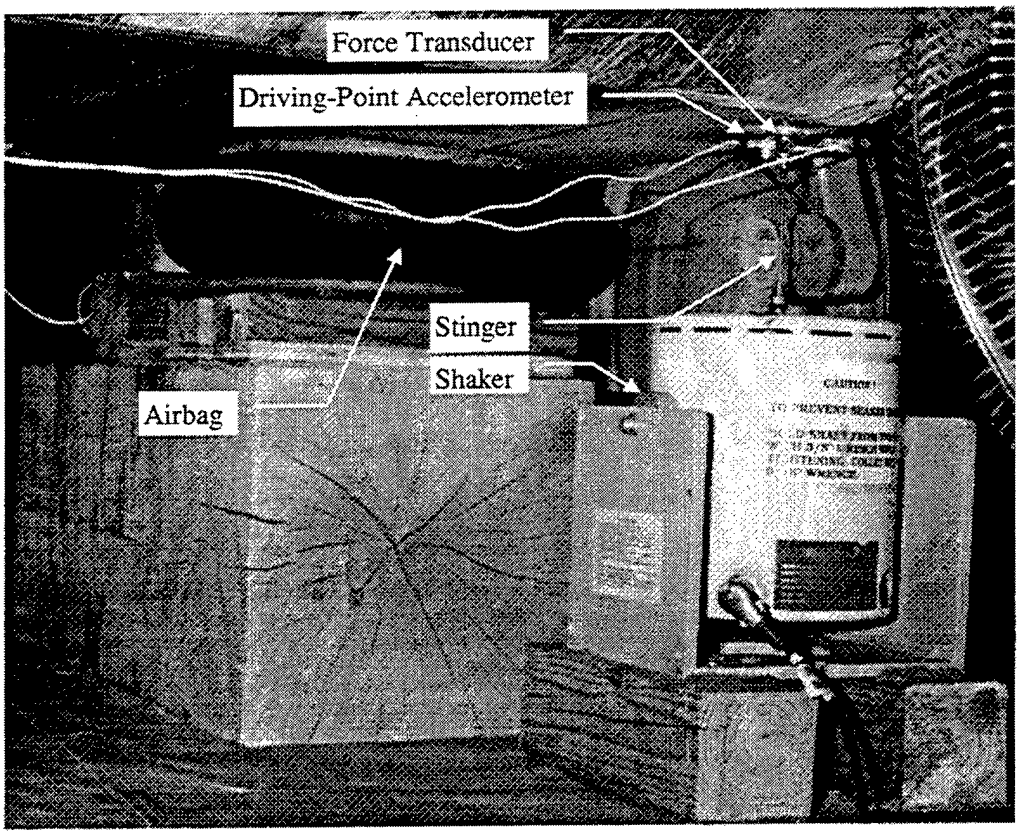

Figure 2. Excitation Setup.

The burst random method of excitation was chosen for this test. This excitation method minimizes the leakage and is well suited to heavily damped structures such as this vehicle hull. The bandwidth of the excitation was identical to the measurement bandwidth.

2.2 Response Measurement. Endevco Model 7254A and Model 61 accelerometers were used. Both the 100- and 500-mV/g sensitivity versions of these sensors were utilized. The less-sensitive sensors were placed closer to the sources of excitation to maximize the signal-to-noise ratio. The 7254A accelerometers were used for the driving-point acceleration measurements.

The data acquisition was performed using a Hewlett-Packard 725 workstation and a Hewlett-Packard 3565 data-acquisition front end. A PCB data harvester was utilized to provide low-pass analog signal filtering and to provide power to the accelerometers. The 3565 front end was configured with 40 input channels and 4 output channels. Data were collected up to 100 Hz at a resolution of 0.0625 Hz. Datasets were also collected to ascertain the degree of nonlinearity, as well as the predominate noise floor.

2.3 Modal Model. The modal model consists of 164 nodes. It is pictured in Figure 3. The nodal locations were chosen to provide a complete geometric description of the basic AGS hull. In addition, a set of sensors was allocated for each panel and hatch that could move independently of the basic hull. A set of transducers was allocated to the gun tube and another set to the engine/transmission assembly. The additional sensors permit the description of localized motion of the various parts of the hull. Although these modes have little effect on the overall flexibility of the structure, they account for the majority of differences between the various mode shapes.

2.4 Qualitative Data Assessment of Results. A noise floor measurement (NFM) was taken in addition to the data that were acquired for analysis. This dataset is acquired in an identical fashion to the other datasets. The only difference between the two datasets is that the NFM has

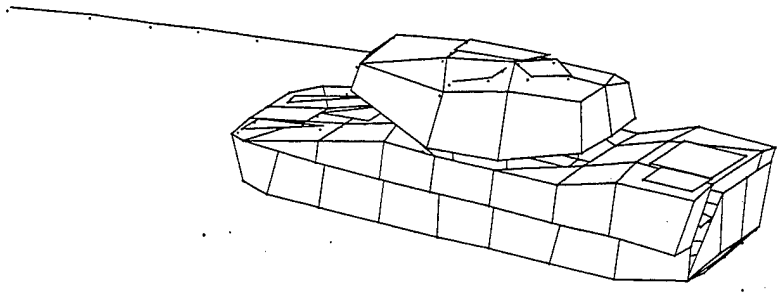

Figure 3. Modal Model.

the excitation signal turned off. Therefore, any signal present in the NFM is due to a noise source. A comparison of the NFM with the analyzed data indicates that the noise floor is at least one order of magnitude less than the data signal in most of the measurements.

Due to limited funds, the test was completed with a limited number of transducers and acquisition channels. Twenty-two different patches were required to obtain the complete dataset. As a result, several patches of data had to be taken over several days. A complete set of driving-point measurements was acquired during every acquisition cycle. A comparison of these records yields a measure of the time variance of the acquired data. Figure 4 is a plot of the FRFs from driving-point 3. Each curve on this plot utilizes the same excitation amplitude, excitation point, and response point. If the system were time invariant, these 18 curves would overlap each other identically. However, due to the time variance, there is a difference between the curves. In some frequency ranges, the difference is severe.

As previously mentioned, modal analysis assumes that the structure under test is linear. A simple technique of verifying this assumption is to input varying force levels to the structure and measure the ensuing FRFs. For an ideal linear structure, all of the FRFs overlay each other exactly. The FRFs measured from three force levels are shown in Figure 5. Since a single 50-lb shaker was utilized for the linearity check, the total force input level was small. A driving-point response location was utilized for these measurements. At the these small force levels, the structure appears to be linear.

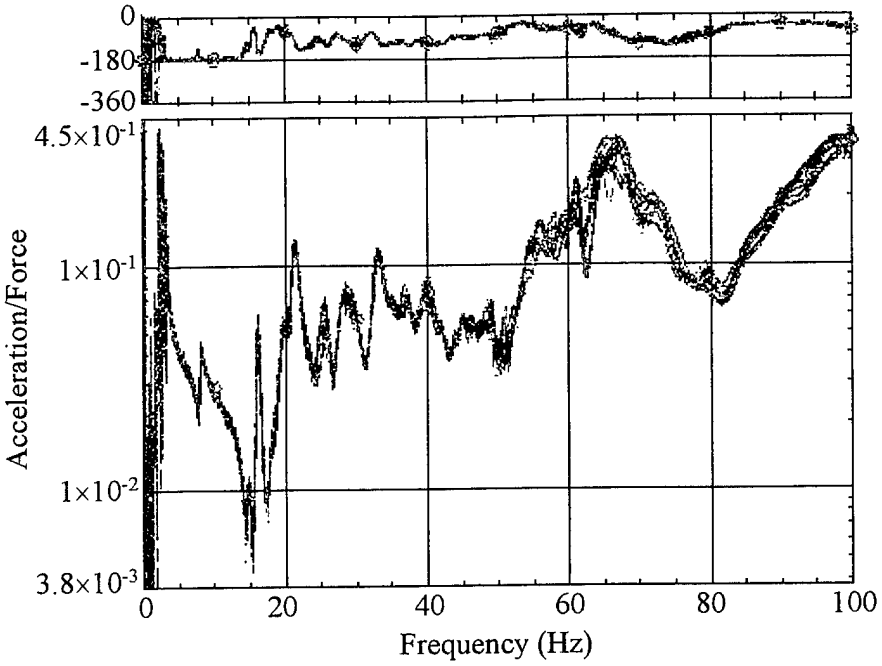

Figure 4. Time Variance of Driving-Point Measurements.

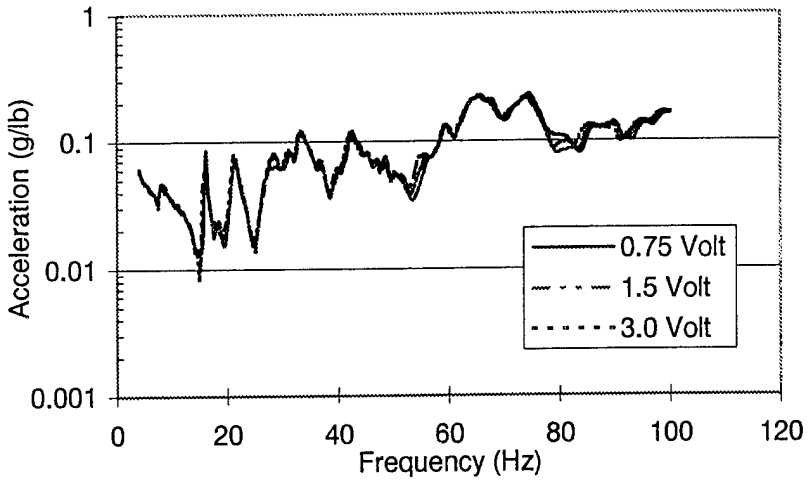

Figure 5. Linearity Check for Three Excitation Levels.

2.5 Parameter Extraction. All parameter extraction and data acquisition were performed on an HP725 workstation, utilizing SDRC's I-DEAS software. The time-domain polyreference method of curve-fitting was used throughout the analysis. The FRFs of interest are inverse

transformed into their impulse response functions (IRFs). Then these IRFs are curve-fit with a least-squares curve-fitter to extract the modal parameters. A complete description of this curve-fitting technique can be found in Brown, Allemang, and Zimmerman [4].

2.6 Accuracy and Certainty. The accuracy and uncertainty of the extracted modal parameters are heavily dependent on the nature of the structure under test. In a lightly damped structure with distinct modes, high accuracy is easily obtained. However, if the structure is heavily damped with many closely coupled modes, the extraction of individual modal parameters proves to be extremely difficult.

Unfortunately, the AGS vehicle, as tested, falls into the latter class of structures. The frequencies less than 50 Hz extracted in the modal analysis are accurate to within 3%. The frequencies over 50 Hz are accurate to within 7%. Clusters of extracted modes exist at various frequencies. In some instances, these clusters result from time-variant measurement data. The extracted damping parameters are accurate to with 10% below 20 Hz and 50% over 20 Hz. The damping values are extremely difficult to extract from these measurements. Since many of the extracted modes entail movement of various hatches, the damping and frequency parameters are heavily dependent on the condition of the rubber gaskets on those panels, as well as the tightness of the fasteners used to secure them.

2.7 Mode Shapes and Frequencies. Due to the complexity of the AGS structure, this report does not attempt to describe each mode shape, but they are illustrated in Appendix B. A description of the common features of groups of mode shapes is included in this report and a digital copy of the full set of mode shapes will be provided upon request. (A set of ARL-authored MATLAB scripts can also be supplied to facilitate viewing the mode shapes on any computational platform supporting MATLAB V4.2c.m files.)

Figure 6 displays the four driving-point FRF measurements from the AGS vehicle test. The measurements are the highest quality FRFs measured and give an indication of the modal density, as well as an indication of the form and quality of the response FRFs.

Table 1. AGS Modal Parameters

Mode No.	Frequency (Hz)	Damping (% Critical)	Mode No.	Frequency (Hz)	Damping (% Critical)	Mode No.	Frequency (Hz)	Damping (% Critical)
1	7.9	2.408	19	33.1	1.884	37	51.1	0.451
2	14.5	1.859	20	33.2	0.798	38	51.2	0.491
3	16.0	1.171	21	33.5	1.595	39	54.8	0.507
4	16.1	1.198	22	36.3	1.770	40	57.8	0.406
5	19.7	3.518	23	36.9	1.347	41	57.9	0.318
6	21.7	0.533	24	38.6	0.960	42	57.9	0.394
7	22.6	1.256	25	40.6	1.899	43	58.1	0.293
8	24.9	0.685	26	42.1	1.724	44	59.3	0.297
9	26.2	0.665	27	43.9	0.860	45	60.4	0.282
10	26.2	0.665	28	44.9	1.151	46	60.5	0.621
11	26.9	0.354	29	45.3	0.523	47	61.4	1.311
12	27.9	3.024	30	46.2	1.005	48	64.3	1.332
13	28.6	0.338	31	47.2	1.671	49	67.5	1.190
14	28.6	0.459	32	48.3	0.044	50	73.9	1.040
15	28.8	0.465	33	48.7	0.881	51	80.6	0.678
16	31.0	1.846	34	48.9	0.874	52	85.2	0.541
17	32.0	0.215	35	49.1	0.994	53	89.0	0.320
18	32.9	1.091	36	50.6	0.861	—	—	—

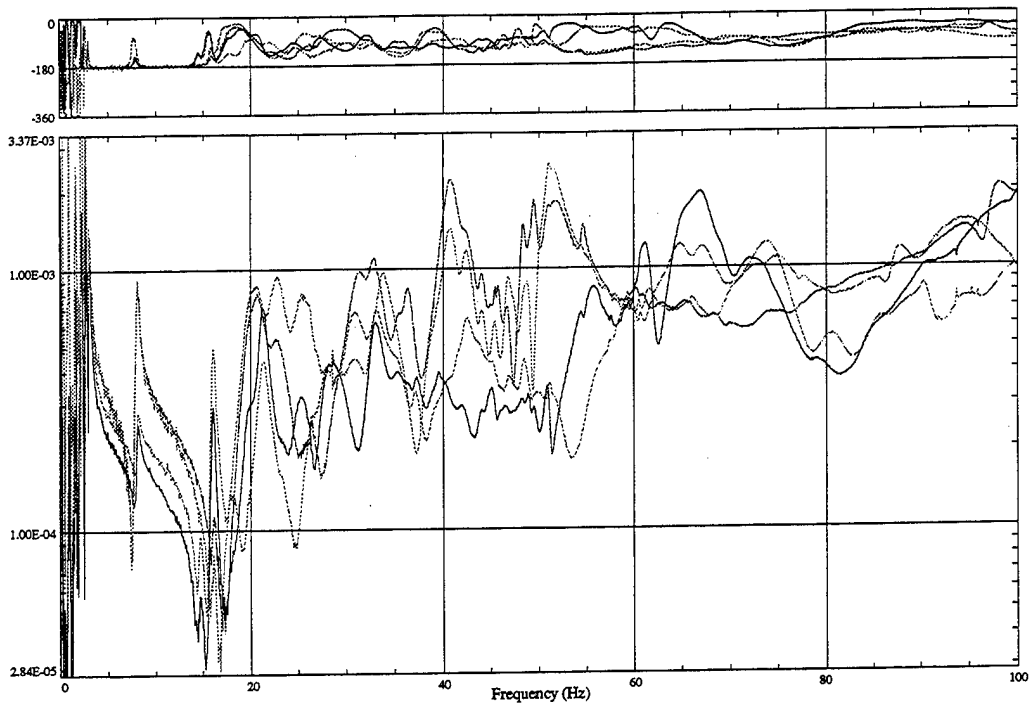

Figure 6. Driving-Point FRFs.

The mode indicator function (MIF) is shown in Figure 7. Minimas in the solid dark curve of this function indicate the presence of modes at those frequencies. The sharper the minima, the stronger the mode. Minimas in the other curves may indicate a cross-over point or a double mode.

The MIF can be used to ascertain the modal density of the structure. Many closely spaced minimas indicate high modal density and a high degree of modal coupling. Sharper minimas with more space between them indicate a low modal density with little interaction between modes. The AGS has a high modal density with significant coupling between modes.

A heavily coupled dynamic response makes the extraction of modal parameters very difficult. The MIF shown in Figure 7 is heavily coupled and exhibits a high modal density.

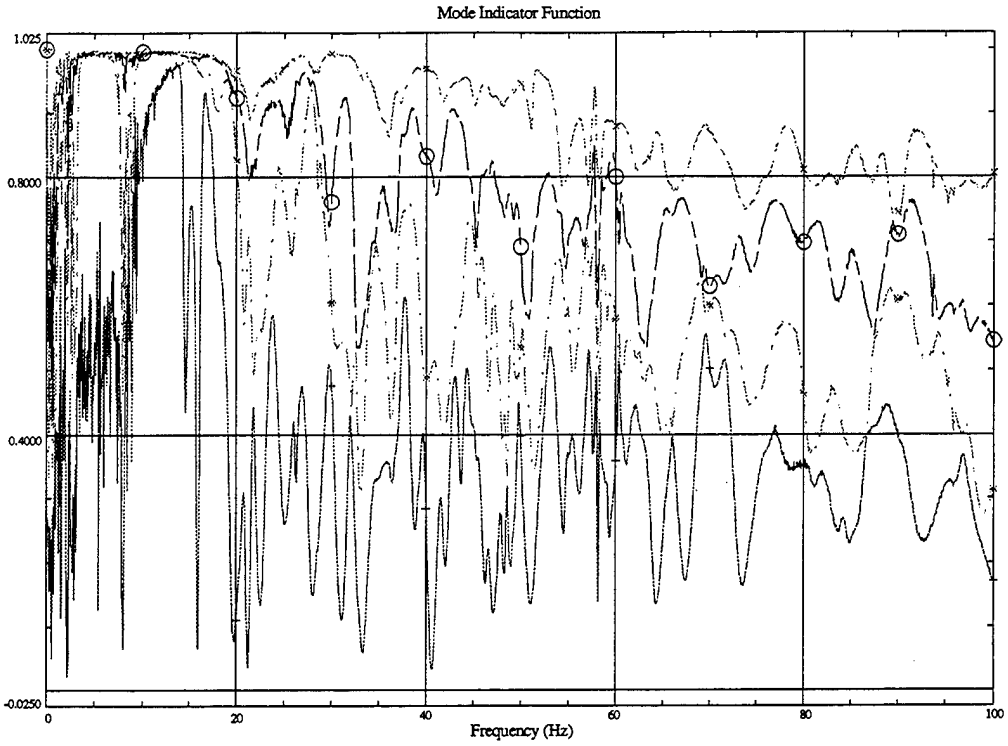

Figure 7. Mode Indicator Function.

Figure 8 is a graphical representation of the modal assurance criterion (MAC) matrix. The MAC provides an indication of the linear independence of each mode. In an ideal analysis, the MAC will have a value of 1 along the diagonal and value of 0 everywhere else. The majority of the modes extracted from this analysis are linearly independent. However, the duration over which a single dataset was measured resulted in time-varying data. This variance is somewhat accounted for by curve-fitting multiple modes where a single mode exists. This effect accounts for a portion of the linearly dependent mode shapes.

The first extracted mode of the AGS entails movement of the main weapon (7.9 Hz). The driver's hatch is the primary participant in the second mode (14.5 Hz). The next several modes include various combinations of motion in the turret hatches in conjunction with gun tube motion. The gun tube moves in both the vertical and horizontal planes. Mode 9 (26.2 Hz) begins to include some elements of motion on the rear deck of the hull.

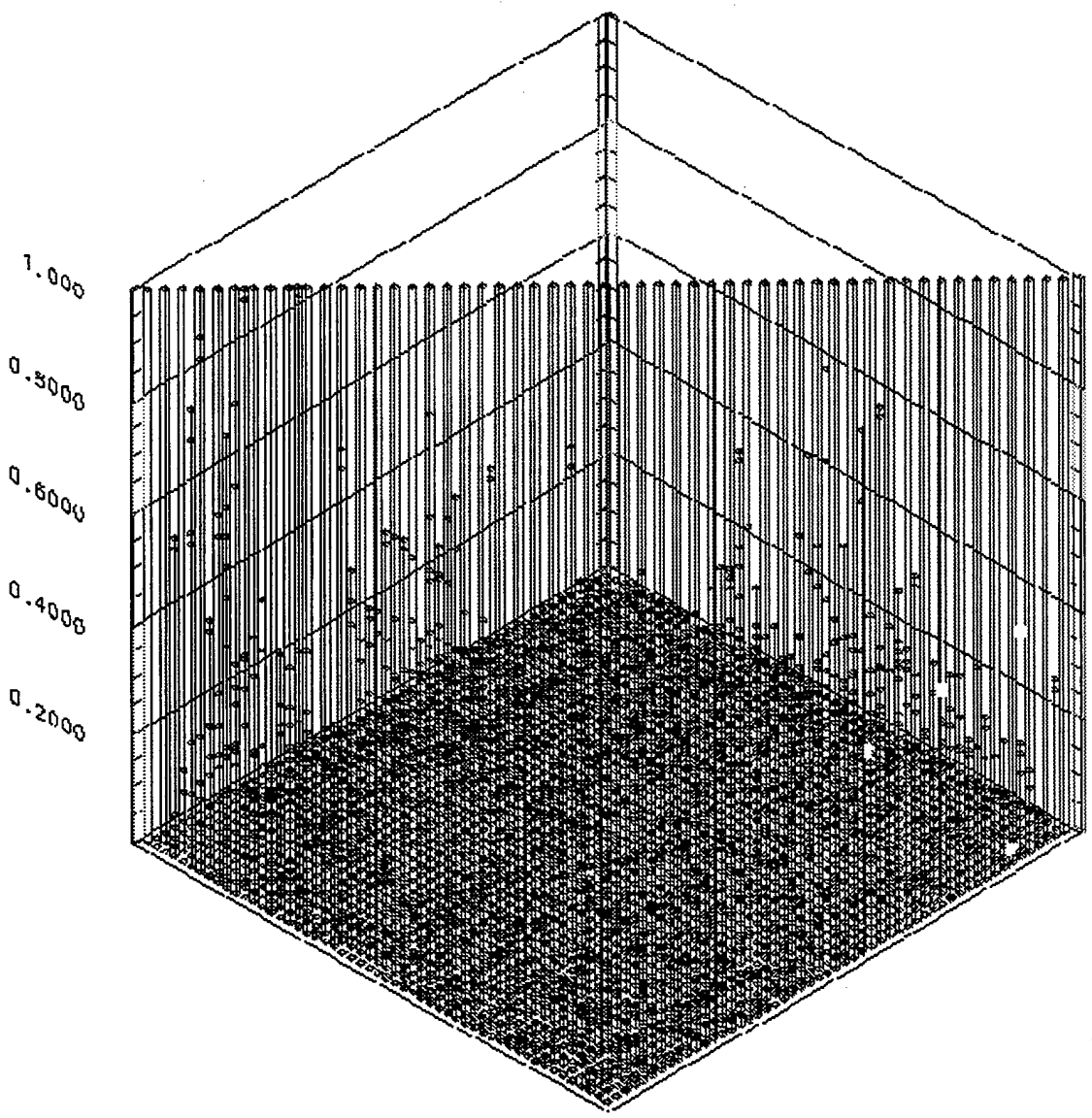

Figure 8. MAC Matrix Representation.

Mode 12 (27.9 Hz) begins to show an indication of global motion as the hull twists slightly in the rear sections. Mode 14 (28.6) begins to show some interactive motion between the turret and the hull. The next several modes include various combinations of tube motion, slight hull twisting, and hull/turret interaction.

Mode 21 (33.5 Hz) begins to show flexibility of the sponson. This type of motion is very similar to the flexibility that was seen in testing other vehicles of similar design. Mode 23

(36.9 Hz) includes significant flexure of the upper surface of the hull deck, particularly in the rear portion. The first primary global torsional mode is mode 25 (40.6 Hz). Although this mode includes motion of various hatches, its dominant feature is global torsion of the hull.

Mode 28 (44.9 Hz) begins to indicate flexibility in the hull floor and Mode 31 (47.2 Hz) indicates flexibility in the forward section of the hull. The next several modes include various combinations of the previous motions. Mode 37 (51.1 Hz) shows motion of the engine within its mounts. Sponson rotation is the primary motion exhibited by Mode 48 (64.3 Hz). The intervening modes, as well as the remaining modes, include various combinations of hatch, engine, floor, hull, and tube motion.

3. High-Frequency Dynamics Test

3.1 Experimental Damping Analysis Methods. Four different methods are utilized to determine damping.

(1) The conventional modal analysis theory based method works on high-quality FRFs. Results from the AGS modal test and analysis were obtained via this method and are presented elsewhere in this report. The method is very accurate when structural modes are well separated. As a result, this method is limited to the lower frequency range where distinct modes exist.

(2) A technique relying on narrow-band filtering and exponential curve-fitting was utilized. The accuracy of this method is reduced by two conflicting factors. When a passband is too wide, modal coupling can lead to a "beating" phenomena, which degrades the exponential curve-fit quality. When the passband is too narrow, the filtering itself causes unwanted distortion in the time domain signal. Nevertheless, this method is conceptually simple and easy to understand. It is also recommended by the MANTA developer. Therefore, AGS damping values used for MANTA predictions were obtained from this method.

(3) The power injection method evolved from Statistical Energy Analysis (SEA) and is based on energy conservation between input power and structural response. This method works well on simpler structures where response velocity and mass are known or can reliably be measured. This method is usually implemented in conjunction with obtaining vibration transmission coefficients (VTC) that are needed for certain analytical predictions. Some recent work, performed on the composite armored vehicle (CAV) composite panels, utilized this method and resulted in reasonable damping estimates. The method requires a response energy measurement on all structural panels, which was well beyond the scope of the AGS test. In general, experience has shown that this method is not practical for complex structures due to its tedious test process and a potential numerical difficulty resulting from matrix inversion.

(4) Initial experiments on a wavelet-transform-based new method seem promising, but further investigations are needed.

Method 1 is used to analyze the low-frequency modal data (to 100 Hz), while methods 2 and 4 were used to analyze the high-frequency data (to 10 kHz) in the AGS test.

3.2 High-Frequency Damping Determination by Wavelet Transform. The continuous wavelet transform (CWT) expands a signal into a time-scale space via correlation with a wavelet, generating a CWT coefficient Φ. When the wavelet is chosen such that its spectral energy includes only a single mode, the scale of the transform is correlated to frequency. In other words, wavelet transforms decompose the signal in the frequency spectrum while retaining the time-domain information.

$$\Phi_{a,b(x)} = \int_{-\infty}^{\infty} x(t) h^{*}_{a,b}(t)\,dt, \tag{1}$$

where Φ is the wavelet transform coefficient, $x(t)$ is the time signal to be transformed, and $h_{a,b}(t)$ is the family of wavelets scaled and shifted from $h(t)$ and is defined as

$$h_{a,b}(t)=\frac{1}{\sqrt{a}}h\left(\frac{t-b}{a}\right). \tag{2}$$

The CWT process is computationally intensive, but its concept is straightforward, as shown in Figure 9.

(1) Starting from the left, compute the coefficient (1) between the wavelet and that section of the signal.

(2) Shift the wavelet to the right and repeat step 1 until the end of the signal. This results in a row of the coefficient matrix C.

(3) Change the scale/frequency of the wavelet (by stretching or compressing it) and repeat steps 1–2 to cover the entire frequency range of interest.

The aforementioned process generates the desired wavelet transform coefficient matrix C, where each scale forms a row and each wavelet time shift forms a column. From the definition of CWT, it can be seen that each element of the C matrix represents how closely the wavelet correlates to the signal at certain frequencies and times. When a typical structure is subjected to impact, its exponentially decaying responses are indicative of the damping characteristics. As energy is dissipated through various structural damping mechanisms, the unimodal energy (a row in C matrix) decreases along the time axis of the matrix. This time-dependent behavior of the CWT coefficients is observable and can be used to calculate the damping as follows:

$$\varsigma_m=\frac{1}{2\omega_m}\ln\left(\left|\frac{\Phi_{a,b_2}}{\Phi_{a,b_1}}\right|\right)\frac{a}{b_2-b_1}\ . \tag{3}$$

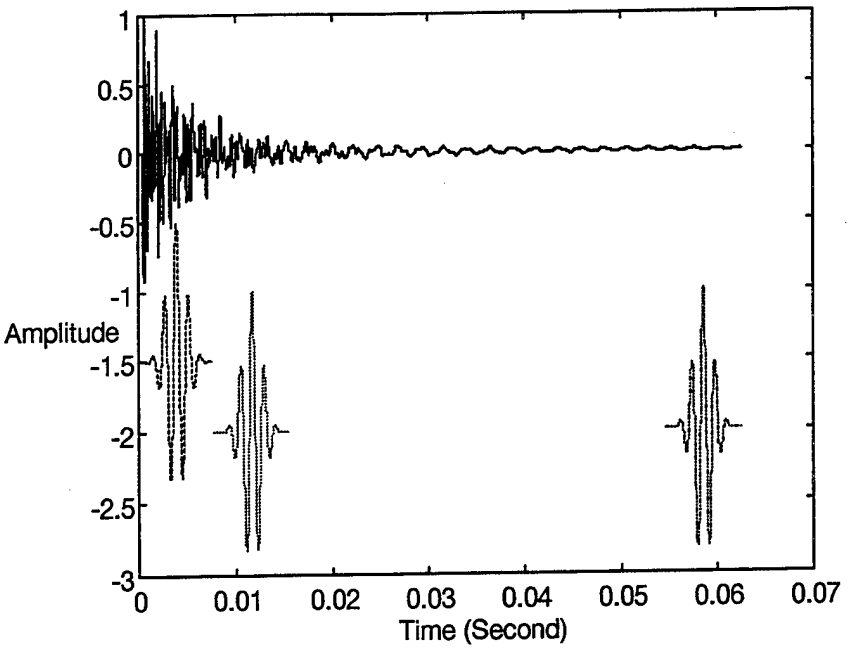

Figure 9. Time Shifting of Wavelet in CWT Process.

The damping ratio (ς_m) can be extracted from, (3), where $\frac{a}{b_2 - b_1}$ is the elapsed time between the two wavelet coefficients Φ_{a,b_2} and Φ_{a,b_1}. A better estimate can be made by performing a curve-fit on a range of coefficients with the corresponding time as the ordinate. The process can be further simplified by linear curve-fitting the log of the coefficient ratio. The least-squared curve-fit reduces the effect from experimental noise and therefore generates more accurate damping estimates as can be seen in Figure 10. Because of the nature of wavelet transforms, coefficients of a mode may contain energy from adjacent modes. Therefore, the coefficients should be considered as moving averages in time and scale. Experience indicated that, in practice, high-frequency damping only changes gradually along the frequency axis (i.e., without sudden or wide variations), so the moving averages issue is insignificant.

The computation process is tested and validated using synthesized signals with known damping values. An example of these waveforms is shown in Figure 11, which is synthesized from damped sinewaves of 4, 6, and 7 kHz.

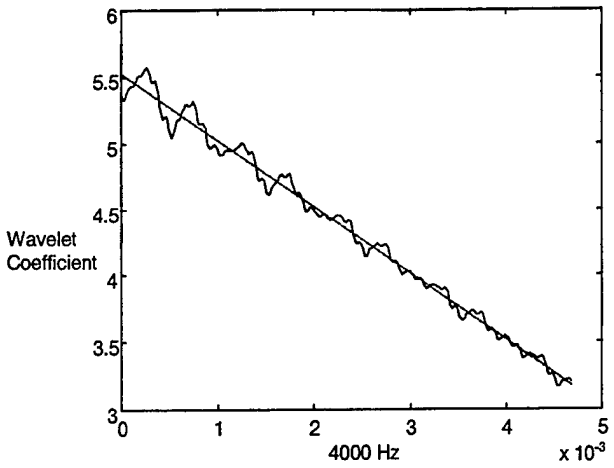

Figure 10. Curve-Fit of CWT Coefficients.

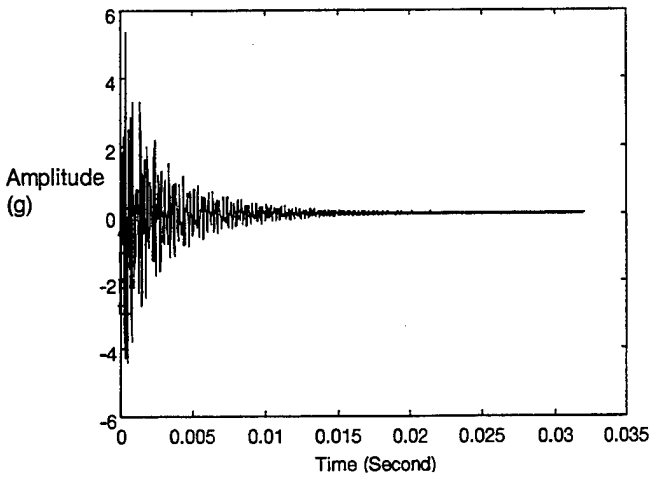

Figure 11. Synthesized Time Domain Signal.

Figure 12 compares the known damping ratios from the synthesized functions with the damping extracted by the CWT method from the same functions. Only a few selected AGS impact responses are analyzed by the wavelet method for comparison purposes. Figure 13 shows the typical structural response (due to hammer impact) and its FFT. Figure 14 is a CWT coefficient matrix of the time history. Figure 15 is an example of curve-fitting a row of CWT coefficients to obtain damping.

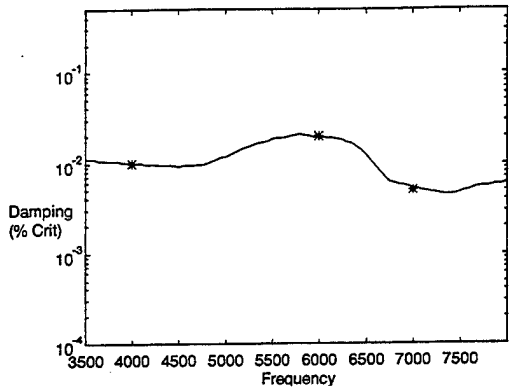

Figure 12. Comparison of Known vs. Synthesised Damping.

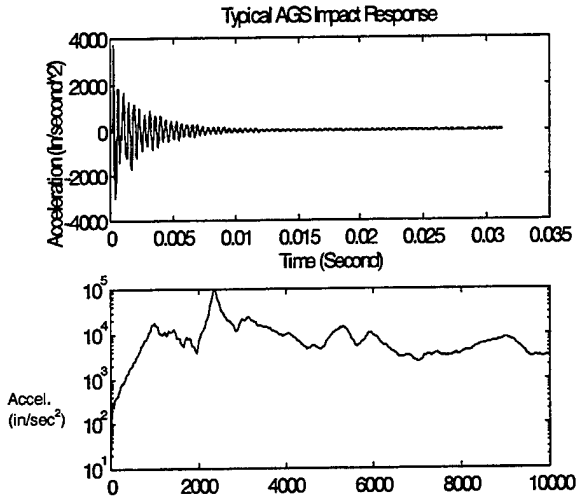

Figure 13. Typical AGS Impact Response.

3.3 Moving Bandpass Filter and Log Decrement Method. This method extends the conventional single-mode log decrement method to a band-filtered signal. The procedure is outlined as follows.

(1) The response signal is band-filtered by a fifth-order Butterworth filter moving from low to high frequency covering the entire 10-kHz range. The typical moving filter center frequency increment is 100 Hz. A synthesized test signal and its FFT ($\varsigma = 0.02$) are shown in Figure 16.

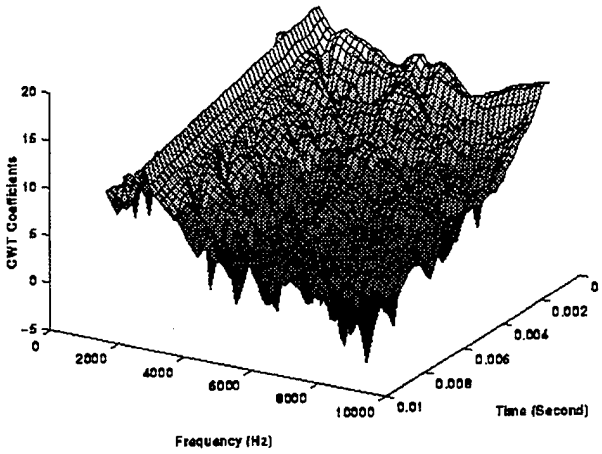

Figure 14. Typical AGS CWT Coefficients.

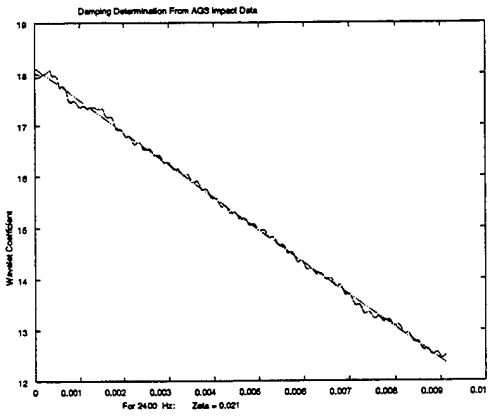

Figure 15. Curve Fit of CWT Coefficients.

(2) Each band-filtered time series now contains only the energy within the passband. Peaks of the damped oscillation are selected as indicated by +'s in Figure 17.

(3) The peaks selected from step 2 are curve-fit based on the formula for an underdamped single-mode time response to an impulse, $x(t) = e^{-\varsigma\omega_n t}\sin\left(\sqrt{1-\varsigma^2}\omega_n + \phi\right)$. When only the oscillation peaks are used for curve-fitting, the sin() factor can be ignored and the peaks fit by $x(t) = e^{-\varsigma\omega_n t}$. Figure 17 shows the synthesized damping curve plotted against the filtered time domain signal.

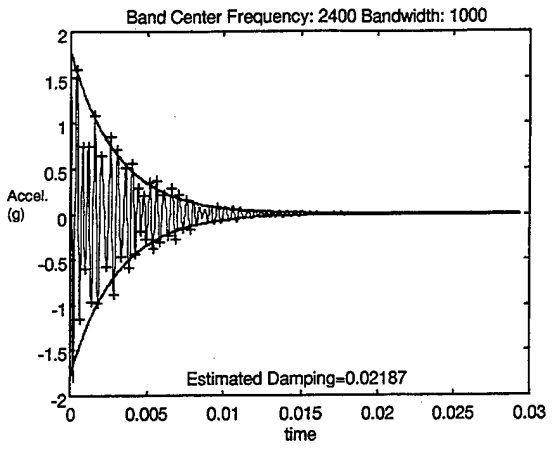

Figure 16. Narrow Band Exponential Curve-Fit.

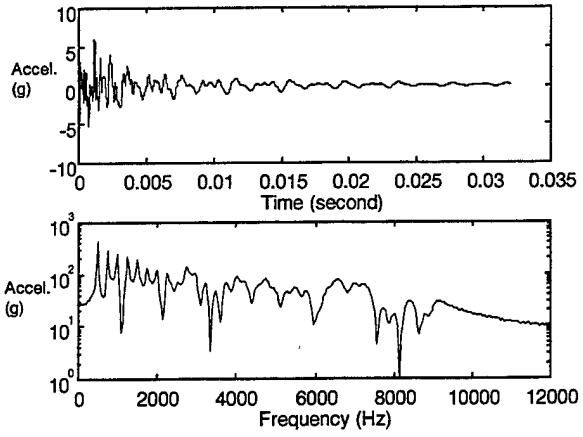

Figure 17. Synthesized Test Waveform With Constant Damping.

(4) This process is then repeated for each filter bank. When the entire frequency range is analyzed, the damping can be plotted as a function of filter bank center frequencies, as shown in Figure 18. Figure 18 compares the synthesized damping values with the damping values obtained by the wavelet method and filtering methods. In general, it is very difficult to accurately extract high-frequency structural damping. All three high-frequency methods described (power injection, bandpass, wavelet) yield approximate damping values.

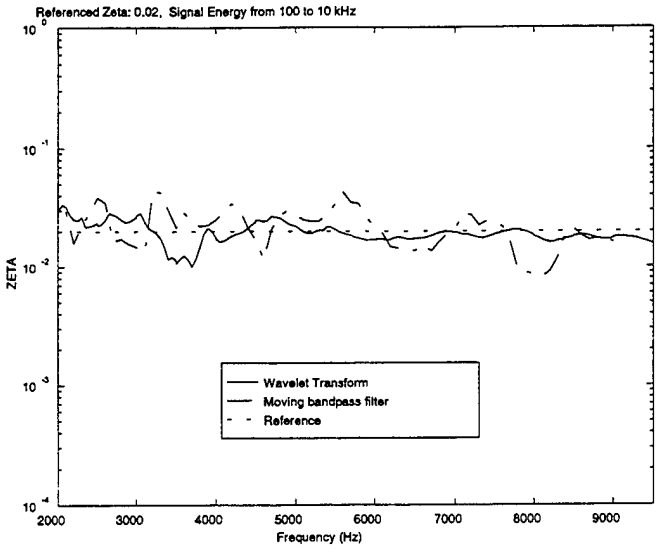

Figure 18. Comparison of Damping Obtained by Wavelet and Exponential Decay Methods.

3.4 High-Frequency FRF Test Description. The data gathered from the high-frequency testing were intended for MANTA model correlation and as a base to obtain live-fire test predictions. Since the vehicle could not be excited at ballistic levels for this test, hammer impact data were obtained from a variety of locations. Consequently, a thorough mapping of FRFs was obtained from this testing. This mapping consisted of 11 excitation input locations and 64 response locations, resulting in over 700 FRFs. Multiple excitation techniques were also used to provide a measure of data consistency and repeatability. These were broadband random, discrete sine sweep, and hammer impact excitations. The data obtained by the alternate excitations were particularly useful for estimating the high-frequency damping, which is a difficult parameter to characterize.

Because of the high-frequency range of this test, careful consideration was given to accelerometer selection and mounting. Also, since the loading levels used in this nondestructive testing were small, sensitive accelerometers were necessary. Endevco Model 7254A accelerometers were selected based on the following factors: (1) acceptable frequency response

to 10 kHz, (2) high sensitivity (500 mV/g for most accelerometers), and (3) extremely low noise floor (the noise floor is equivalent to 0.0002 g for model 7254A_500).

In order to assure a good frequency response measurement of the structure up to 10 kHz without influence of the accelerometer mount, direct screw mounting of the accelerometer is preferable. Fortunately, the threaded bolt holes normally used for attaching armor and accessories could be used with replacement bolts to house the accelerometers. The hex tops of these replacement bolts were drilled and tapped so that each accelerometer could be stud-mounted. The specially prepared replacement bolts were then screwed directly to the vehicle body at or near the desired measurement locations. For vehicle locations where threaded holes were not available, dental cement or glue was used. Experiments were performed prior to the AGS vehicle test to ensure that the adhesive-mount frequency responses, though not ideal, were acceptable. Figure 19 shows a typical stud-mounted sensor.

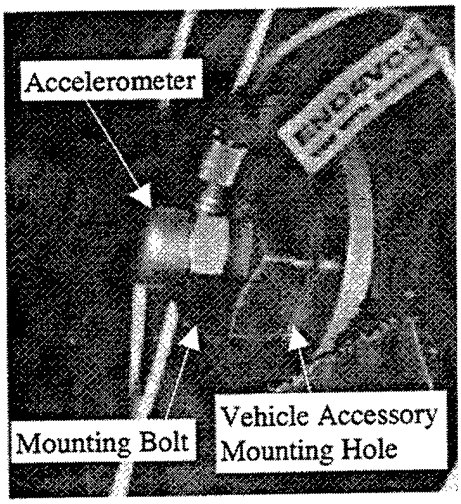

Figure 19. Typical High-Frequency Sensor Attachment.

Careful consideration was also given to exciter selection and technique to ensure that the exciter had sufficient power to propagate vibration throughout this massive structure at levels above noise. It is difficult to provide this excitation since the available electrodynamic shakers are only designed to provide excitation below 5 kHz.

Although these shakers can be used to generate force up to 10 kHz, the force is at a considerably reduced level. Consequently, an instrumented impact hammer was used to provide complimentary FRF data (and also to provide time response data for high-frequency damping estimates). Figure 20 shows a typical hammer force measurement. Note that the relatively flat frequency response extends to 8 kHz, resulting in a force signal with a signal-to-noise ratio of 100 below 8 kHz and only about 10 from 8 to 10 kHz. The hammer provides some improvement at the high frequencies, but not without limitation.

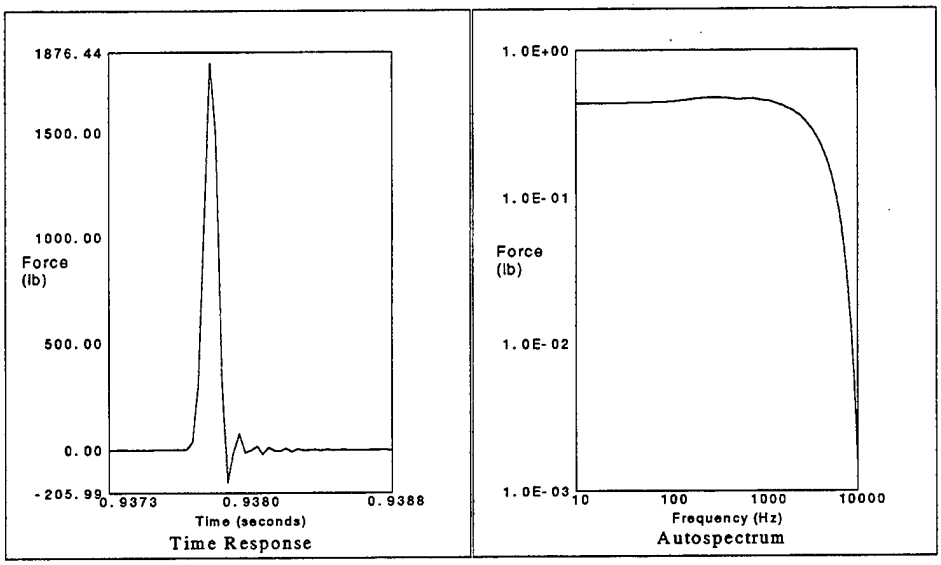

Figure 20. Typical Hammer Impact.

The careful test design yielded data that were high quality and repeatable. Some interesting trends were apparent upon review of the data collection. First, there was a large attenuation of response amplitude at locations of increasing distance from the excitation source. This attenuation was particularly pronounced as frequency increased, as shown in Figure 21 and Table 2. Also noted was that for a remote excitation source, the vibration was typically uniform within a single panel of the vehicle structure. Table 2 compares relative responses of six locations on the right turret panel due to vibration input at five locations.

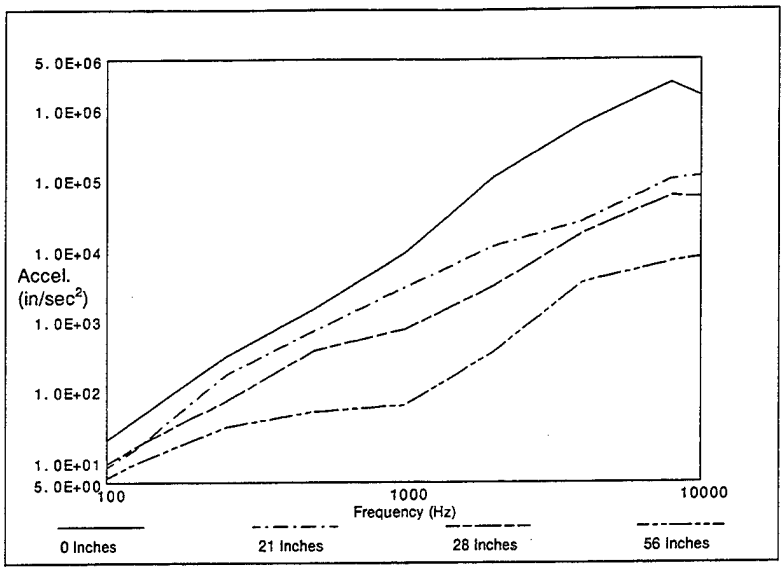

Figure 21. Octave Analysis of FRFs.

Table 2. Response Location Statistics

Response Location	Input 2	Input 3	Input 4	Input 5	Input 6
111	60.3	14.1	15.3	26.9	23.0
112	49.0	15.7	17.4	26.6	25.5
113	50.4	15.6	20.3	26.4	26.6
114	52.3	21.6	24.2	33.7	29.0
115	43.1	15.9	18.1	24.9	24.0
116	49.3	14.5	15.0	25.1	21.8
STD	5.61	2.73	3.45	3.26	2.61
Mean	50.7	16.2	18.4	27.3	25.0
STD/Mean	0.111	0.168	0.188	0.120	0.105

It must be noted that these estimated damping values are very approximate because several modes are usually present within the bandwidth. These additional modes create an apparent damping value as represented by a single theoretical mode.

An important result of the damping estimates that is of particular use to the analytical modeling effort is that the damping of various locations on the structure appeared relatively

uniform. Figure 22 shows a histogram of estimated damping (averaged over frequency) at the various response locations from an impact at the left hull side in the middle. The mean value is seen to be roughly 1.75% critical damping. The damping estimates for these locations do not seem to be dependent on impact location. Figure 23 shows a similar histogram for an impact at the left-turret middle panel. A similar result of 1.6% critical damping is seen.

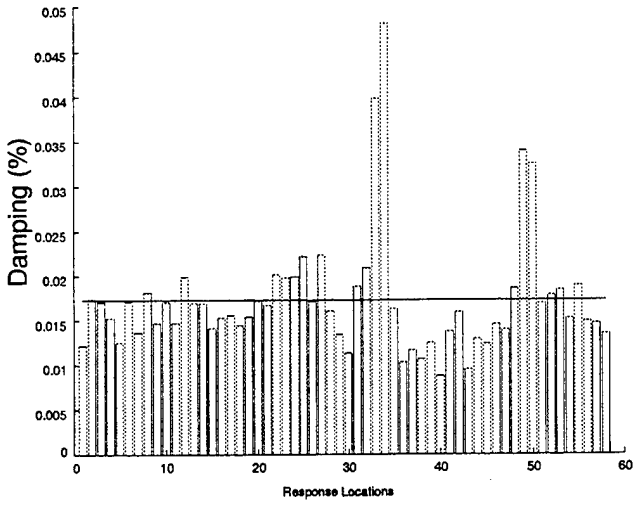

Figure 22. Estimated Average Damping for Various Locations for Hull Impact.

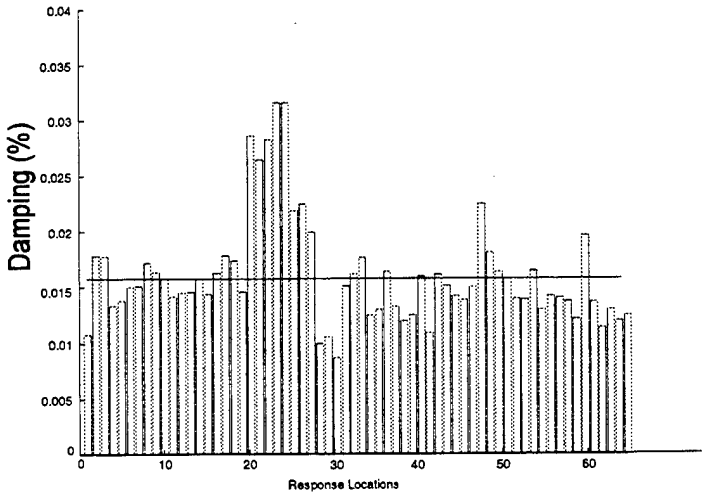

Figure 23. Estimated Average Damping for Various Locations for Turret Impact.

4. Conclusions and Recommendations

Previous modal analyses of the BFV, M113 and heavy composite hull have concentrated on either bare hull or almost completely stripped hull vehicles. Conversely, this modal test and analysis of the AGS was performed on a full-up vehicle. In addition, the test of the AGS included the turret, whereas all of the previous tests excluded the turret from the tested configuration. As a result, the measurements were extremely noisy compared to previous tests. Despite the high noise, modal parameters were extracted from the measured data.

This test has shown that, although modal parameters are extractable from a full-up vehicle, the accuracy of the parameters is much lower. The additional noise greatly reduced the confidence in the mode-shape estimation. The large number of modes resulting from hatches and other subcomponents tended to mask global vehicle modes. However, despite the hatch-induced noise, at least one turret/hull interactive mode was extracted. Removal of hatches and other nonstructural components on future tests will enhance the ability of the analyst to extract meaningful structural modes from future modal tests of similar vehicles.

The analysis was further complicated by time variance in the measured data. The large number of patches required for a single data set required several days to measure. Changes in the structural response of the vehicle occurred during the time span required to complete a single measurement cycle. These changes reduced the accuracy of the modal analysis. More sensors and data acquisition channels in future tests reduce the measurement time, thus increasing the accuracy of the resulting modal parameters. Ideally, a single measurement cycle should be completed within a few hours or, at most, a single day.

Throughout this test and analysis, several methods of damping estimation were used. Based on this experience, there is no single estimation technique that is best on all structures. Where usable, modal damping for individual modes is the most reliable method of damping estimation. The power injection technique is a good method for high frequencies where individual modes

cannot be analyzed. However, power injection is only applicable to simple plate-like structures under free-free boundary conditions.

The remaining two estimation techniques are both applicable to vehicle class structures. Both the narrow-band filtering and the wavelet transform techniques yielded reasonable damping estimates. However, neither method was completely satisfactory. Other time-frequency decomposition techniques should be explored and compared against the modal damping and power-injection damping estimation techniques.

The AGS was heavier than any previous vehicle that the authors have tested. The shakers utilized provided a marginal excitation force. More powerful shakers would have moved the data further above the noise floor, thus permitting high-quality measurements at remote hull locations. In addition, the hammer excitation did not come close to approximating the force levels expected in a live-fire test. For a reasonable comparison to live-fire predictions, the impact excitation should approximate the force levels expected in a live-fire test.

INTENTIONALLY LEFT BLANK.

5. References

1. Berman, M. S., and T. H. Li. "Modal Analysis of the Bradley Fighting Vehicle (BFV): Prototype Composite Hull and Production Metallic Hull." ARL-TR-445, U.S. Army Research Laboratory, Aberdeen Proving Ground, MD, 1994.

2. Berman, M. S. "Modal Analysis of the M113 Armored Personnel Carrier Metallic Hull and Composite Hull." ARL-MR-246, U.S. Army Research Laboratory, Aberdeen Proving Ground, MD, 1995.

3. Berman, M. S. "Modal Analysis of the Heavy Composite Hull." U.S. Army Research Laboratory, Adelphi Laboratory Center, MD, in progress.

4. Brown, D. L., R. J. Allemang, and R. Zimmerman. "Parameter Estimation Techniques for Modal Analysis." Technical Paper Series 90221, Society of Automotive Engineers, Inc., 26 February–2 March 1979.

INTENTIONALLY LEFT BLANK.

Appendix A:

Airmount Data Sheet

INTENTIONALLY LEFT BLANK.

	Description	Order No.
Style 113 Two Ply Bellows	Blind nuts, 1/4 NPT	WO1-358-7103
	Blind nuts, 1/4 NPT, bumper	WO1-358-7104
	Blind nuts, 3/4 NPT	WO1-358-7101
	Blind nuts, 3/4 NPT, bumper	WO1-358-7109
	Button head steel bead rings, 1⅞ bolts, nuts, washers	WO1-358-7110
	Blind nuts, 1/8 NPT	WO1-753-7113
	Blind nuts, 1¼ NPT	WO1-753-7114
	Rubber bellows only	WO1-358-0135
Assembly weight ..... 14.5 lbs.		
Force to collapse to minimum height (@ 0 PSIG)..... 17 lbs.		
Style 128 Four Ply Bellows	Blind nuts, 1/4 NPT	WO1-358-8151
	Blind nuts, 1/4 NPT, rubber bumper	WO1-358-8149
	Blind nuts, 3/4 NPT	WO1-358-8152
	Blind nuts, 3/4 NPT, rubber bumper	WO1-358-8150
	Rubber bellows only	WO1-358-0231

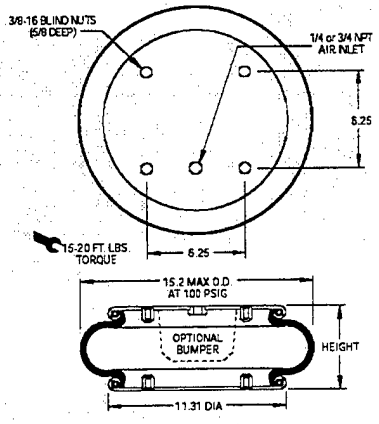

NOTE: This part is also available with bead rings (rather than end plates). SEE PAGE 8.

Dynamic Characteristics at 5.0 in. Design Height
(Required for Airmount isolator design only)

Volume @ 100 PSIG = 585 in³			Natural Frequency	
Gage Pressure (PSIG)	Load (lbs.)	Spring Rate (lbs./in.)	CPM	HZ
40	3,220	2,429	163	2.72
60	5,030	3,432	155	2.58
80	6,890	4,407	150	2.50
100	8,800	5,385	147	2.45

Static Data
4002

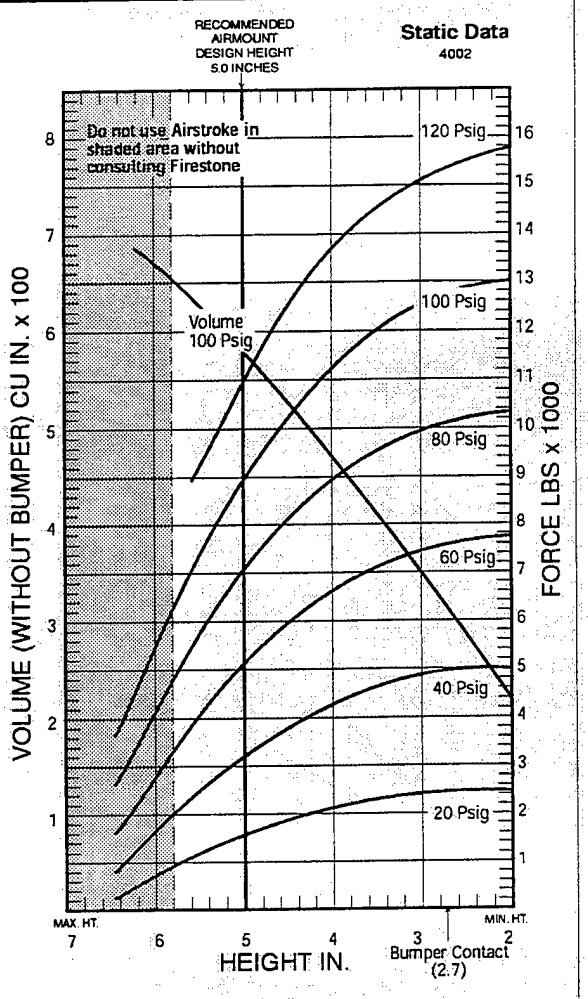

SEE PAGE 12 for instructions on how to use chart.

Force Table (Use for Airstroke® actuator design)

Assembly Height (in.)	Volume @ 100 PSIG (in³)	Pounds Force @20 PSIG	@40 PSIG	@60 PSIG	@80 PSIG	@100 PSIG
5.0	585	1,540	3,220	5,030	6,890	8,800
4.0	477	2,120	4,320	6,600	8,890	11,230
3.0	353	2,390	4,830	7,380	9,900	12,470

INTENTIONALLY LEFT BLANK.

Appendix B:

Mode Shapes

INTENTIONALLY LEFT BLANK.

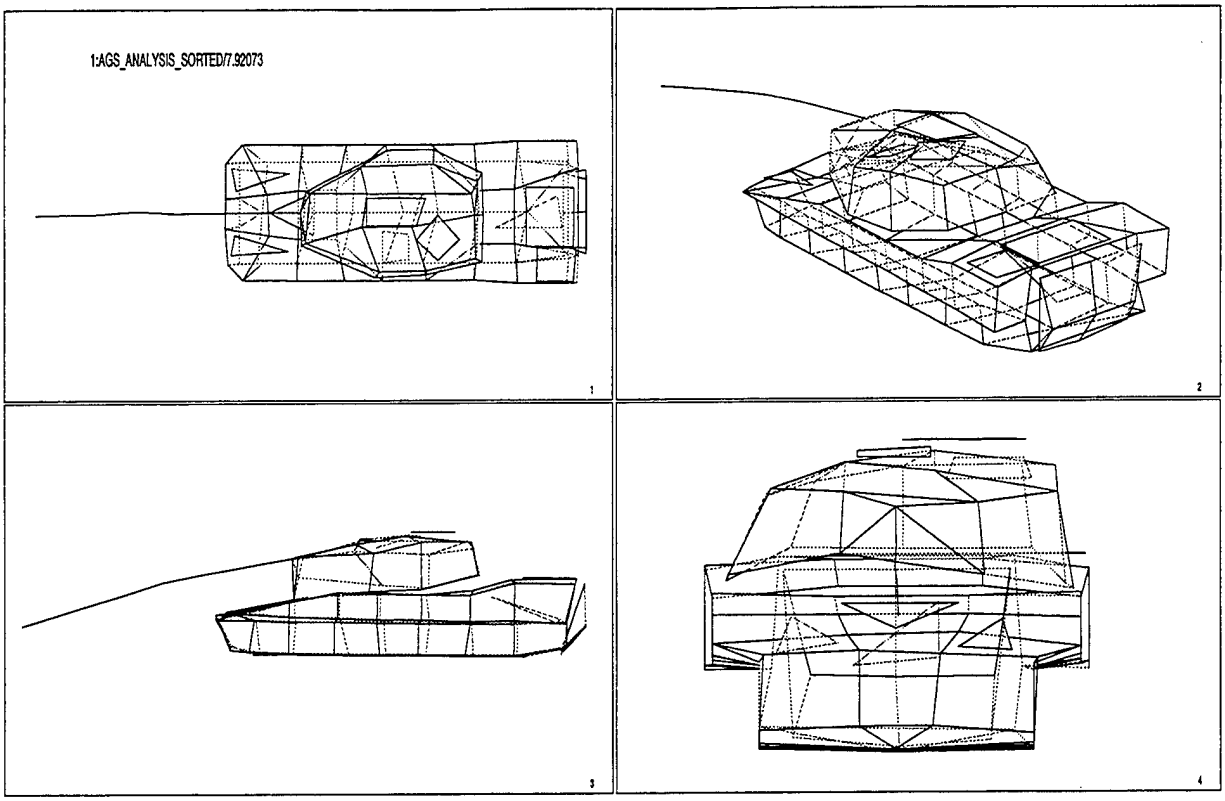
1:AGS_ANALYSIS_SORTED/7.92073
1
2
3
4

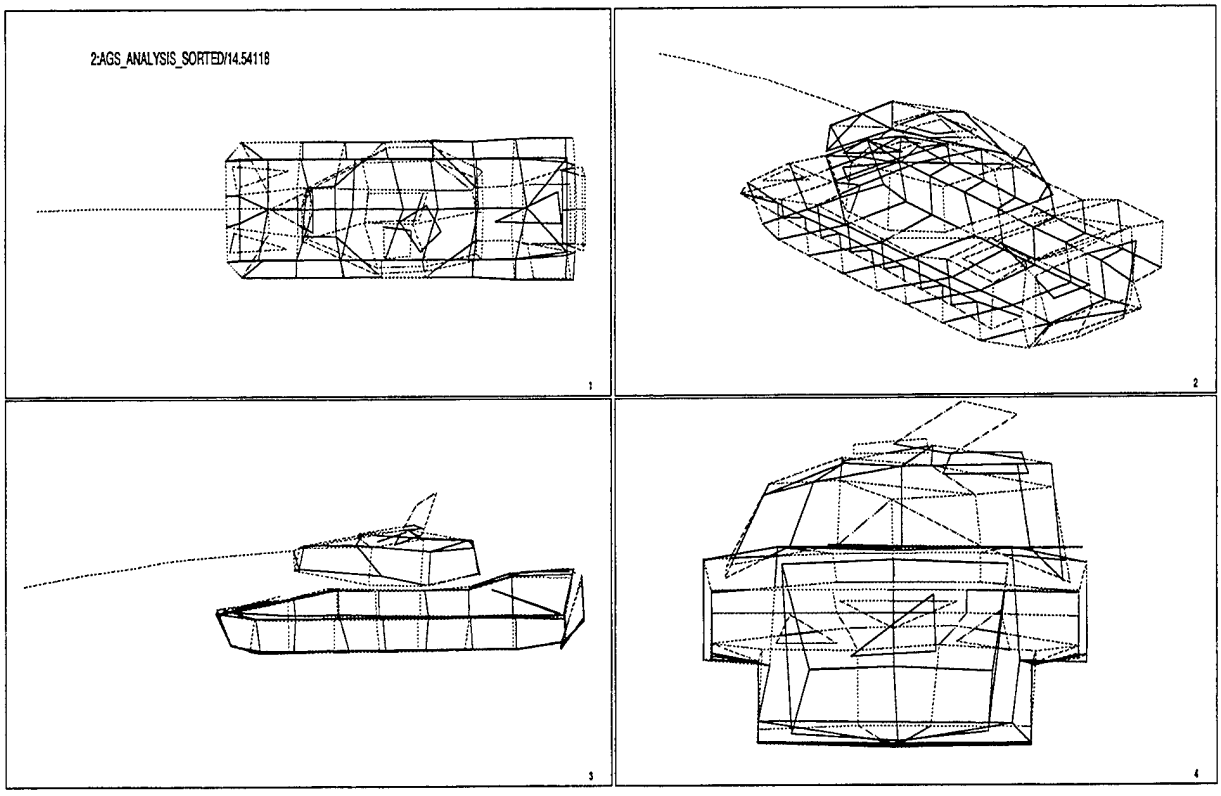
2:AGS_ANALYSIS_SORTED/14.54118
1
2
3
4

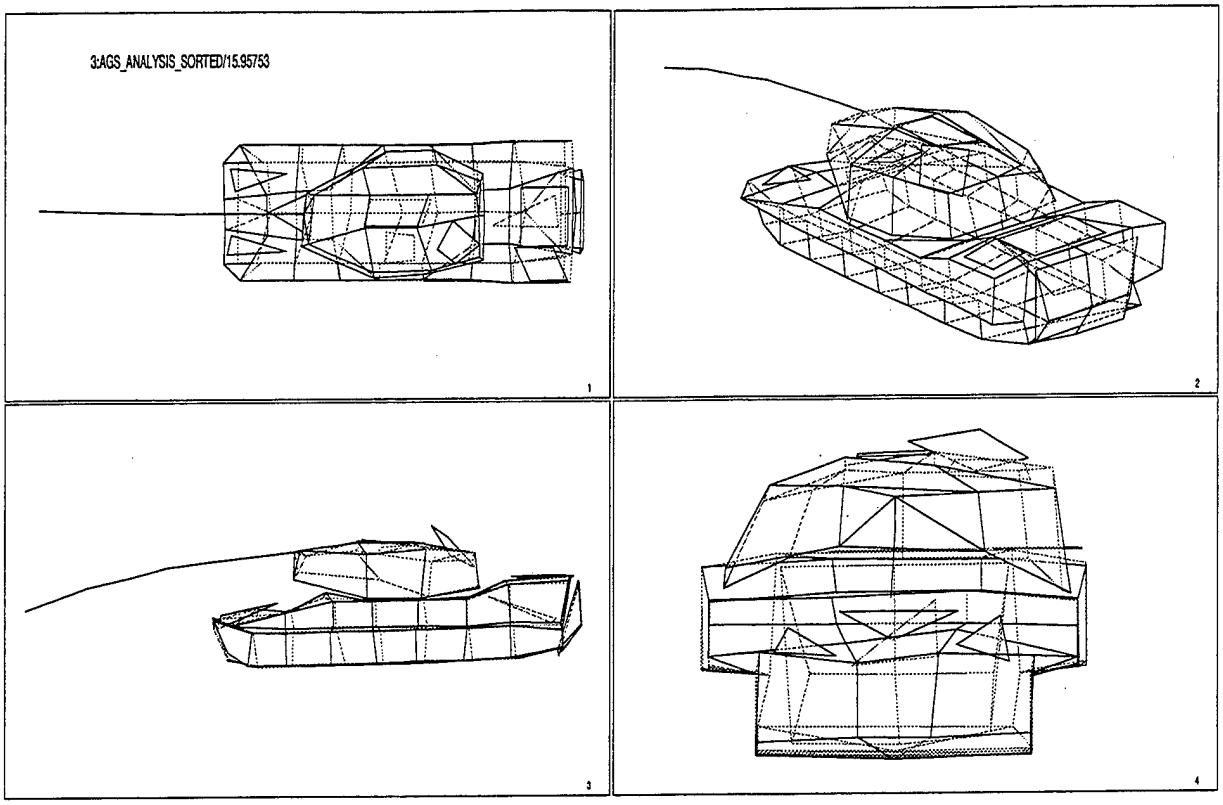
3:AGS_ANALYSIS_SORTED/15.95753
1
2
3
4

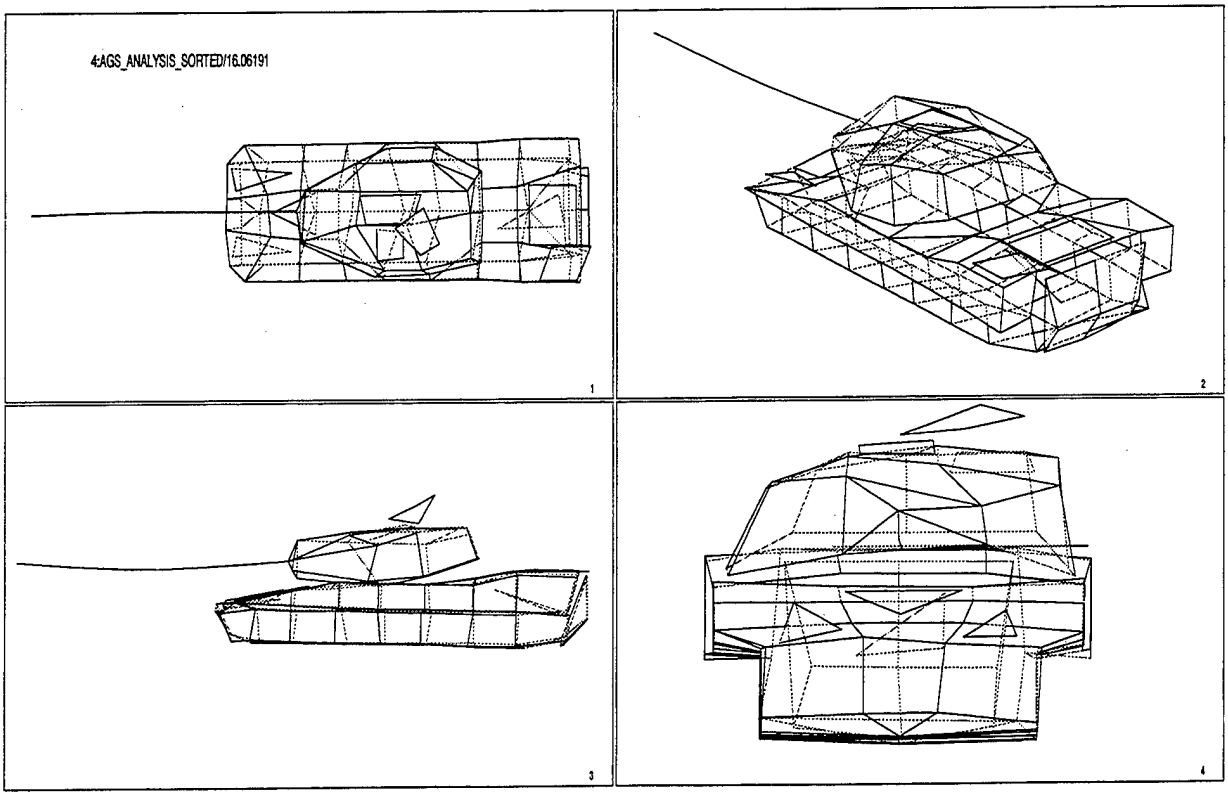
4:AGS_ANALYSIS_SORTED/16.06191
1
2
3
4

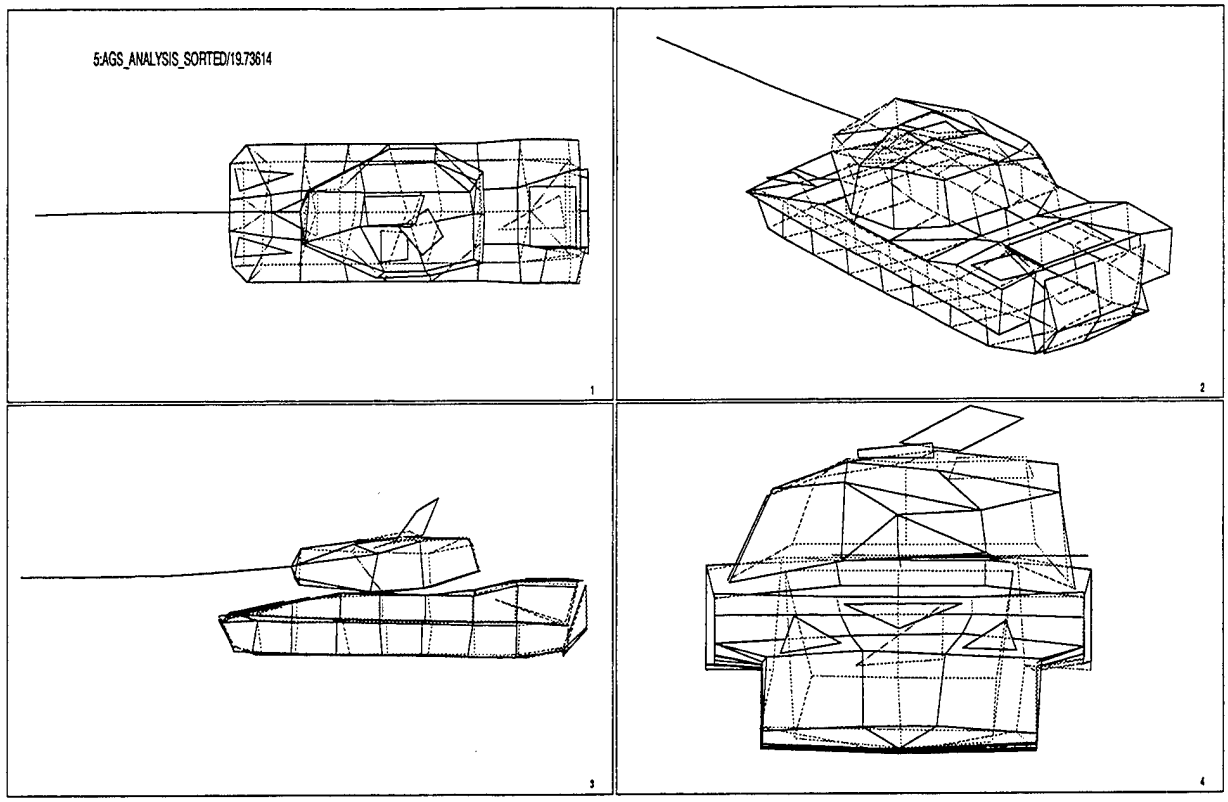
5:AGS_ANALYSIS_SORTED/19.73614
1
2
3
4

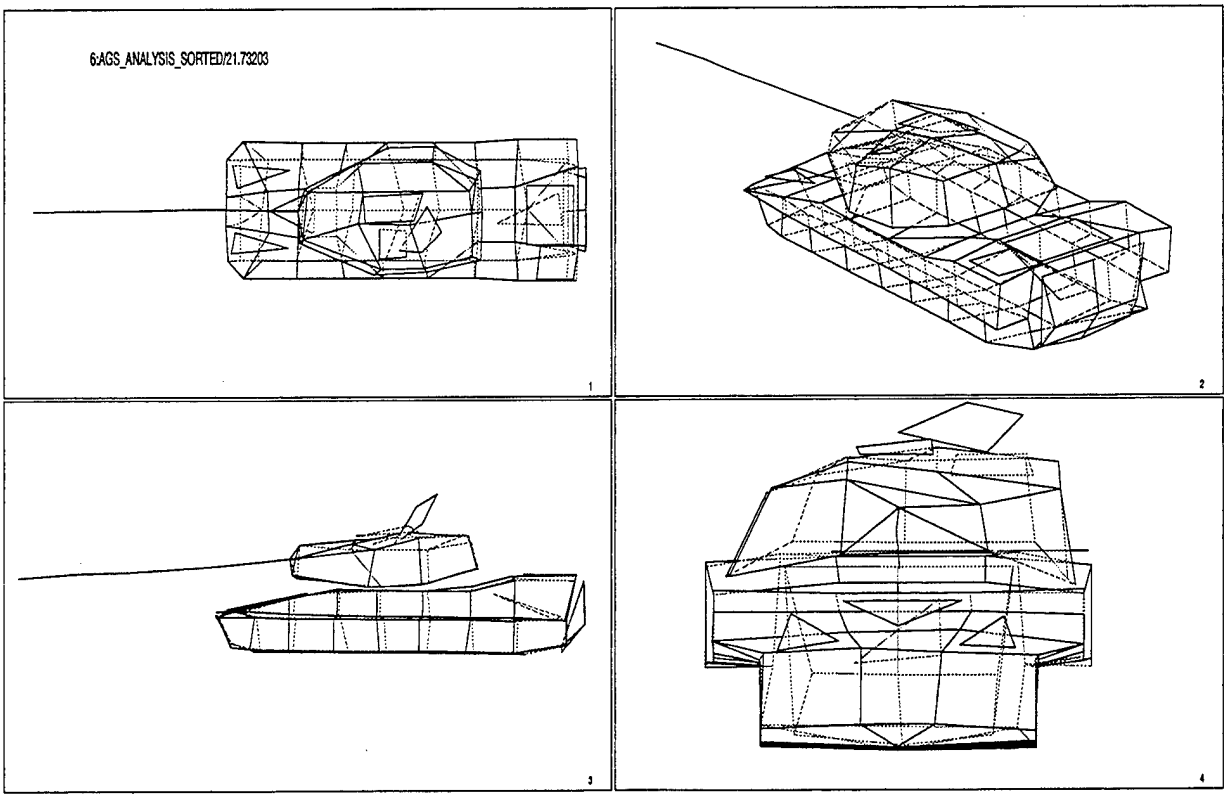
6:AGS_ANALYSIS_SORTED/21.73203
1
2
3
4

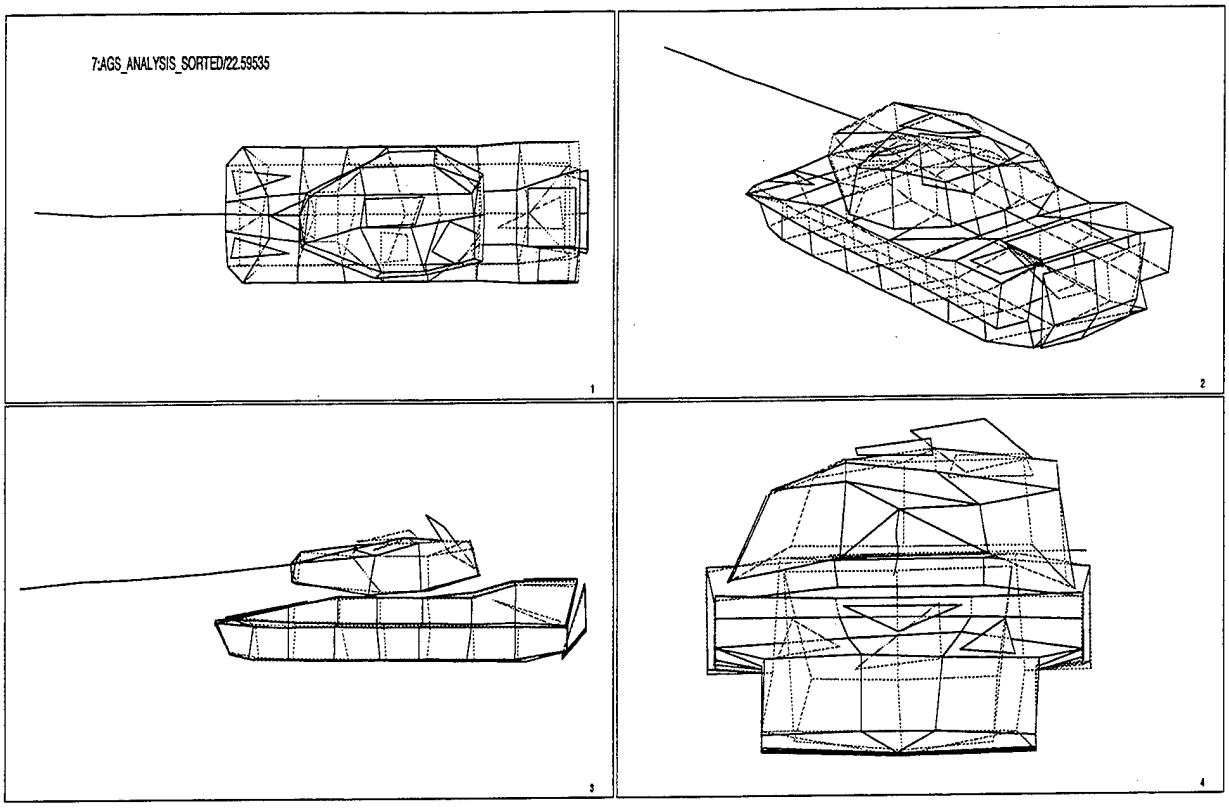
7:AGS_ANALYSIS_SORTED/22.59535
1
2
3
4

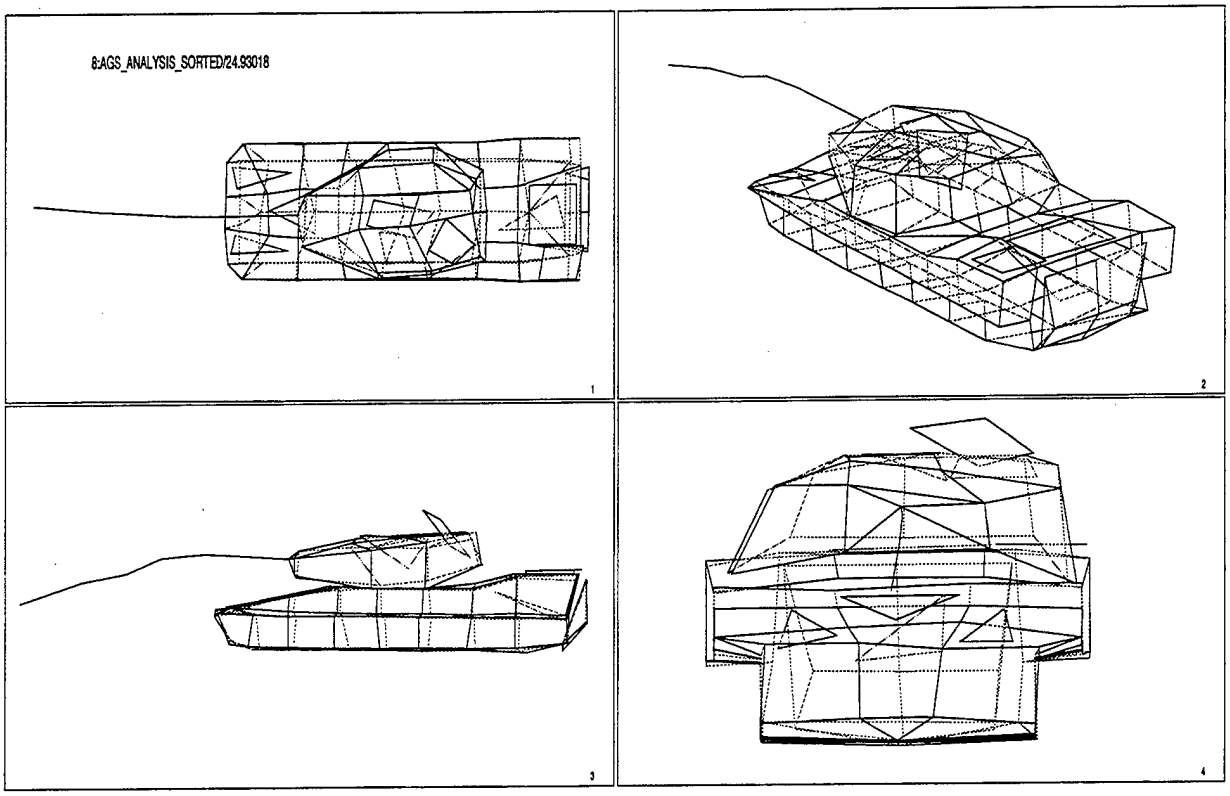
8:AGS_ANALYSIS_SORTED/24.93018
1
2
3
4

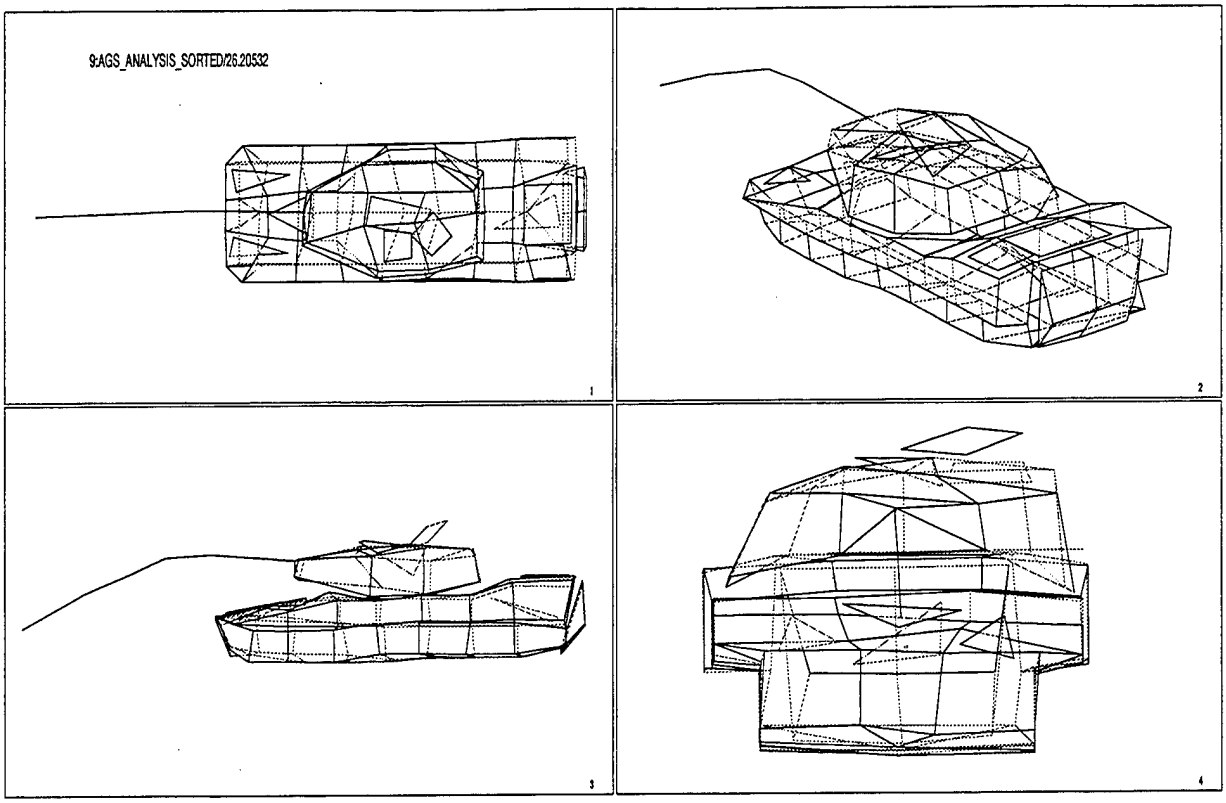
9:AGS_ANALYSIS_SORTED/26.20532
1
2
3
4

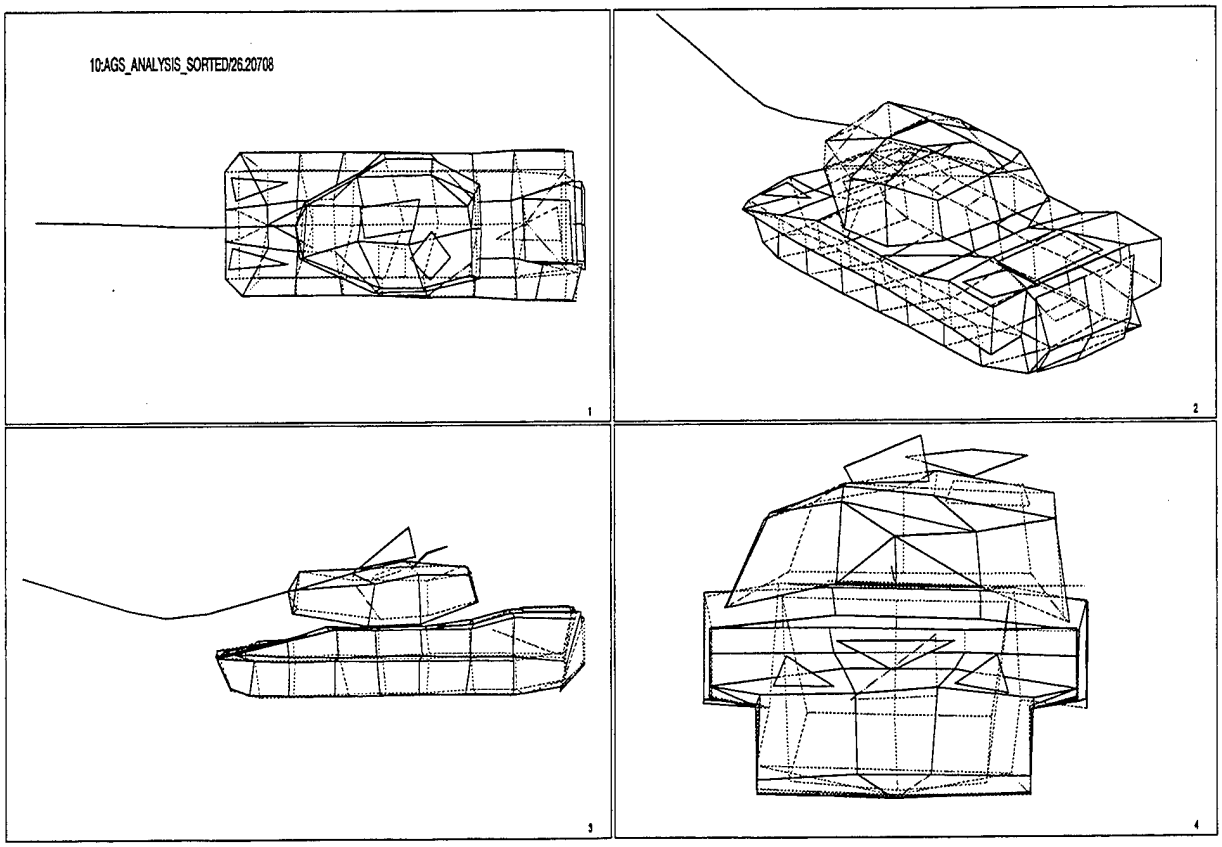
10:AGS_ANALYSIS_SORTED/26.20708
1
2
3
4

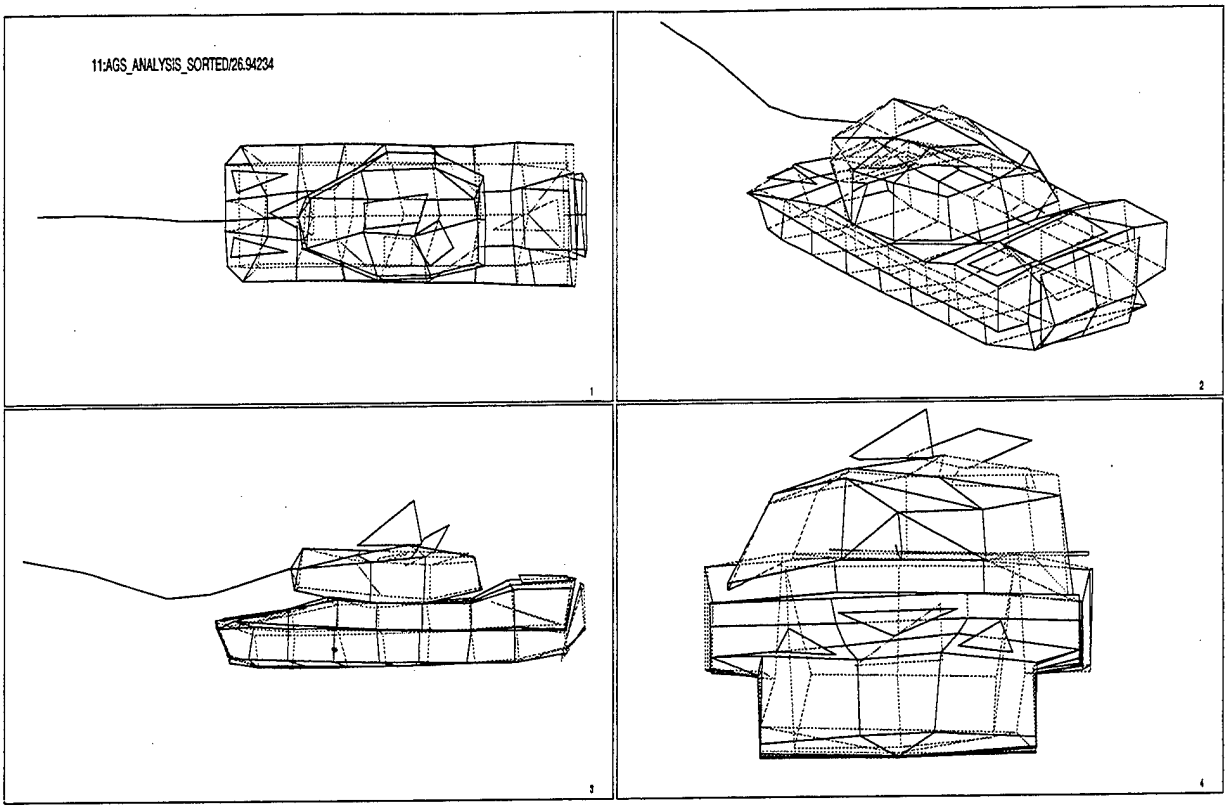
11:AGS_ANALYSIS_SORTED/26.94234
1
2
3
4

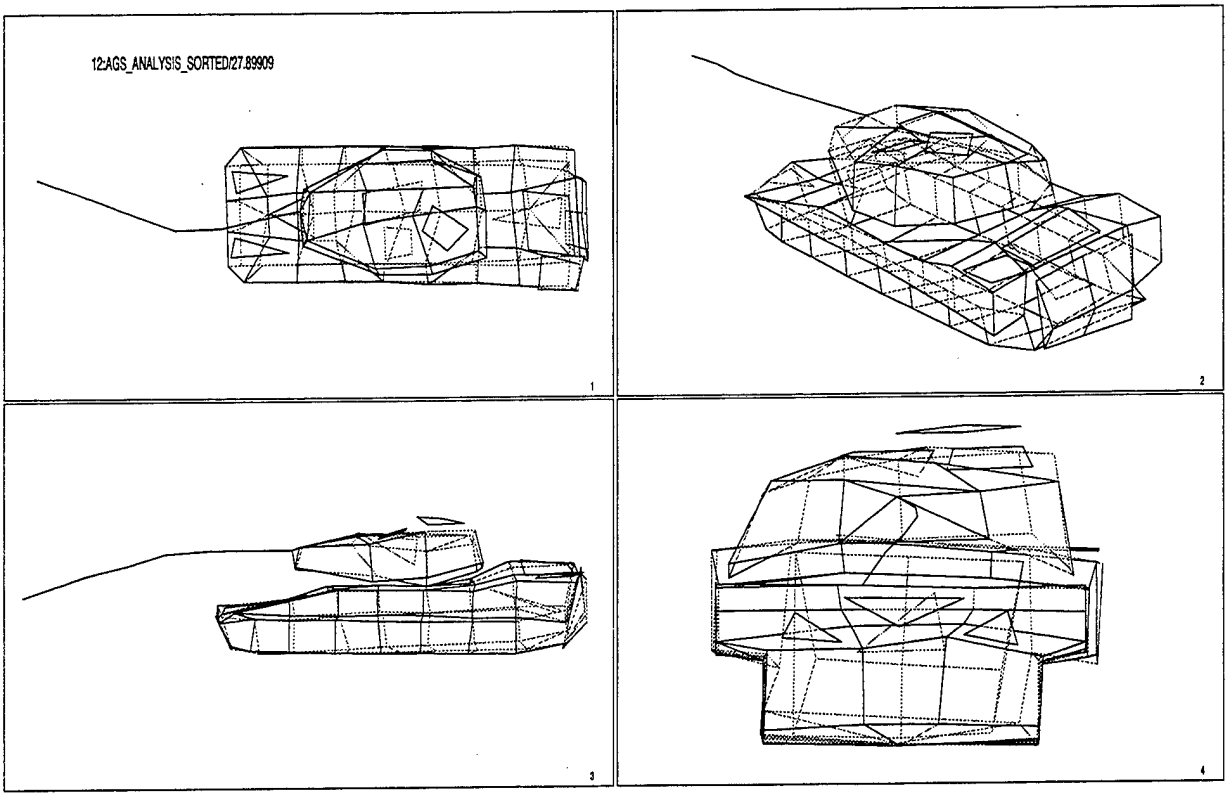
12:AGS_ANALYSIS_SORTED/27.89909
1
2
3
4

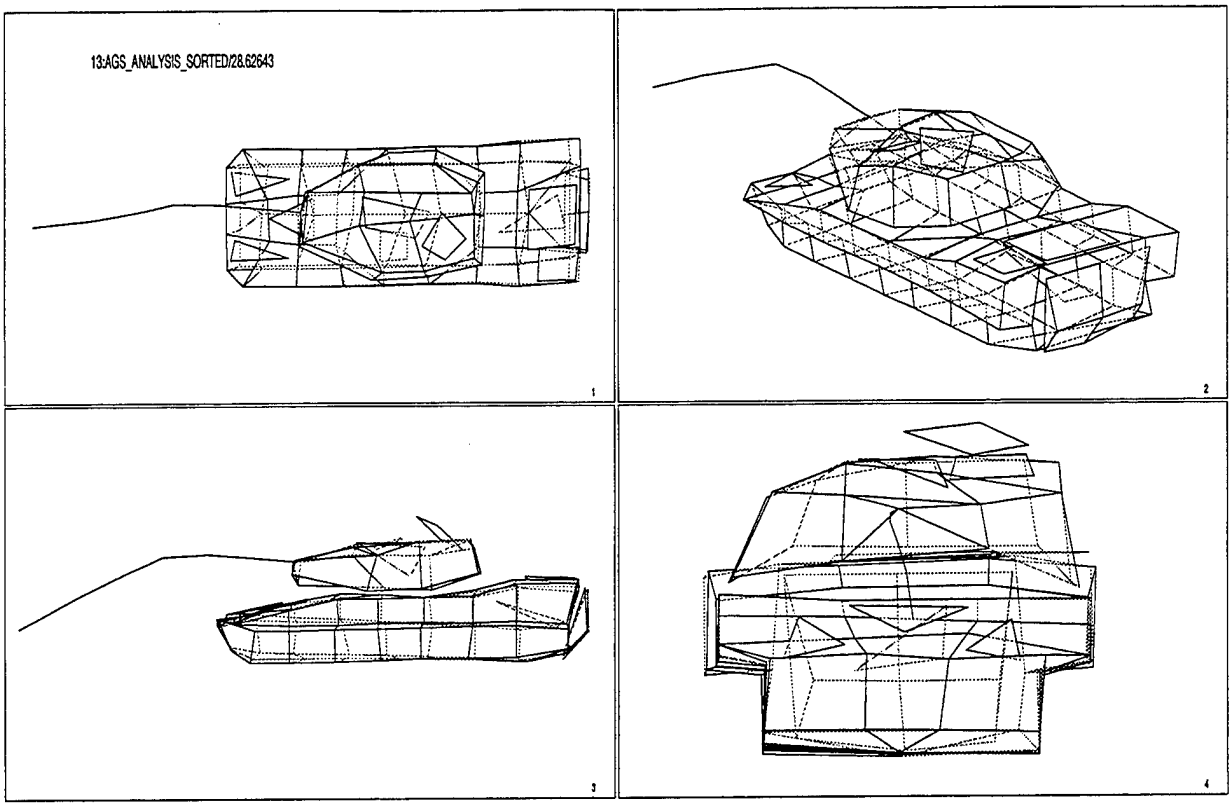
13:AGS_ANALYSIS_SORTED/28.62643
1
2
3
4

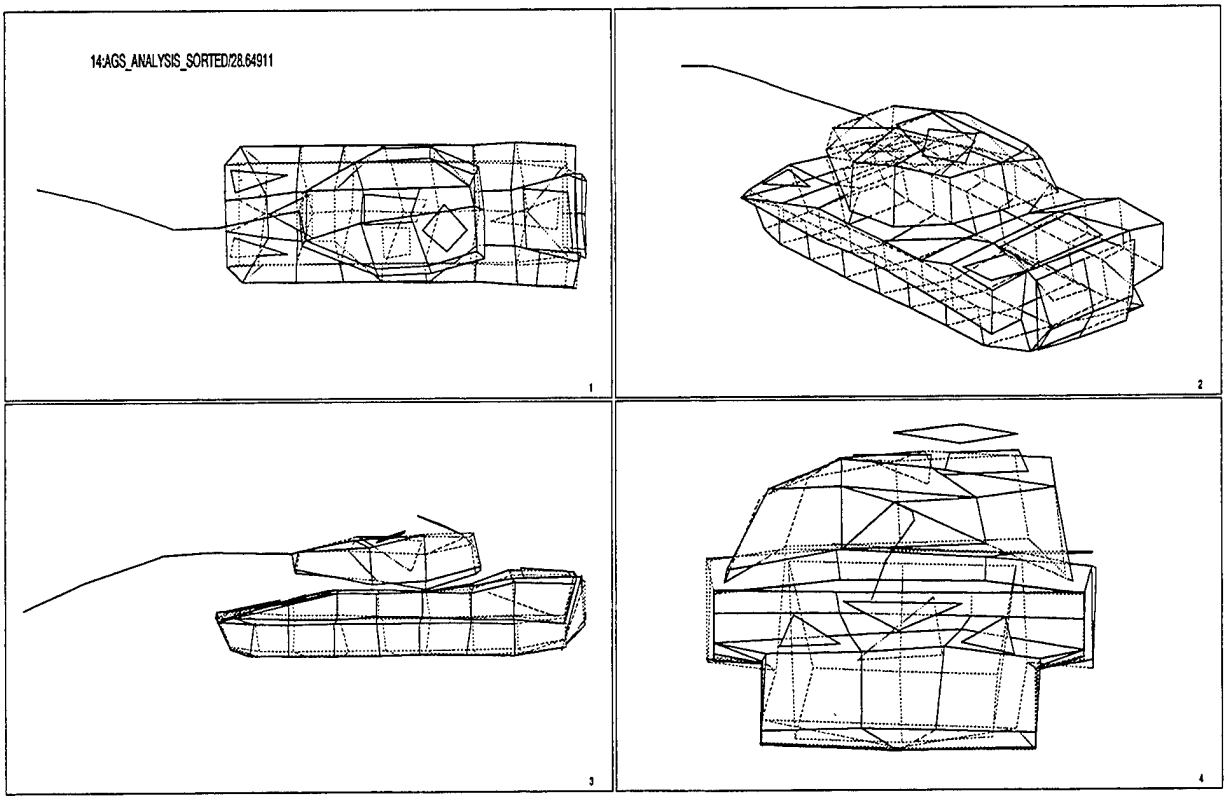
14:AGS_ANALYSIS_SORTED/28.64911
1
2
3
4

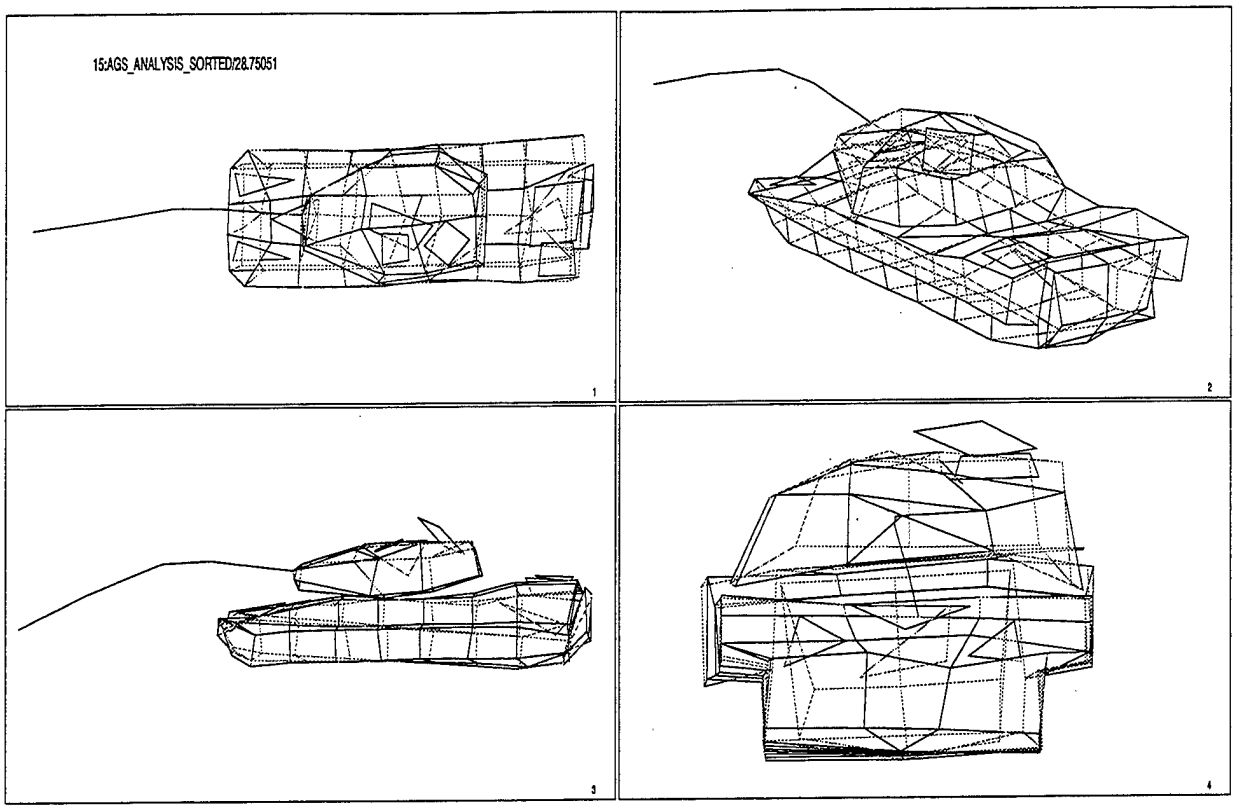
15:AGS_ANALYSIS_SORTED/28.75051
1
2
3
4

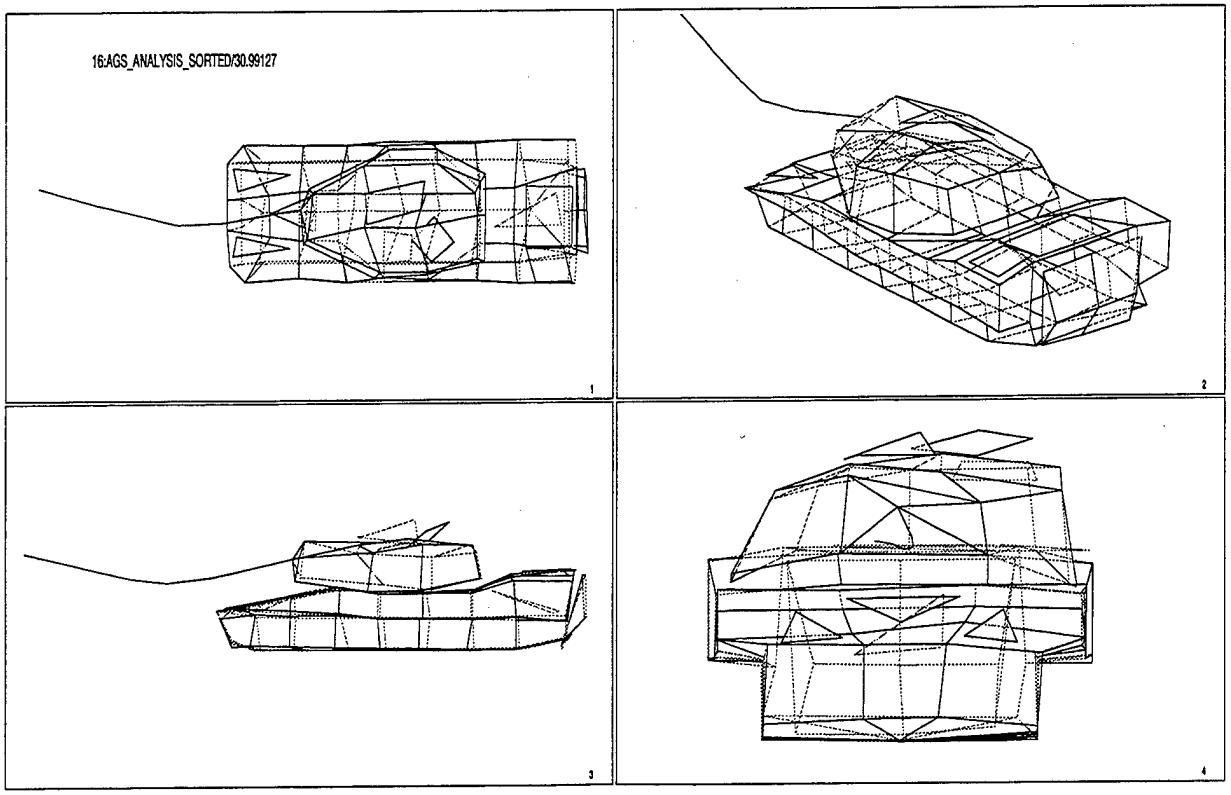
16:AGS_ANALYSIS_SORTED/30.99127
1
2
3
4

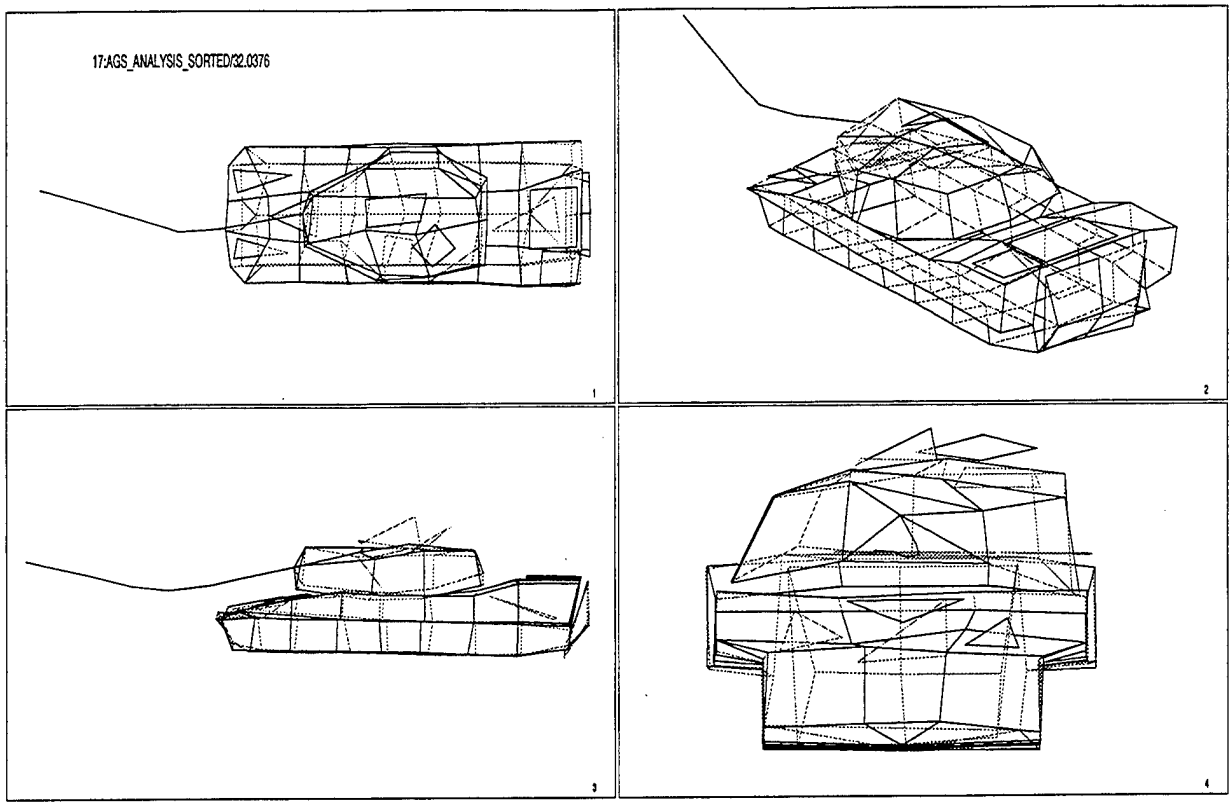
17:AGS_ANALYSIS_SORTED/32.0376
1
2
3
4

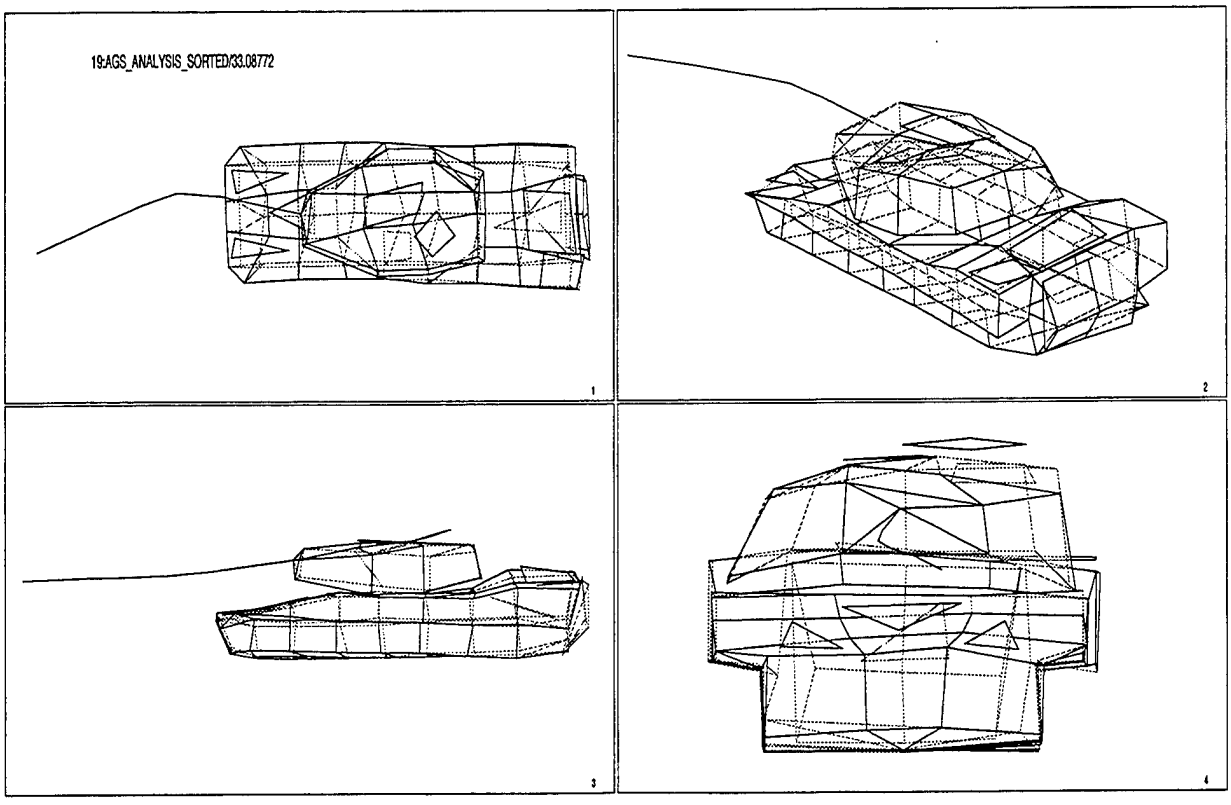
19:AGS_ANALYSIS_SORTED/33.08772
1
2
3
4

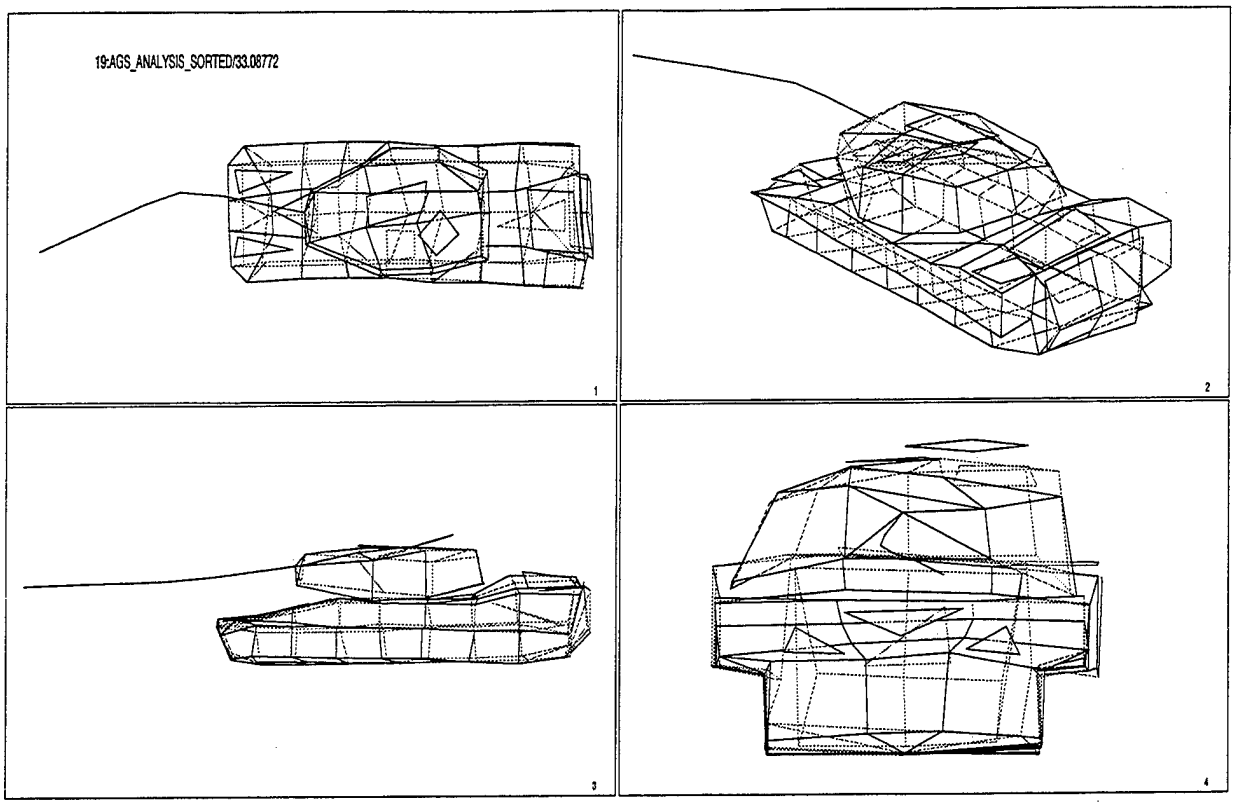
19:AGS_ANALYSIS_SORTED/33.08772
1
2
3
4

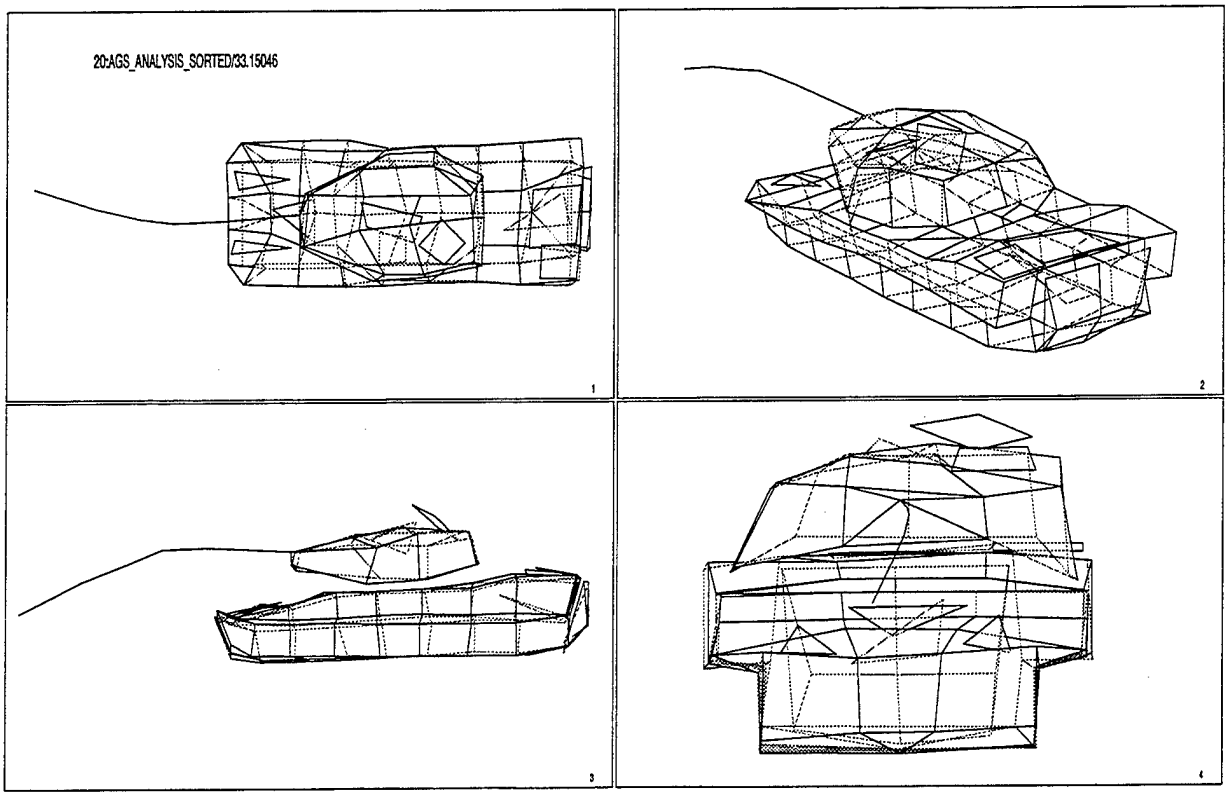
20:AGS_ANALYSIS_SORTED/33.15046
1
2
3
4

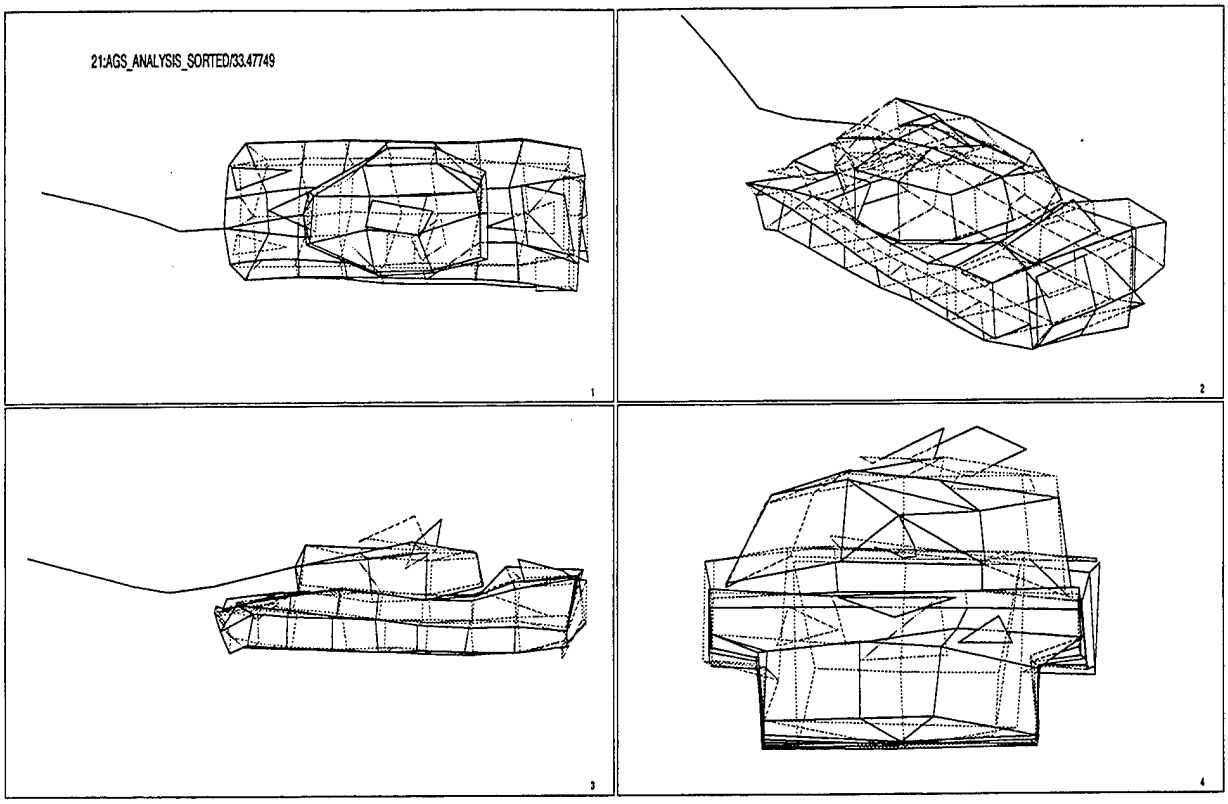
21:AGS_ANALYSIS_SORTED/33.47749
1
2
3
4

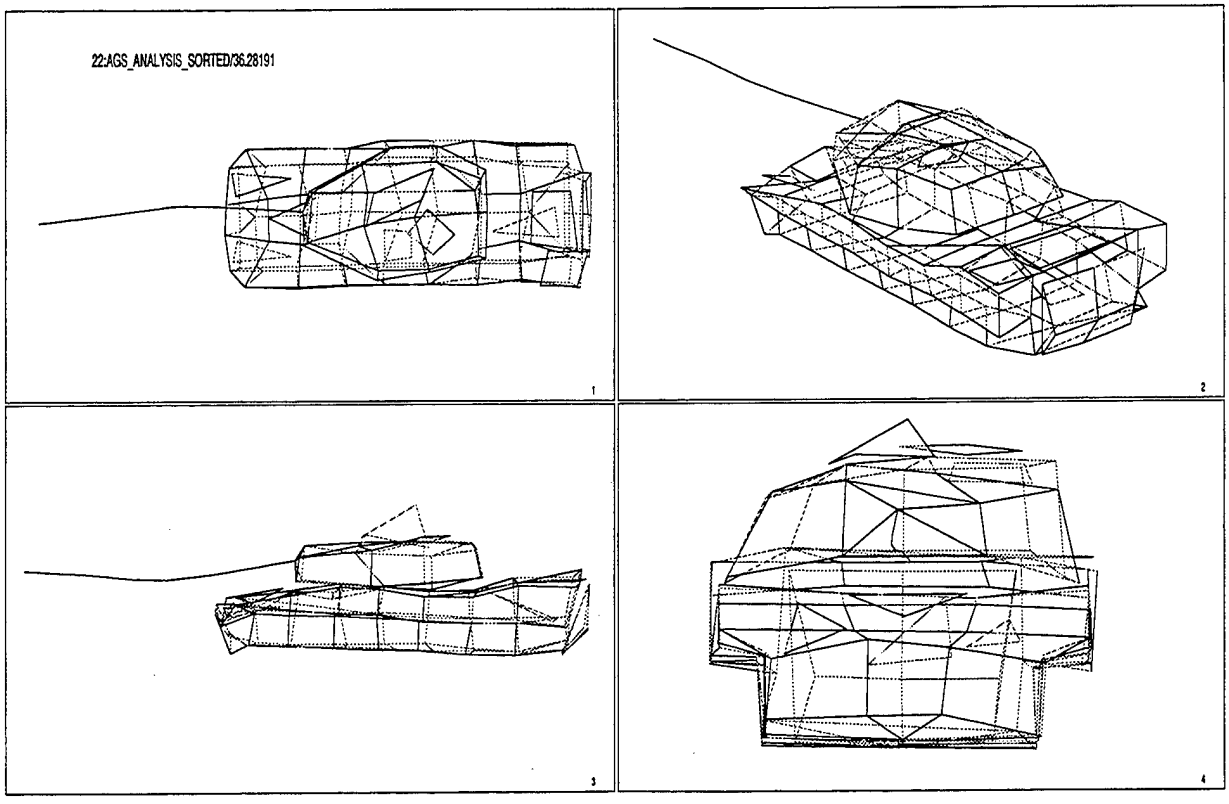
22:AGS_ANALYSIS_SORTED/36.28191
1
2
3
4

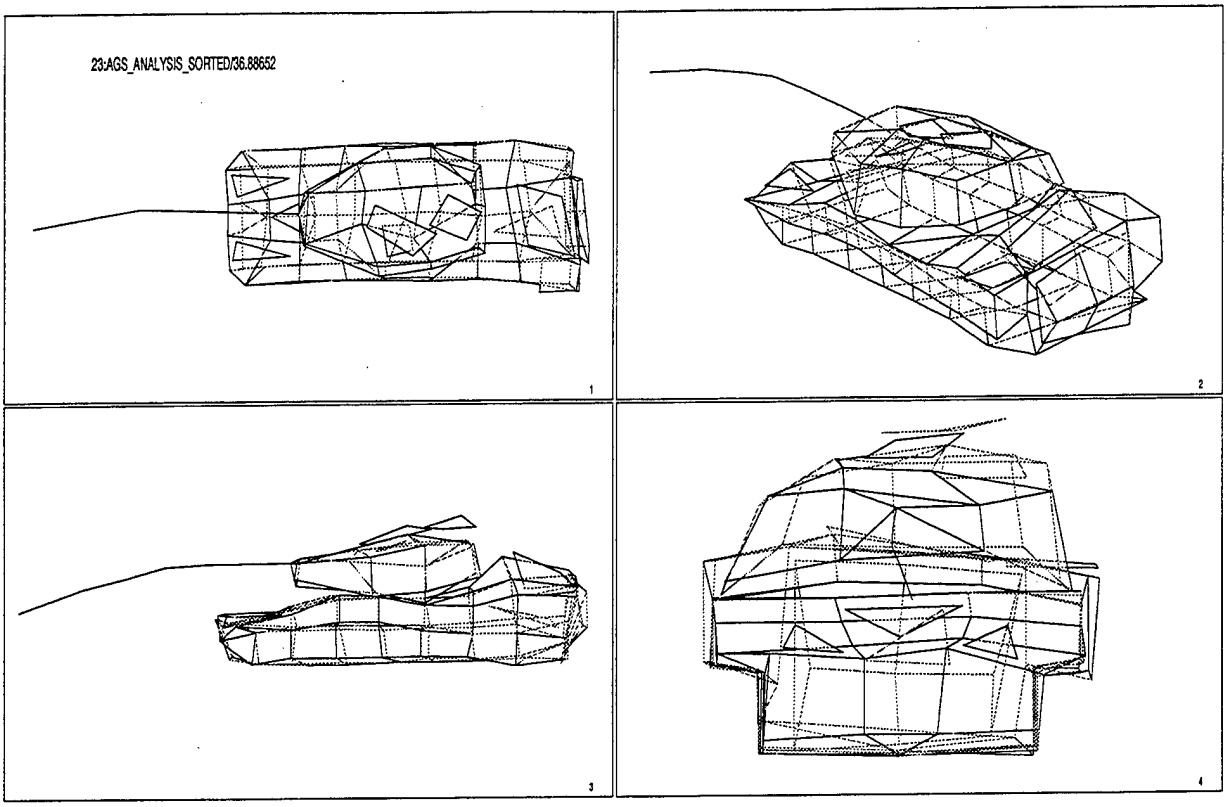
23:AGS_ANALYSIS_SORTED/36.88652
1
2
3
4

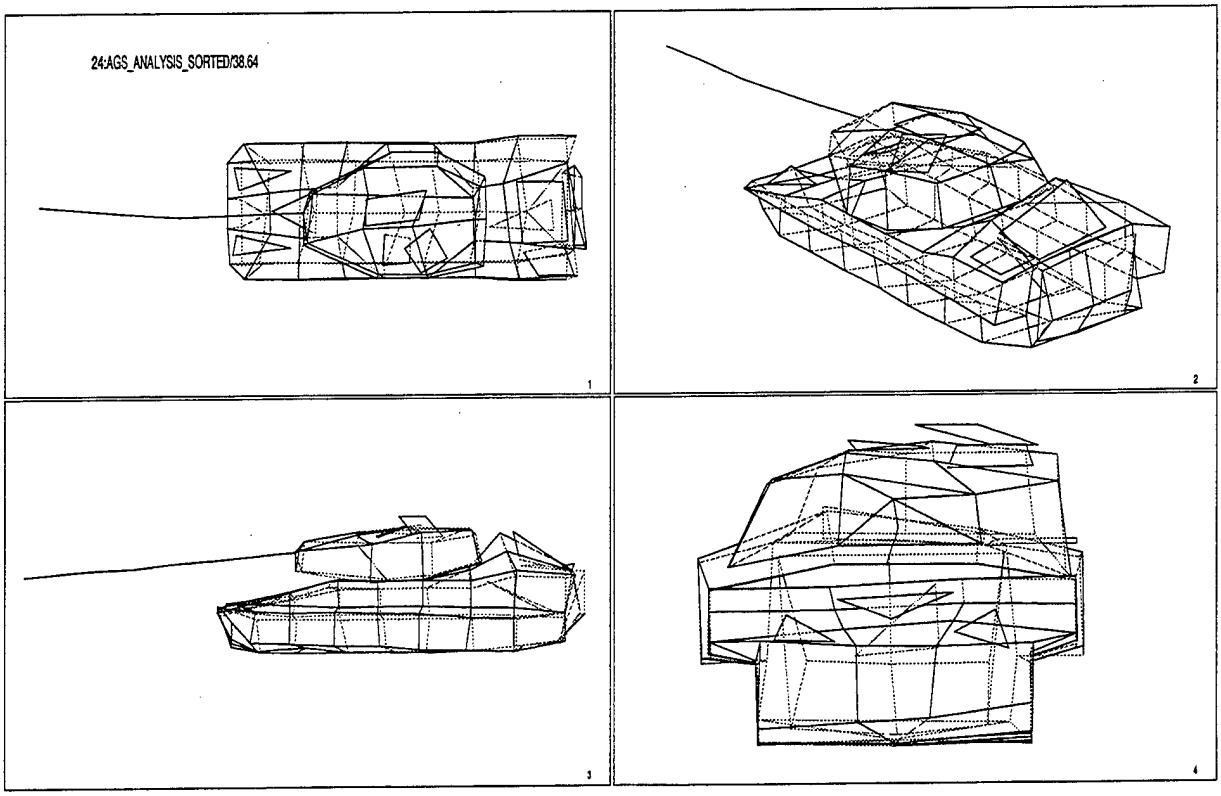
24:AGS_ANALYSIS_SORTED/38.64
1
2
3
4

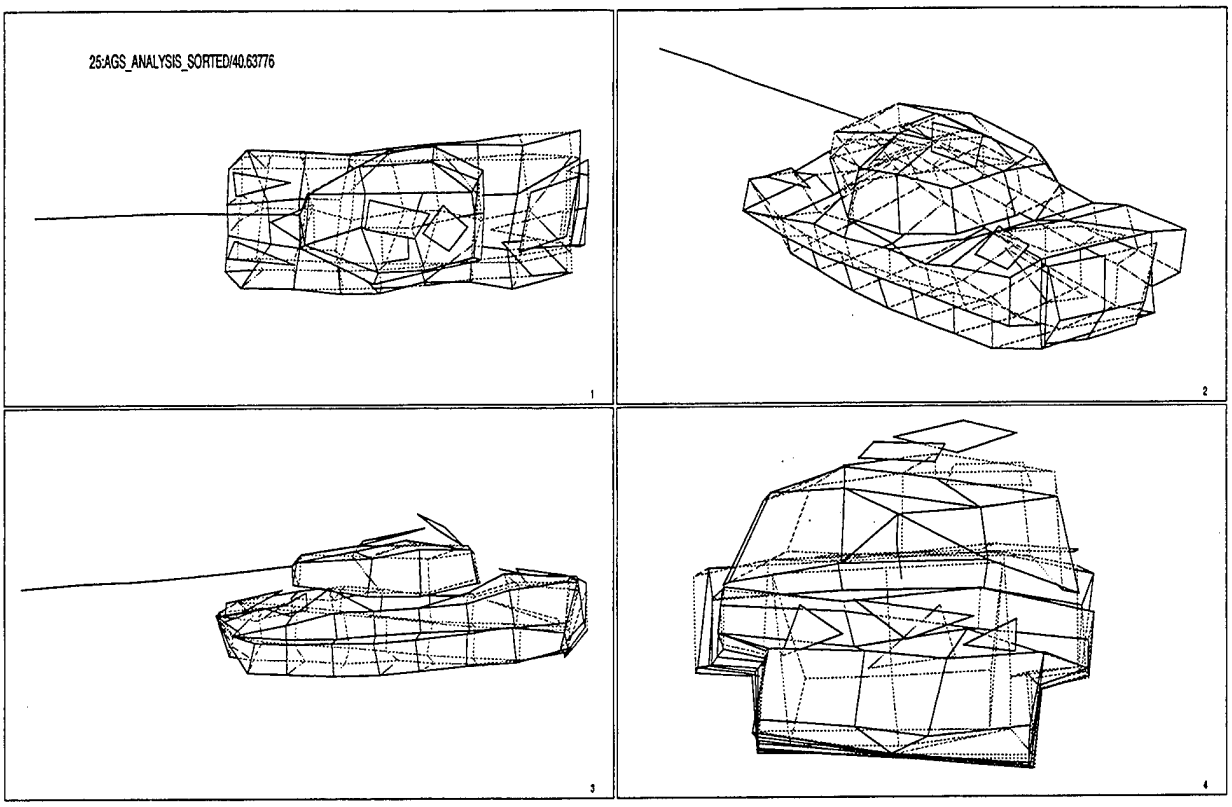
25:AGS_ANALYSIS_SORTED/40.63776
1
2
3
4

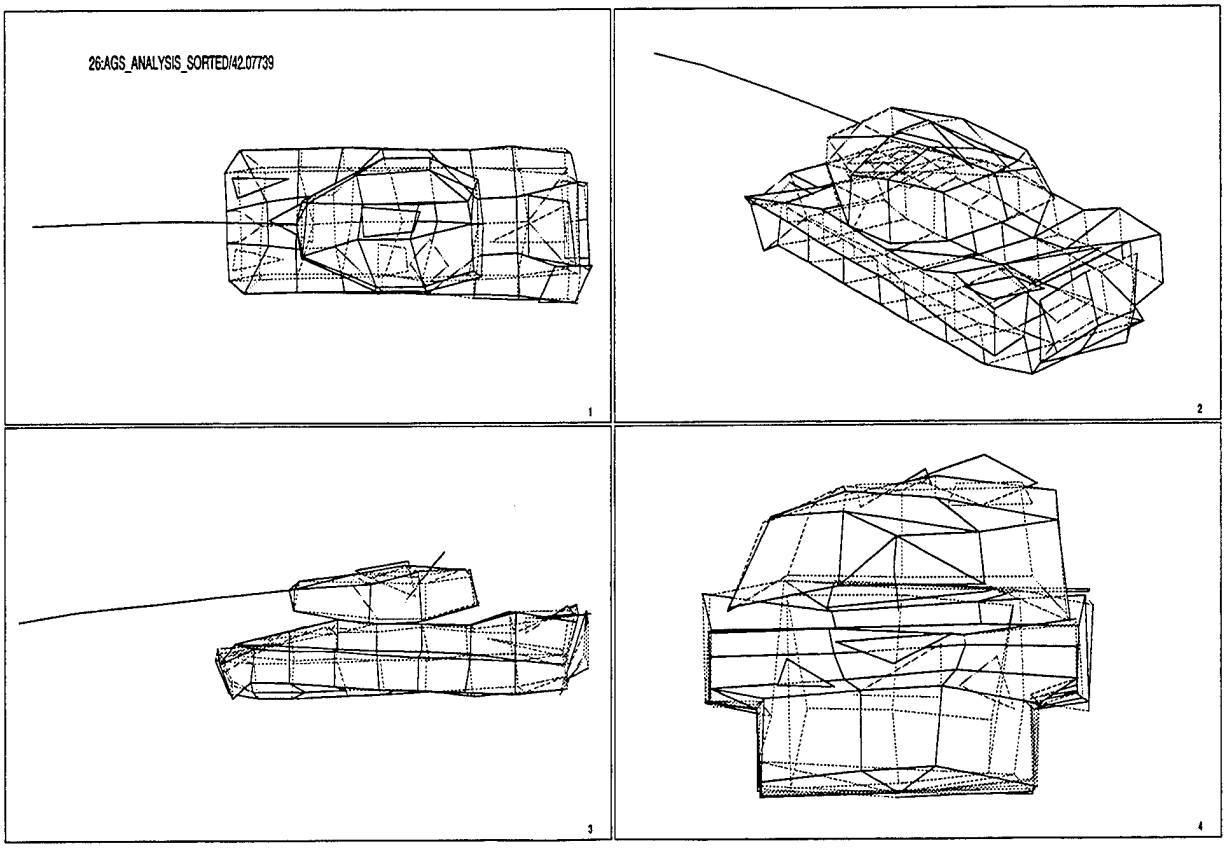
26:AGS_ANALYSIS_SORTED/42.07739
1
2
3
4

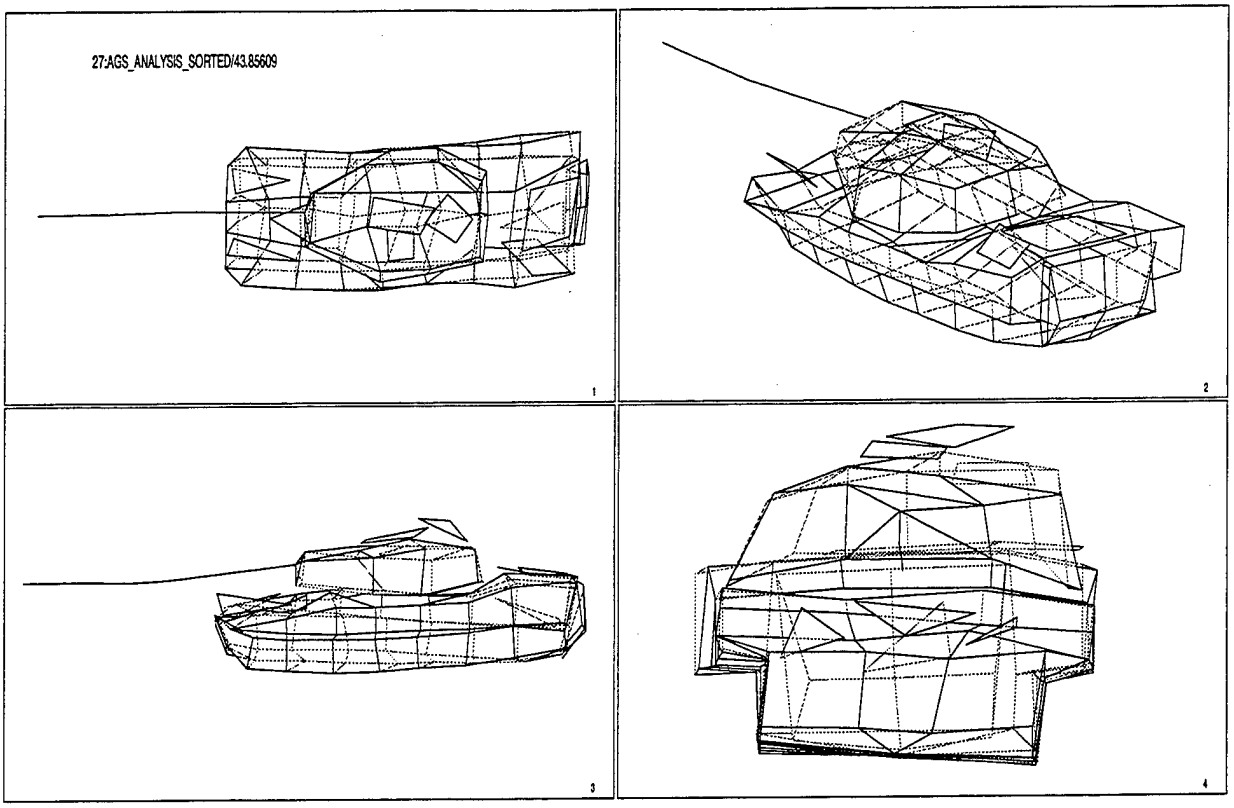
27:AGS_ANALYSIS_SORTED/43.85609
1
2
3
4

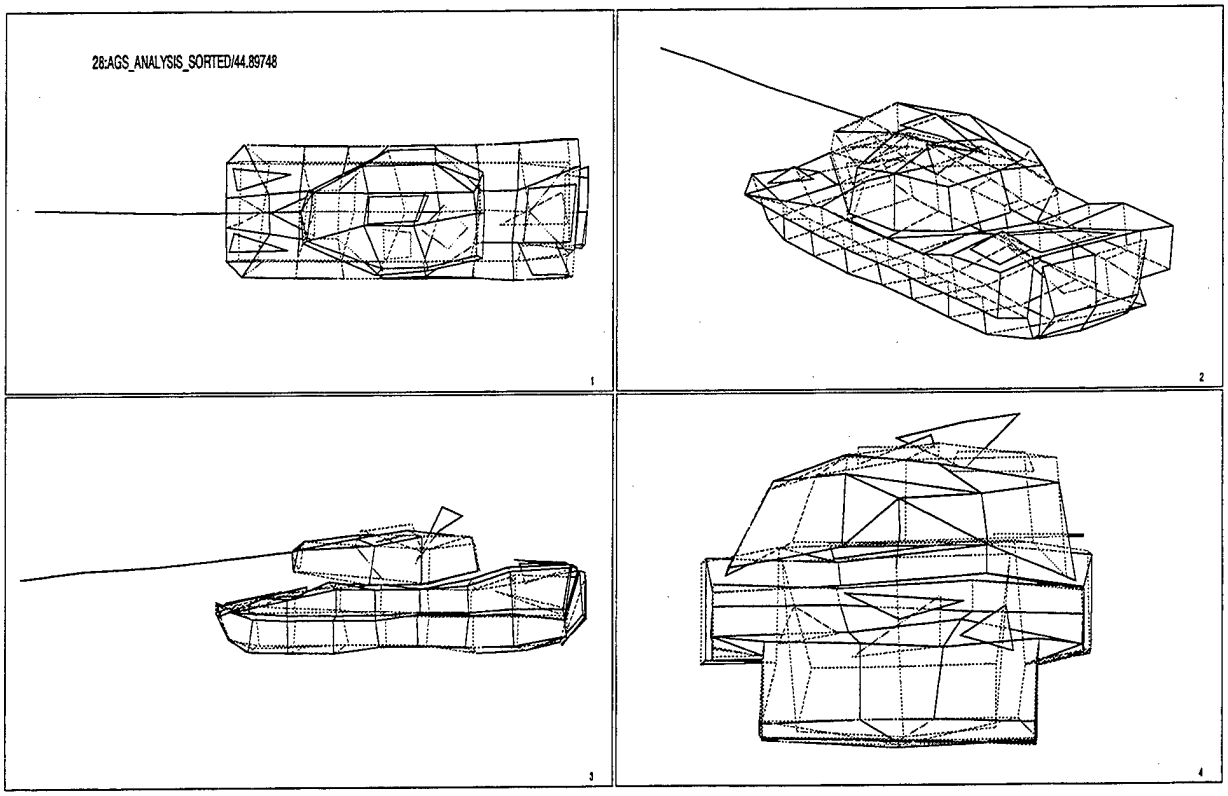
28:AGS_ANALYSIS_SORTED/44.89748
1
2
3
4

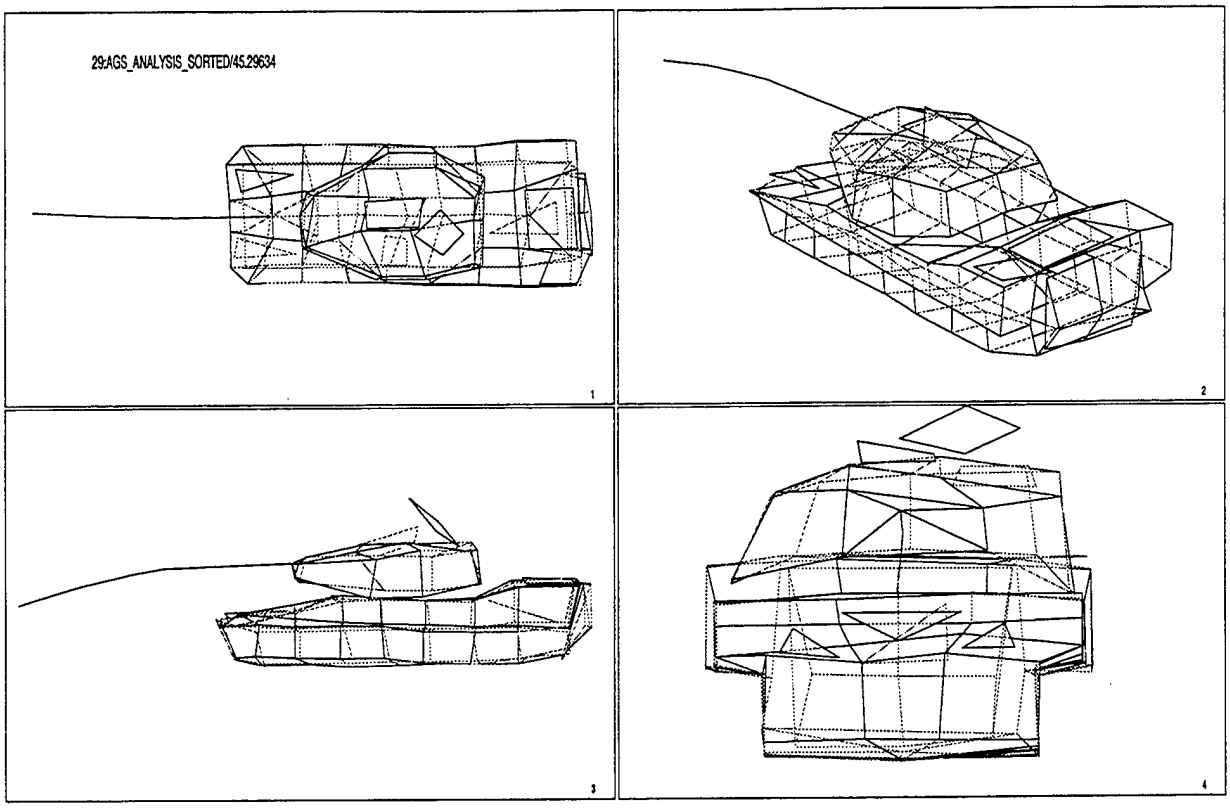
29:AGS_ANALYSIS_SORTED/45.29634
1
2
3
4

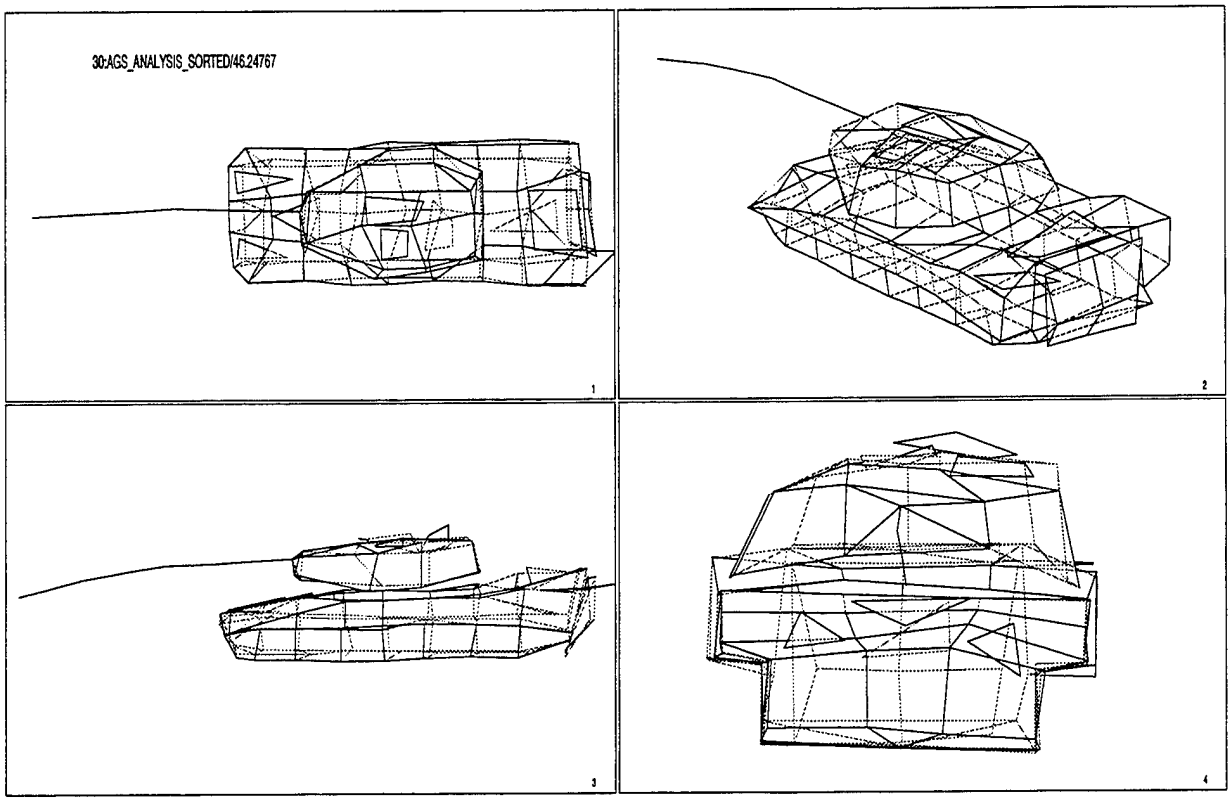
30:AGS_ANALYSIS_SORTED/46.24767
1
2
3
4

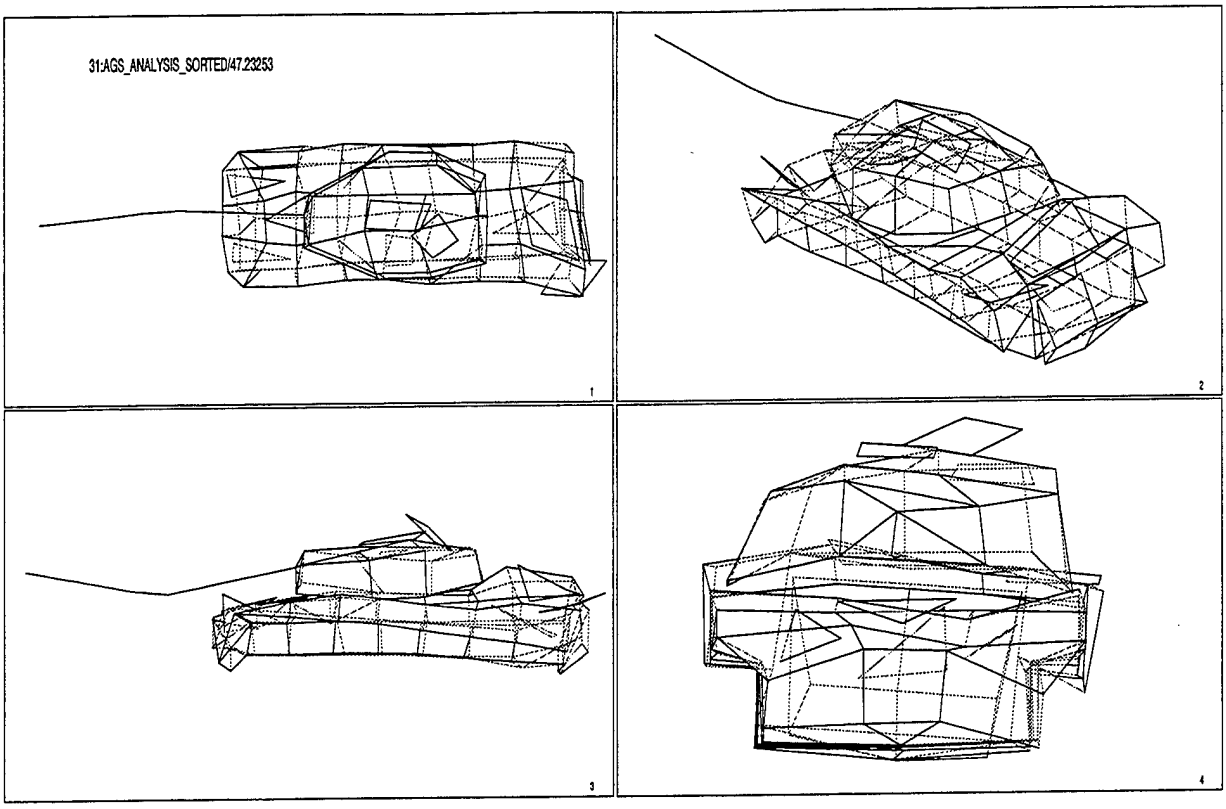
31:AGS_ANALYSIS_SORTED/47.23253
1
2
3
4

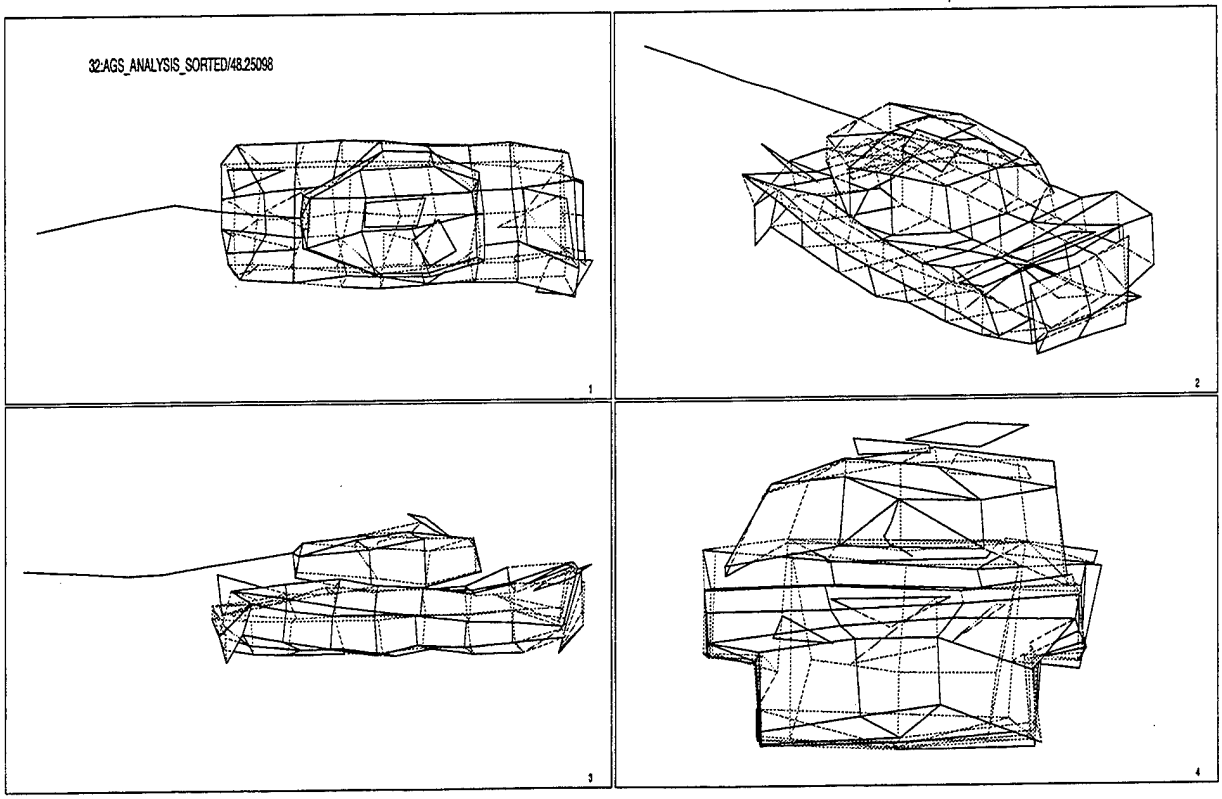
32:AGS_ANALYSIS_SORTED/48.25098
1
2
3
4

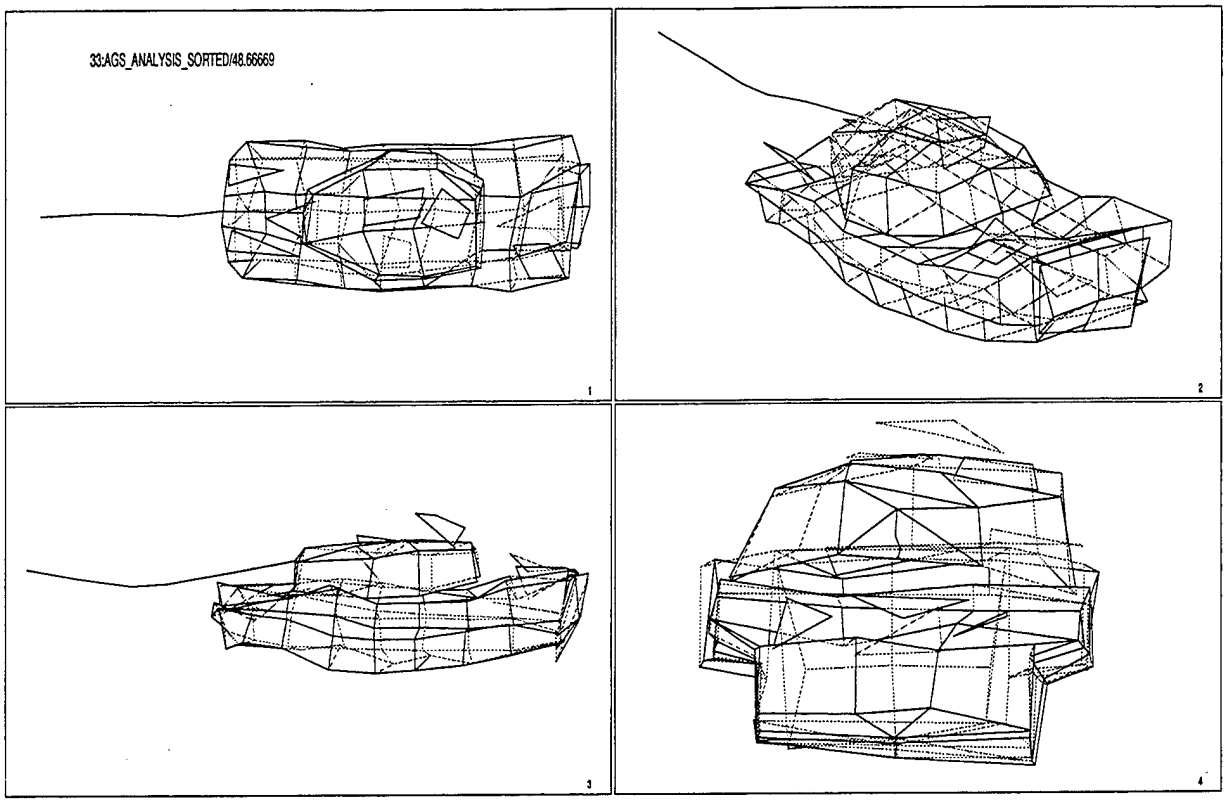
33:AGS_ANALYSIS_SORTED/48.66669
1
2
3
4

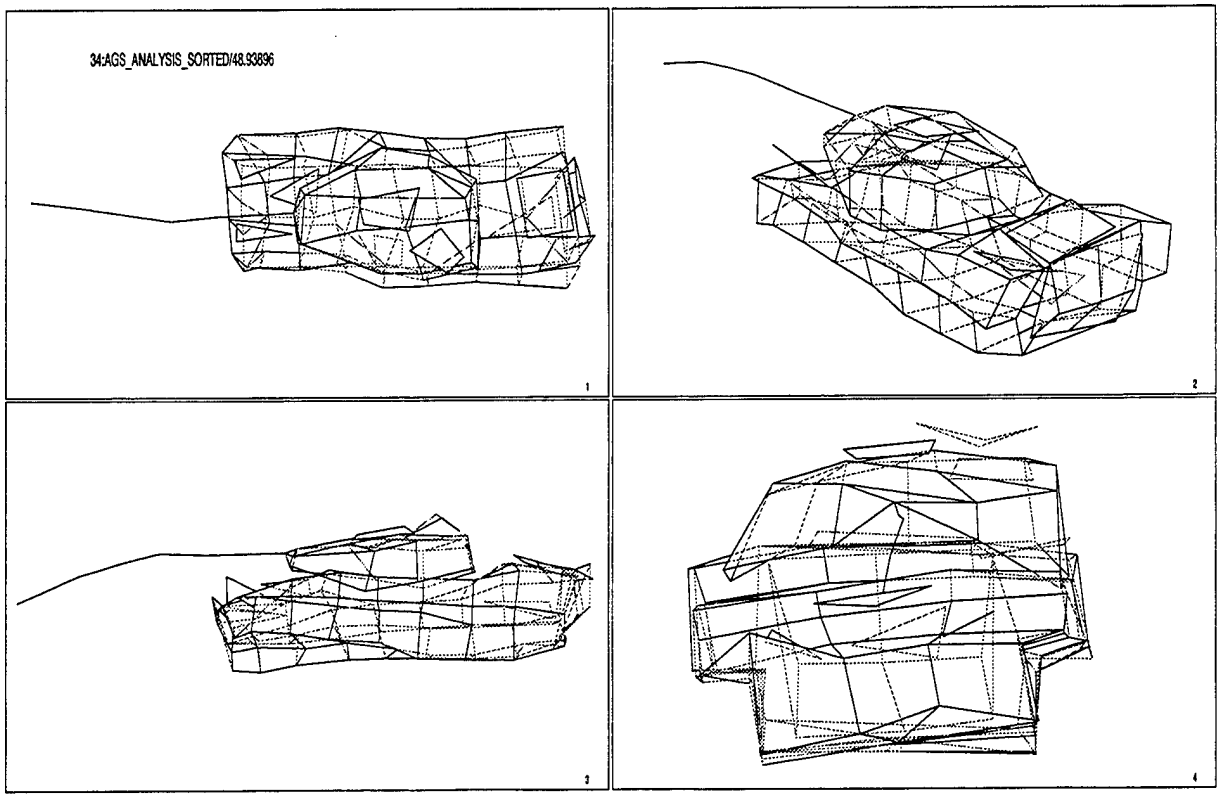
34:AGS_ANALYSIS_SORTED/48.93896
1
2
3
4

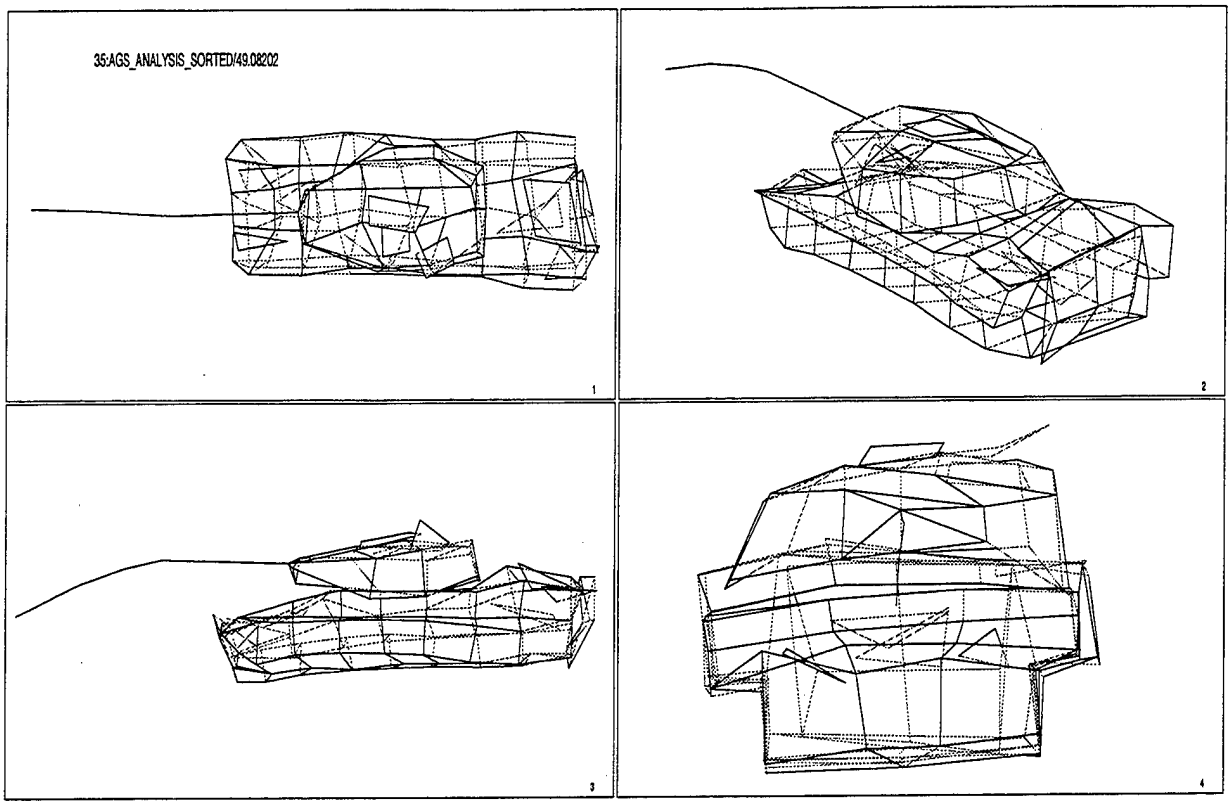
35:AGS_ANALYSIS_SORTED/49.08202
1
2
3
4

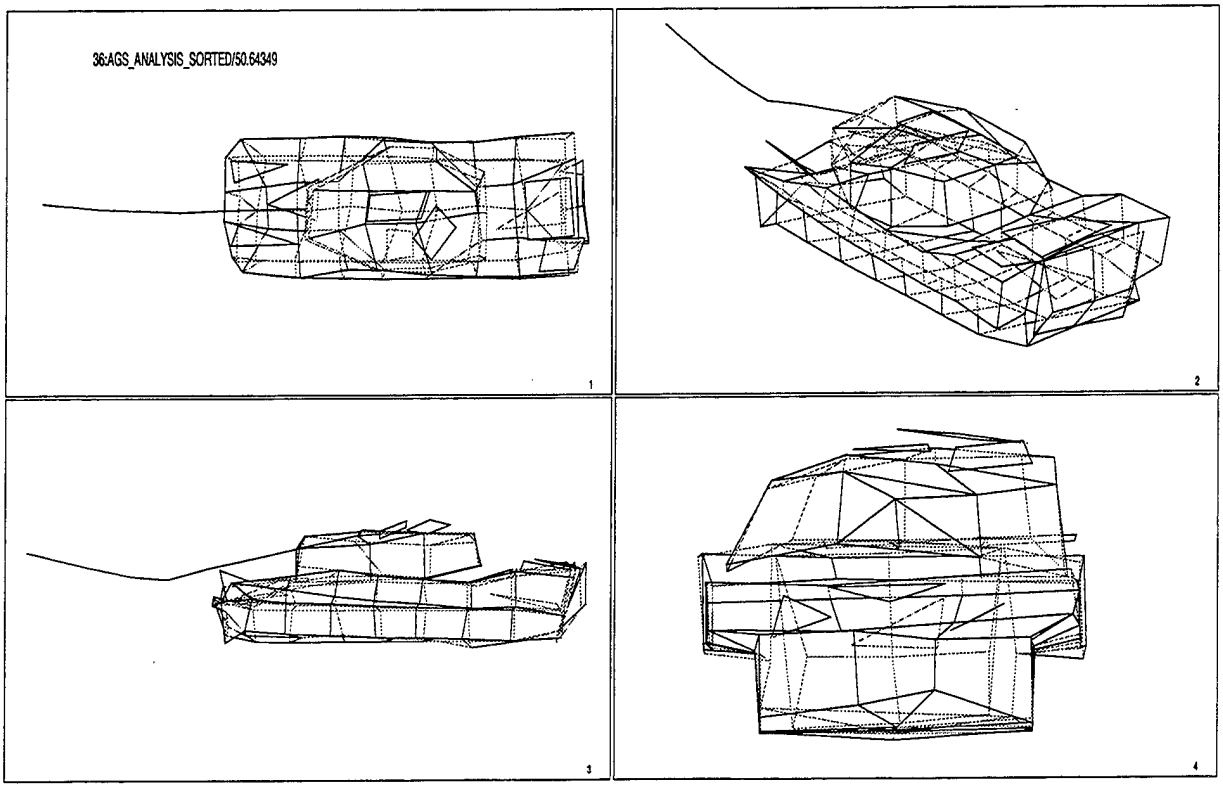
36:AGS_ANALYSIS_SORTED/50.64349
1
2
3
4

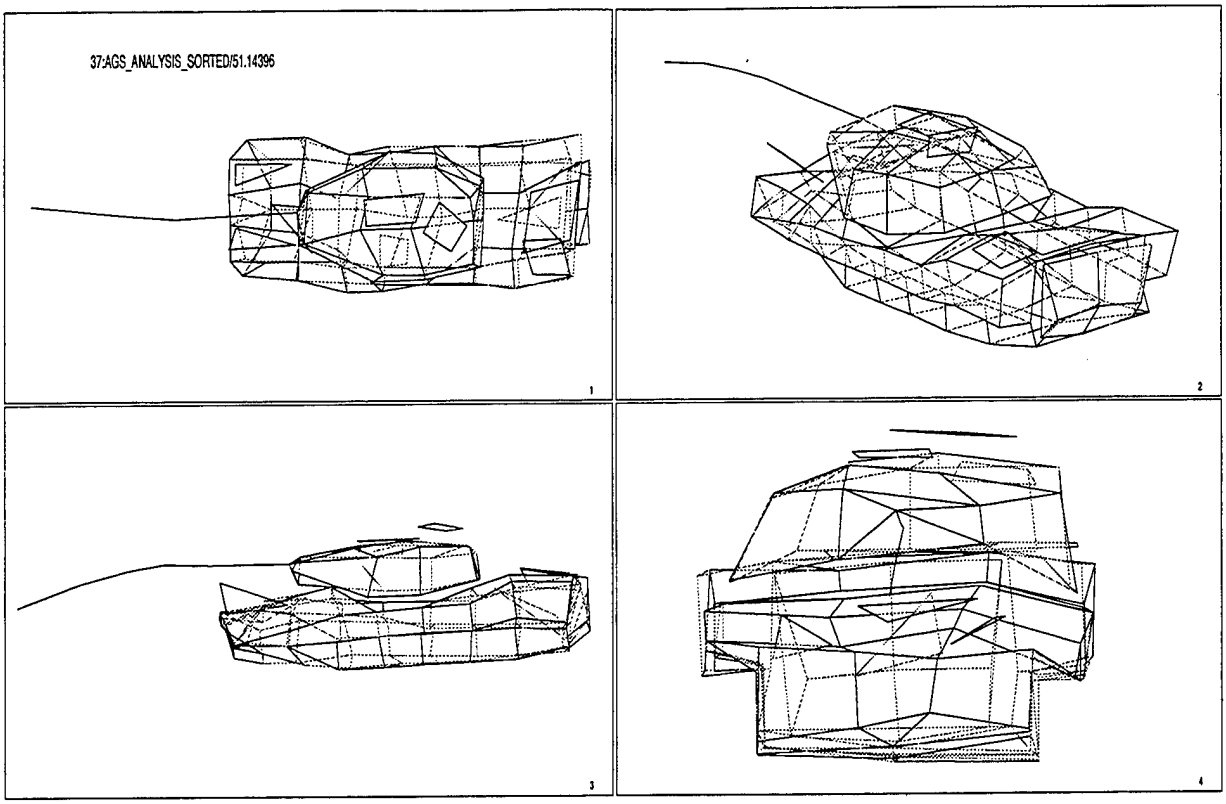
37:AGS_ANALYSIS_SORTED/51.14396
1
2
3
4

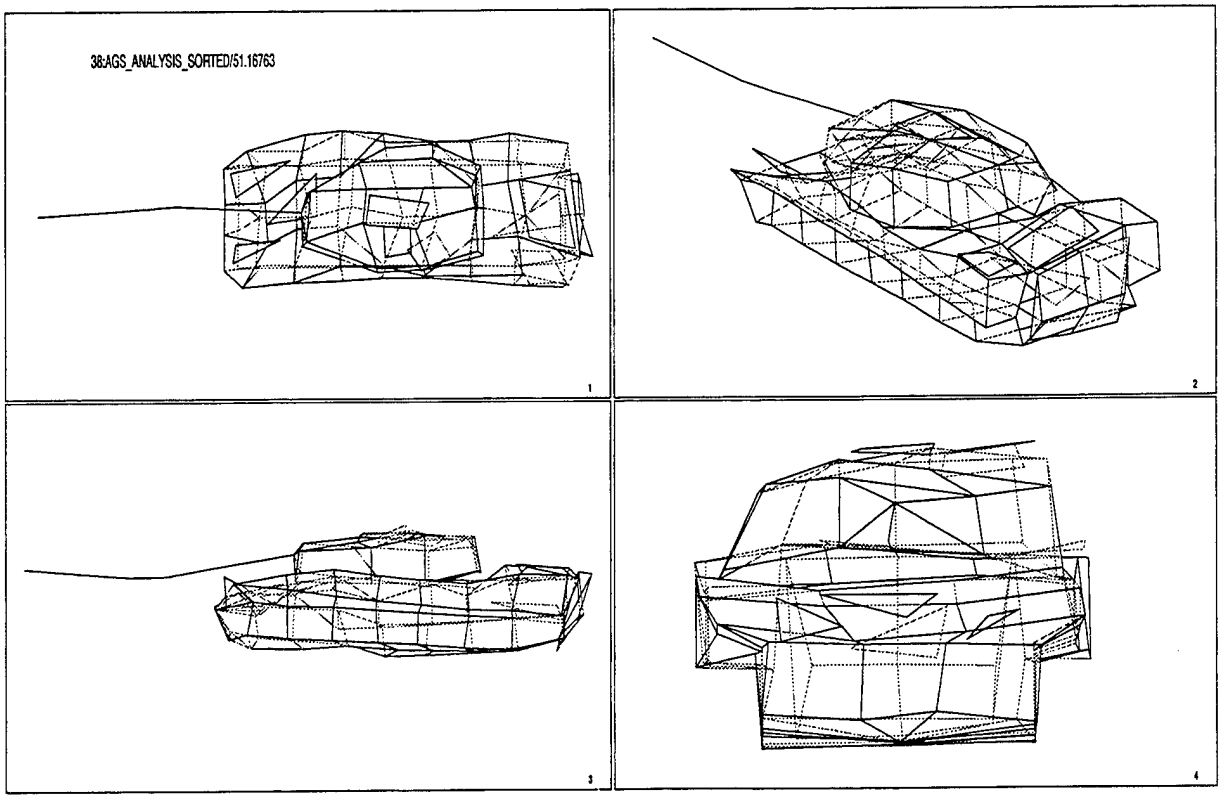
38:AGS_ANALYSIS_SORTED/51.16763
1
2
3
4

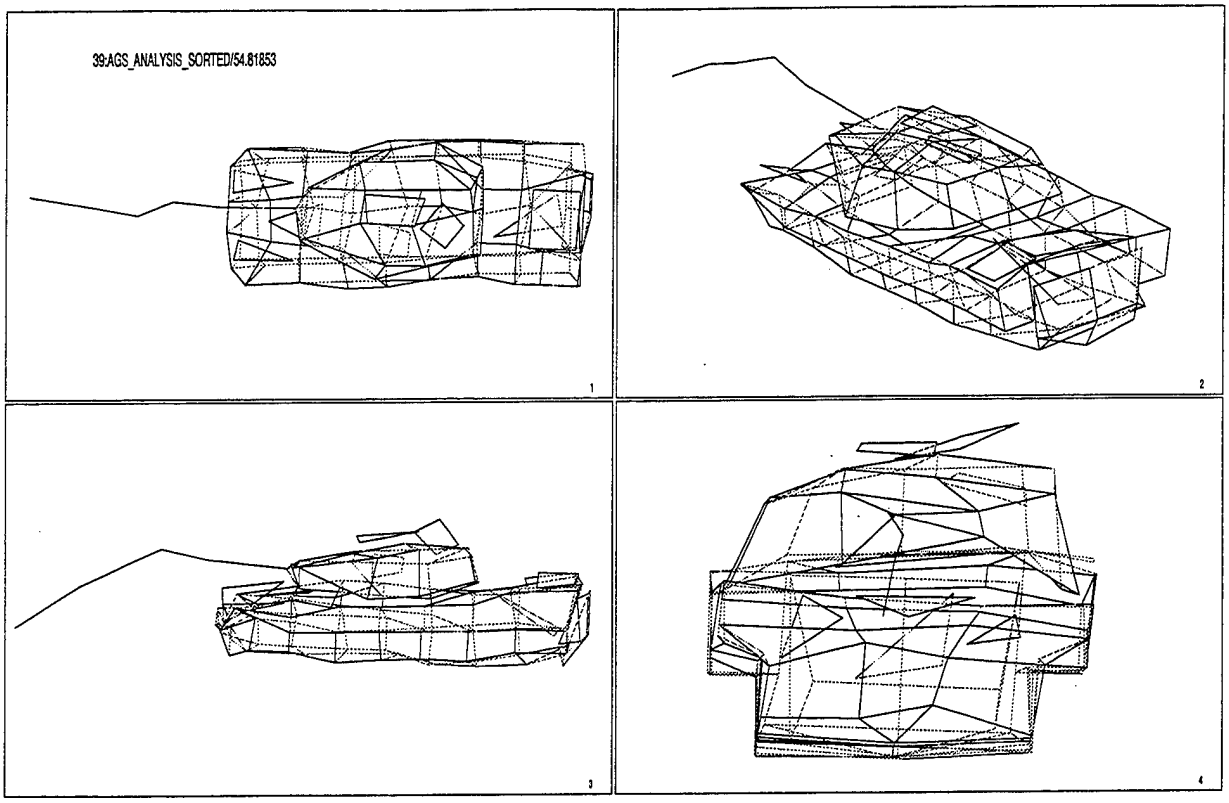
39:AGS_ANALYSIS_SORTED/54.81853
1
2
3
4

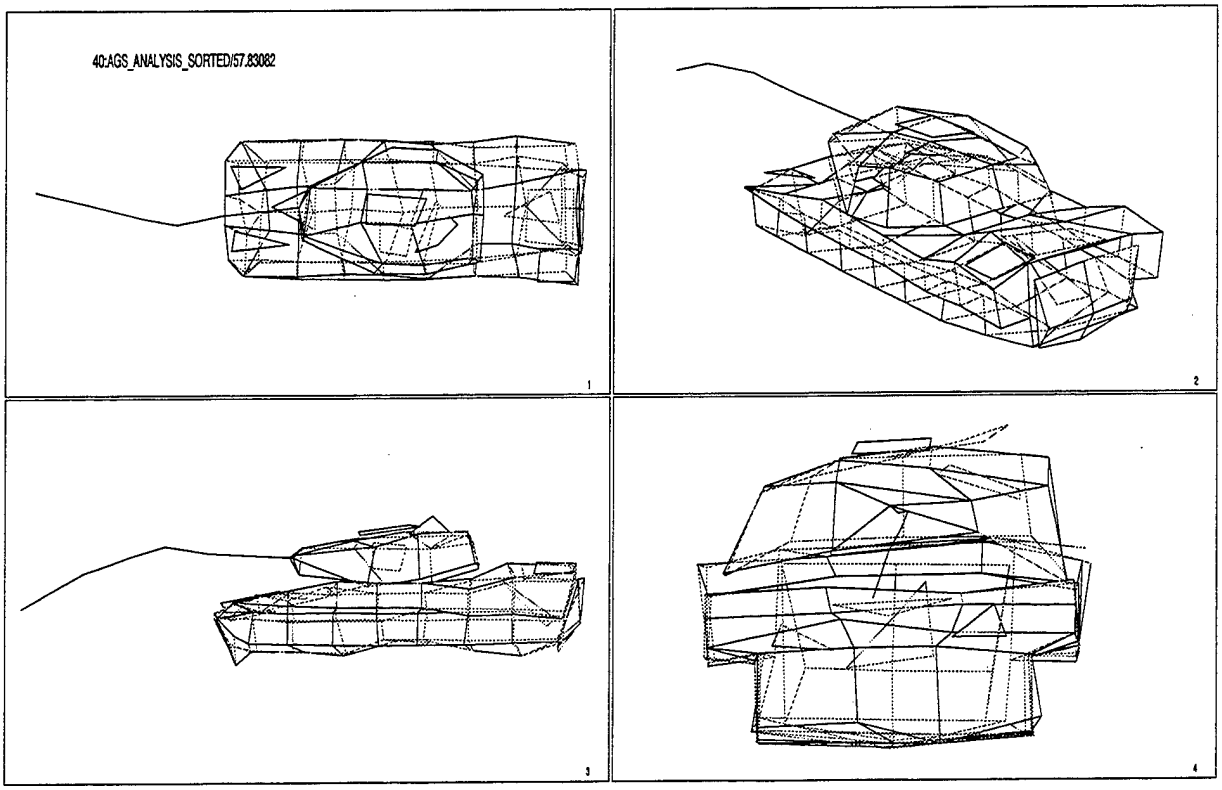
40:AGS_ANALYSIS_SORTED/57.83082
1
2
3
4

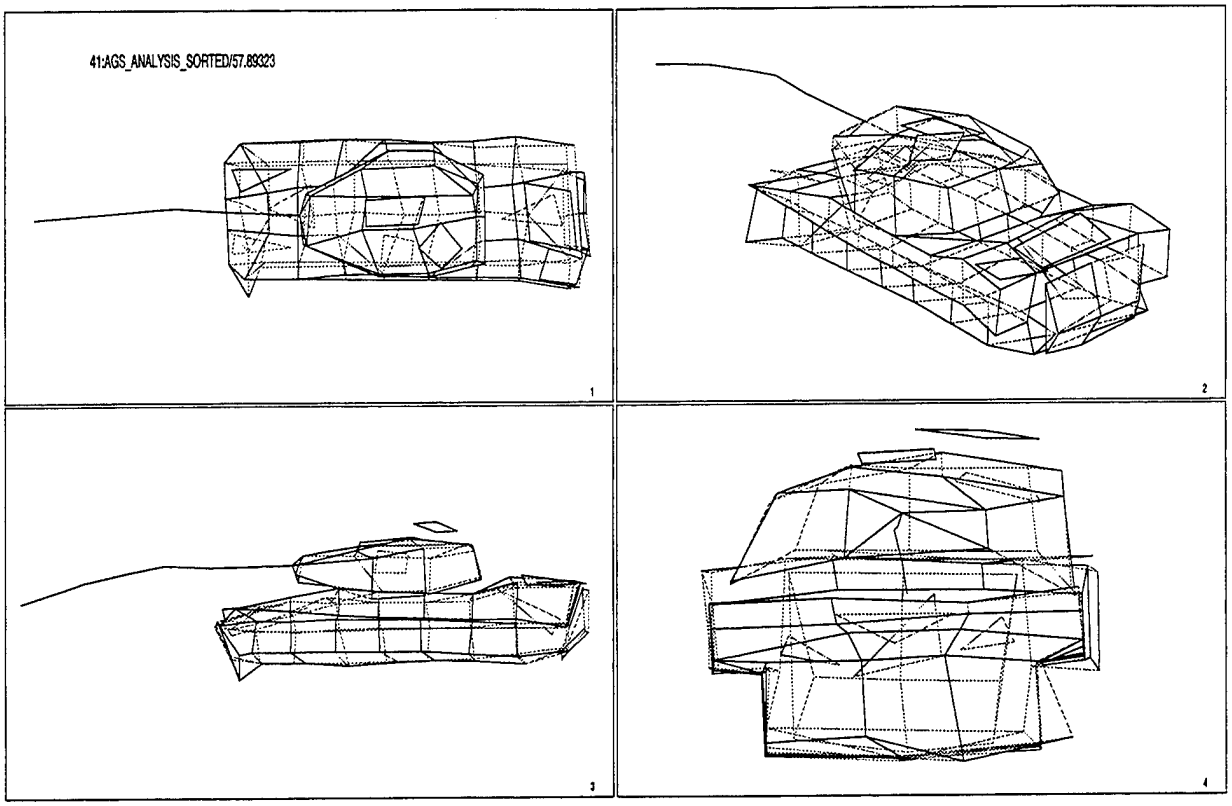
41:AGS_ANALYSIS_SORTED/57.89323
1
2
3
4

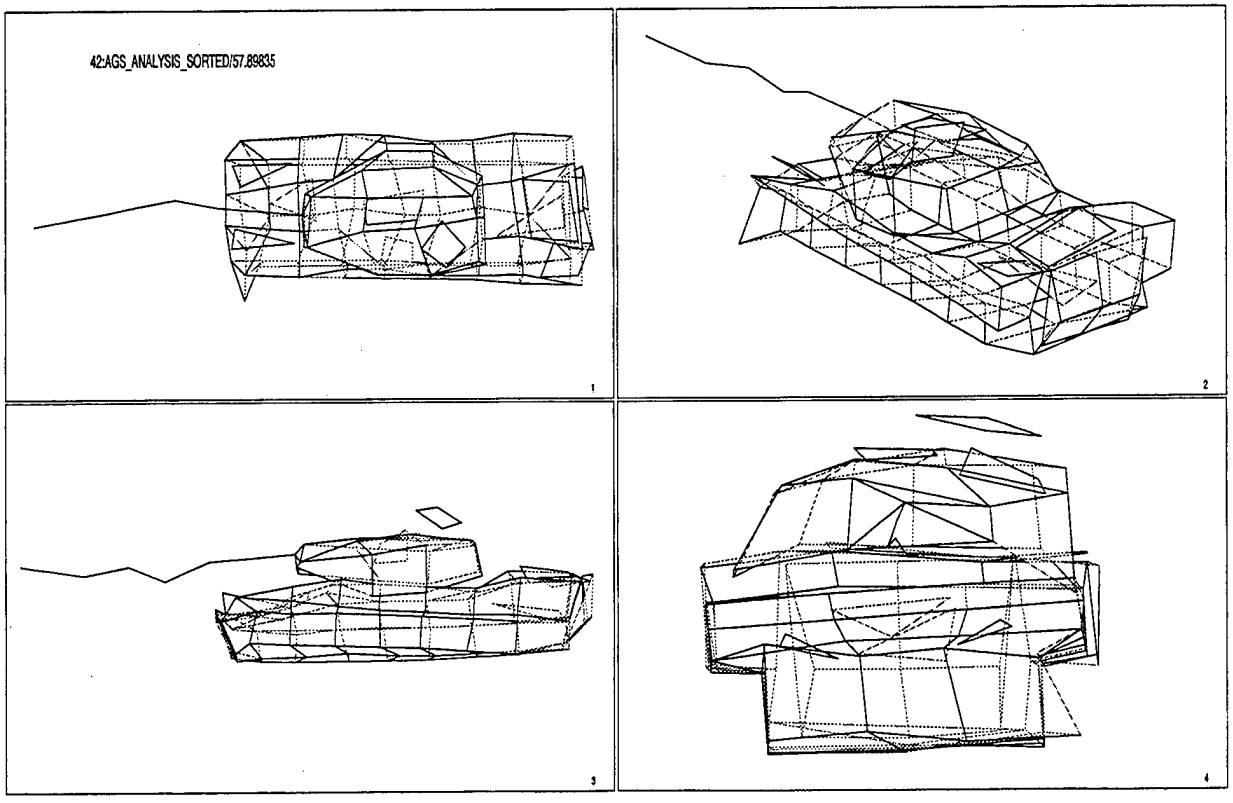
42:AGS_ANALYSIS_SORTED/57.89835
1
2
3
4

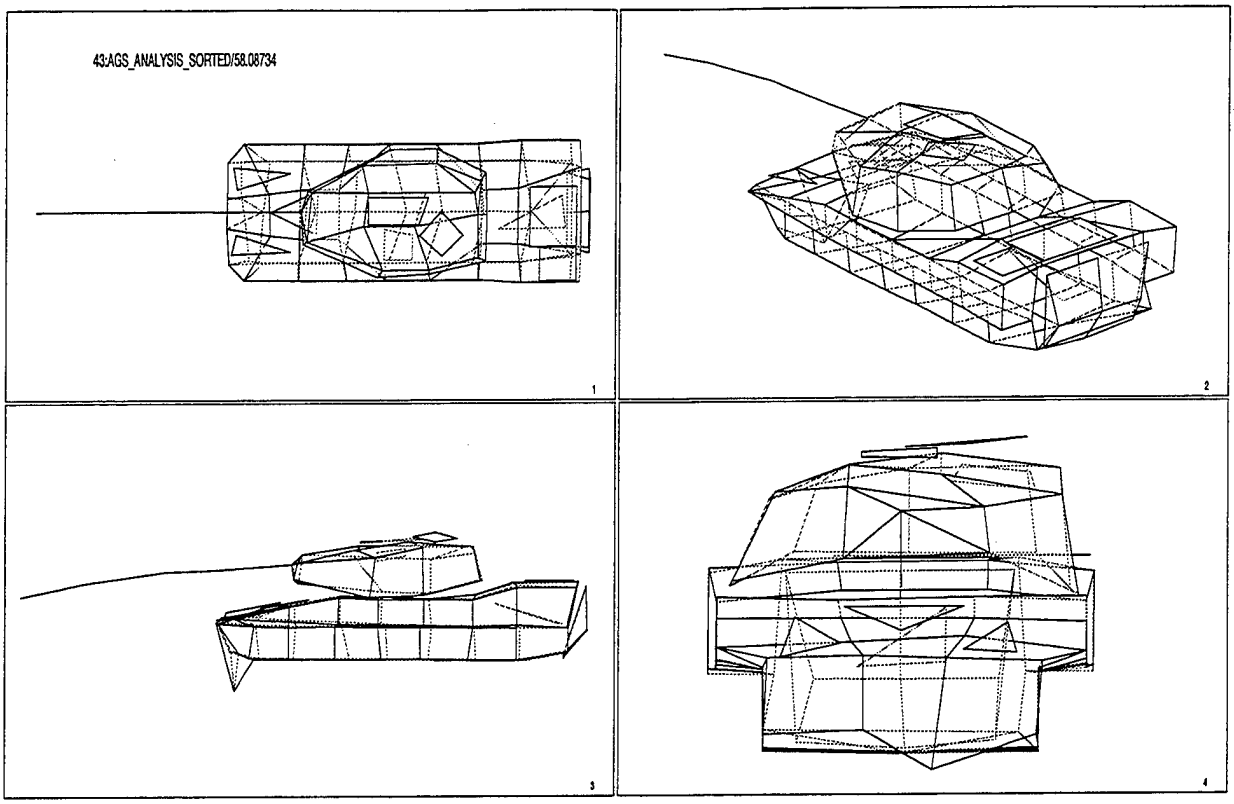
43:AGS_ANALYSIS_SORTED/58.08734
1
2
3
4

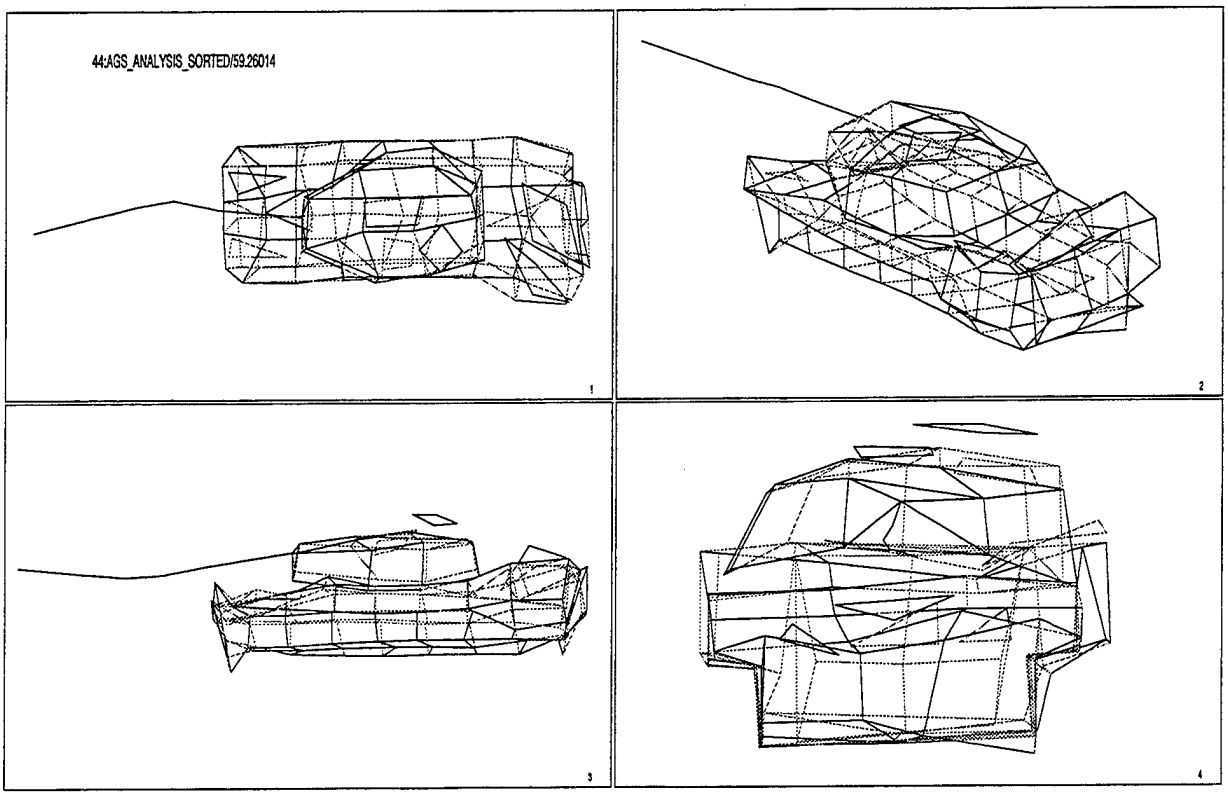
44:AGS_ANALYSIS_SORTED/59.26014
1
2
3
4

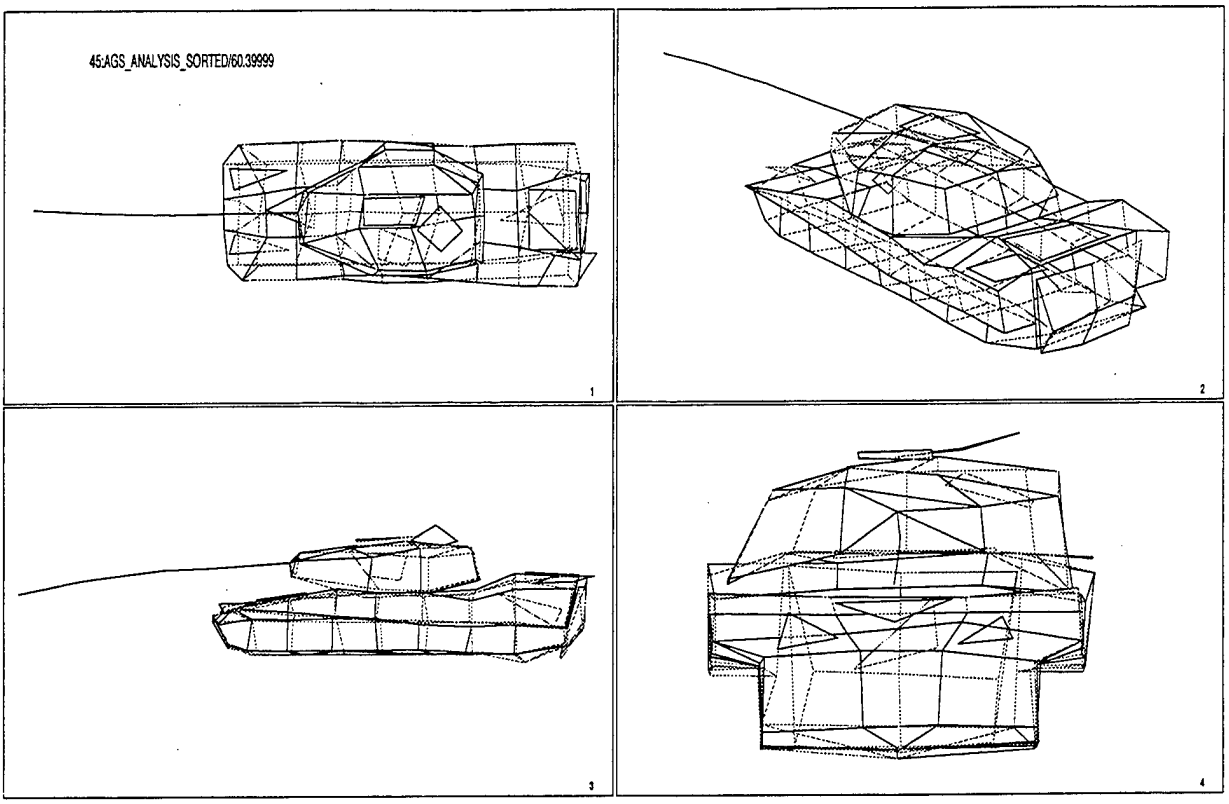
45:AGS_ANALYSIS_SORTED/60.39999
1
2
3
4

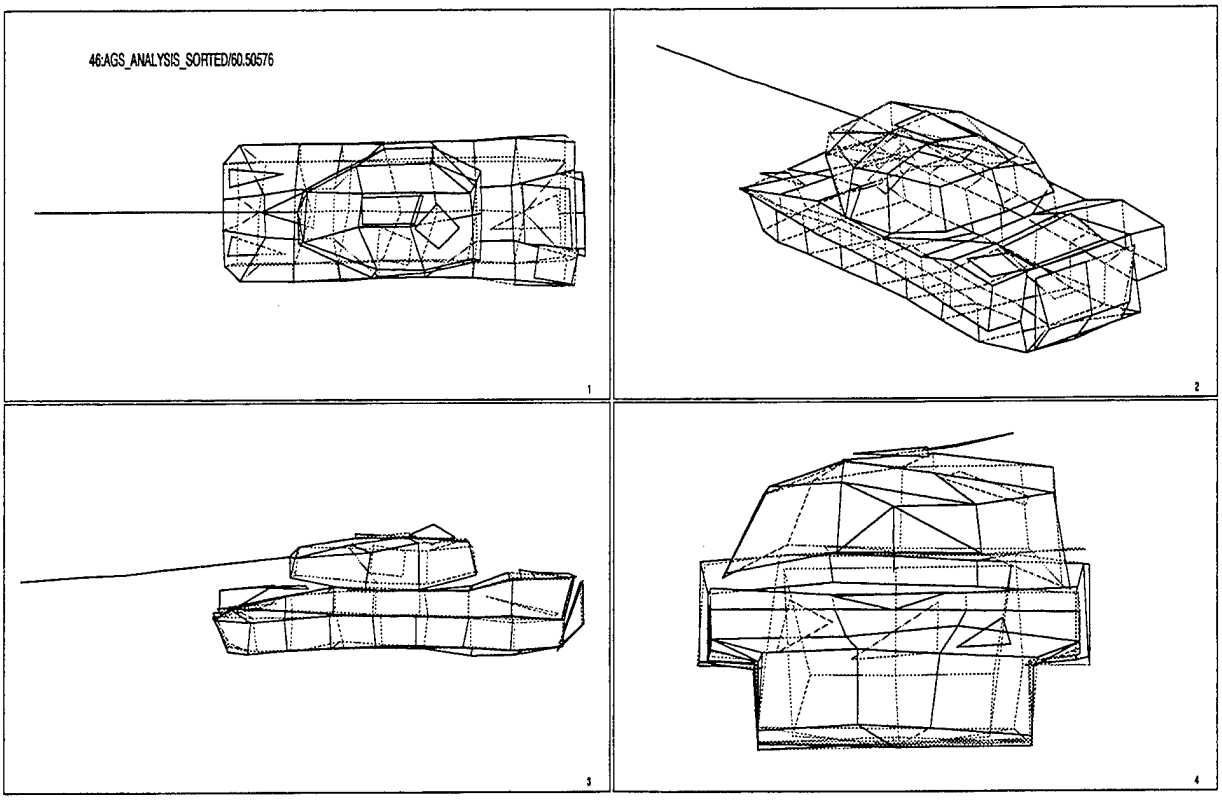
46:AGS_ANALYSIS_SORTED/60.50576
1
2
3
4

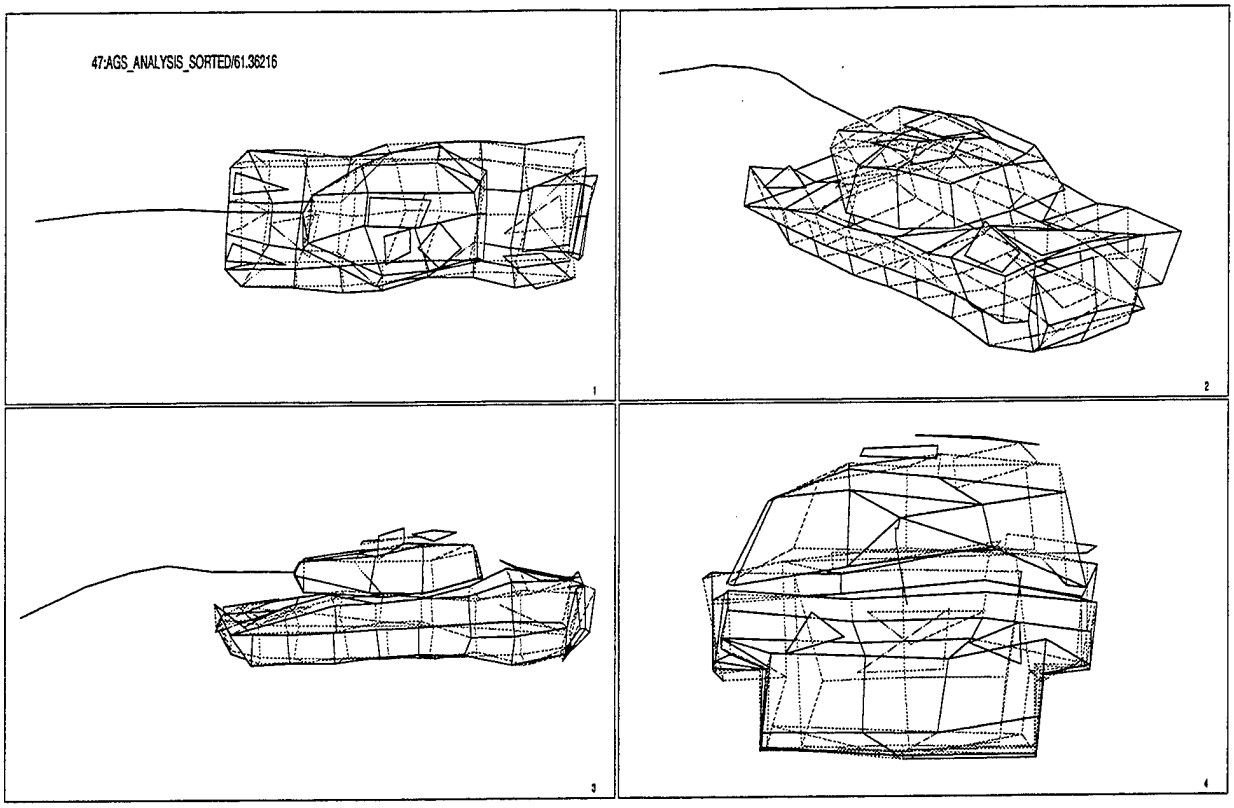
47:AGS_ANALYSIS_SORTED/61.36216
1
2
3
4

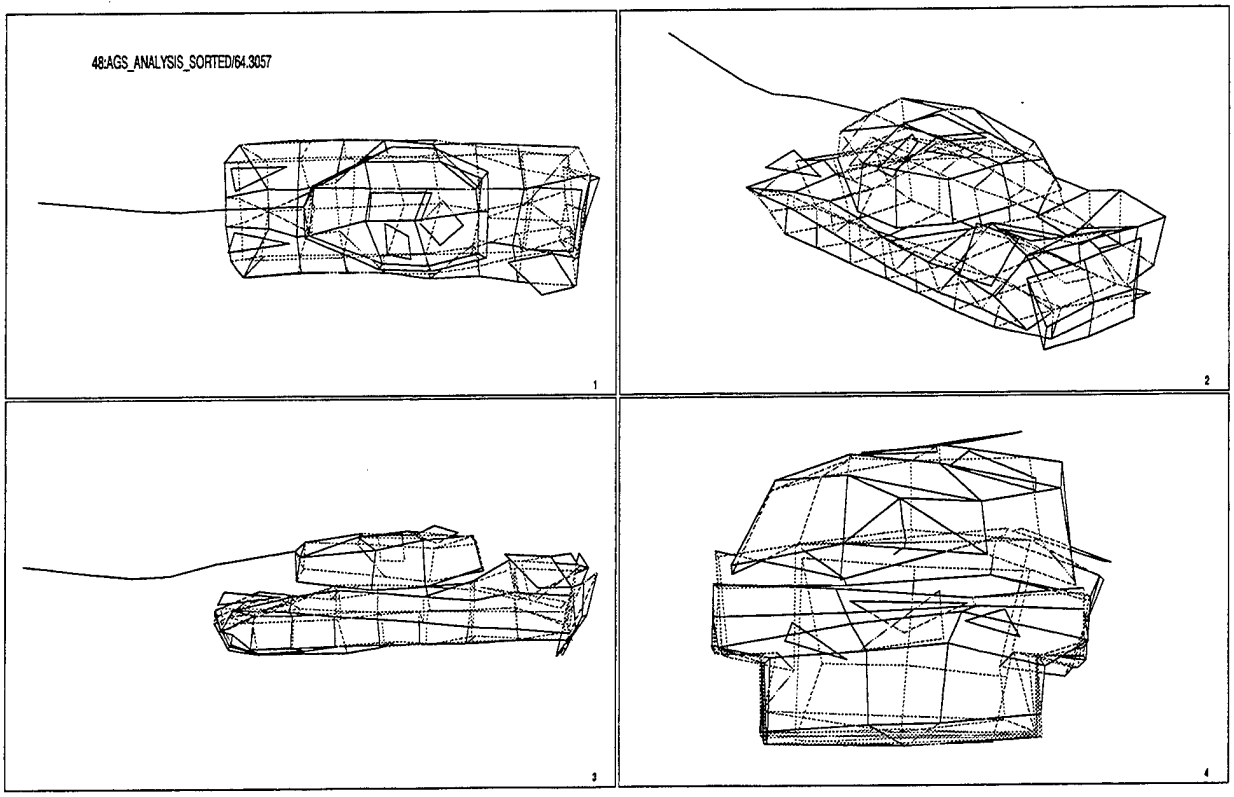
48:AGS_ANALYSIS_SORTED/64.3057
1
2
3
4

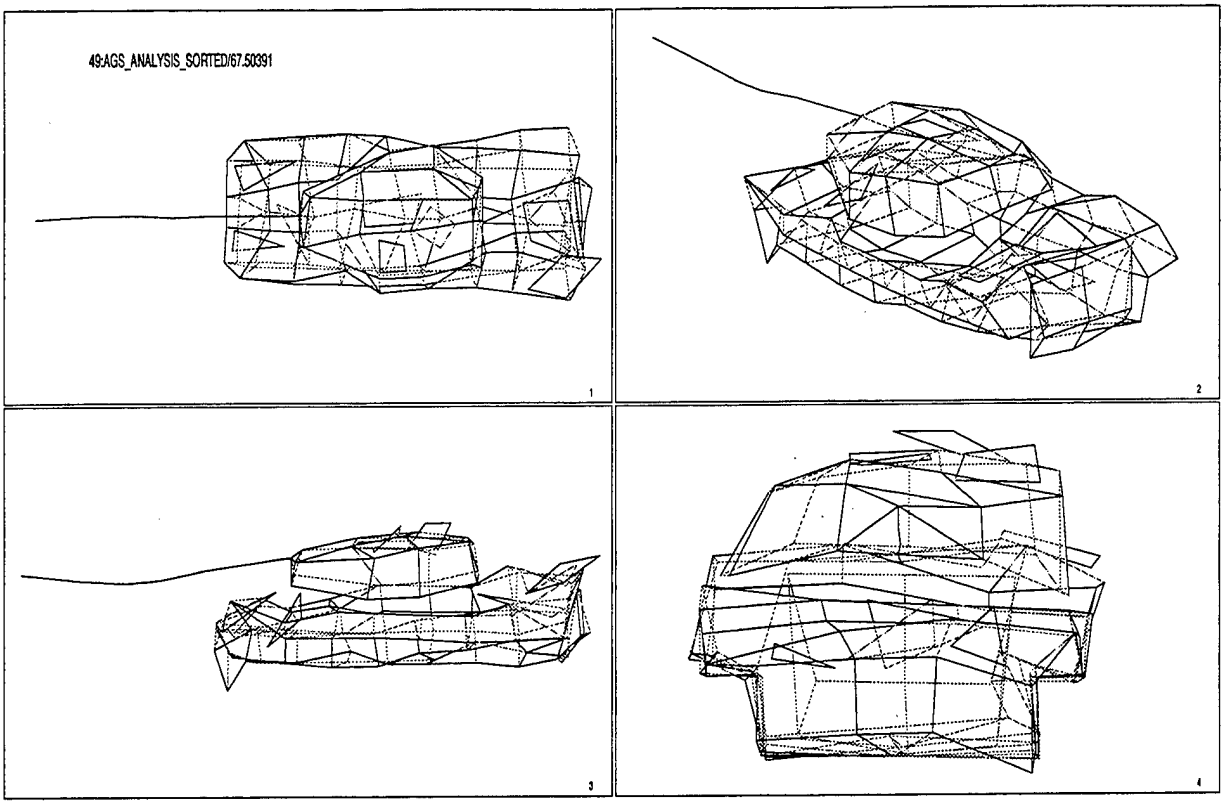
49:AGS_ANALYSIS_SORTED/67.50391
1
2
3
4

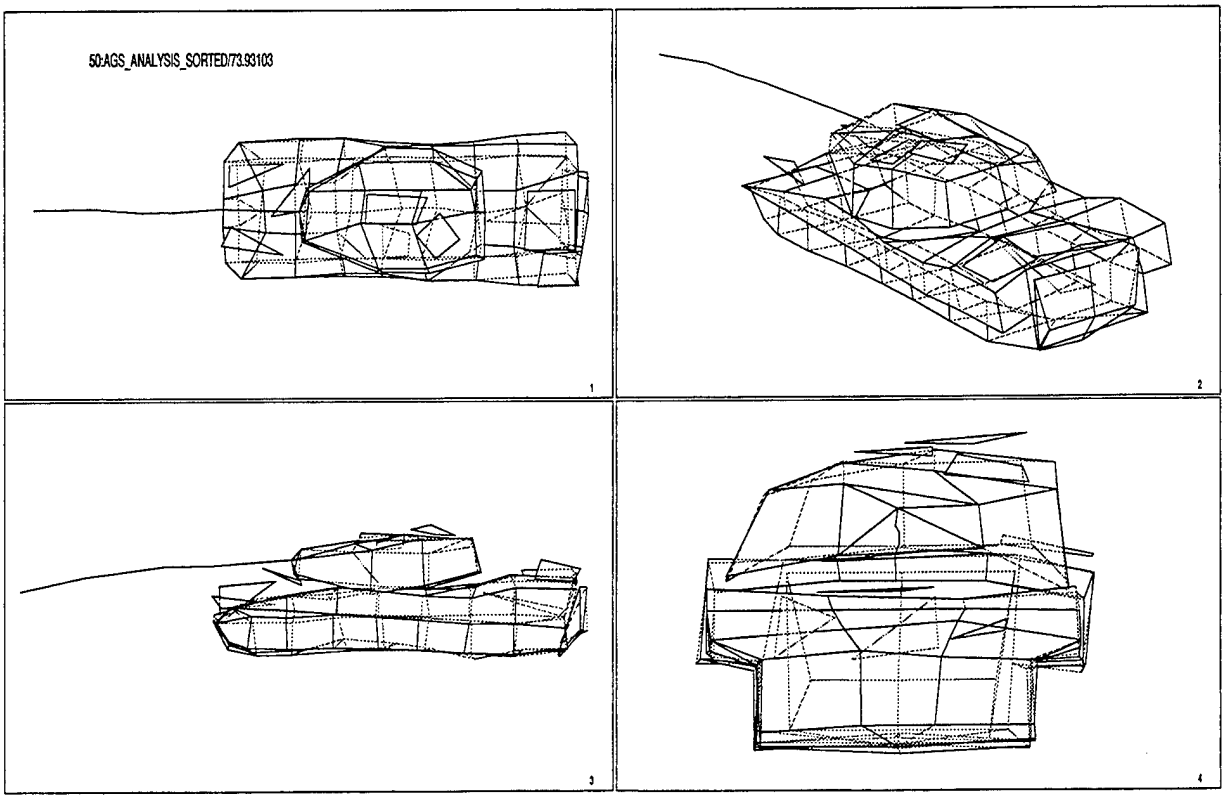
50:AGS_ANALYSIS_SORTED/73.93103
1
2
3
4

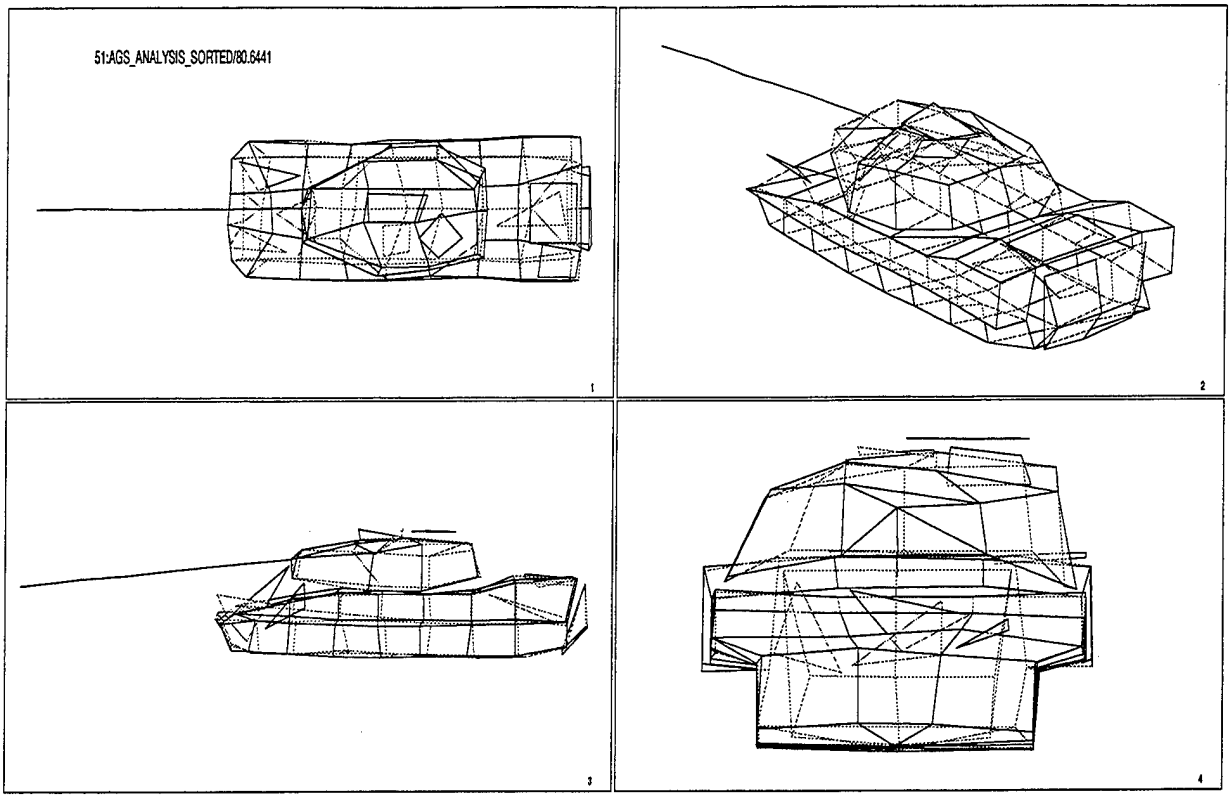
51:AGS_ANALYSIS_SORTED/80.6441
1
2
3
4

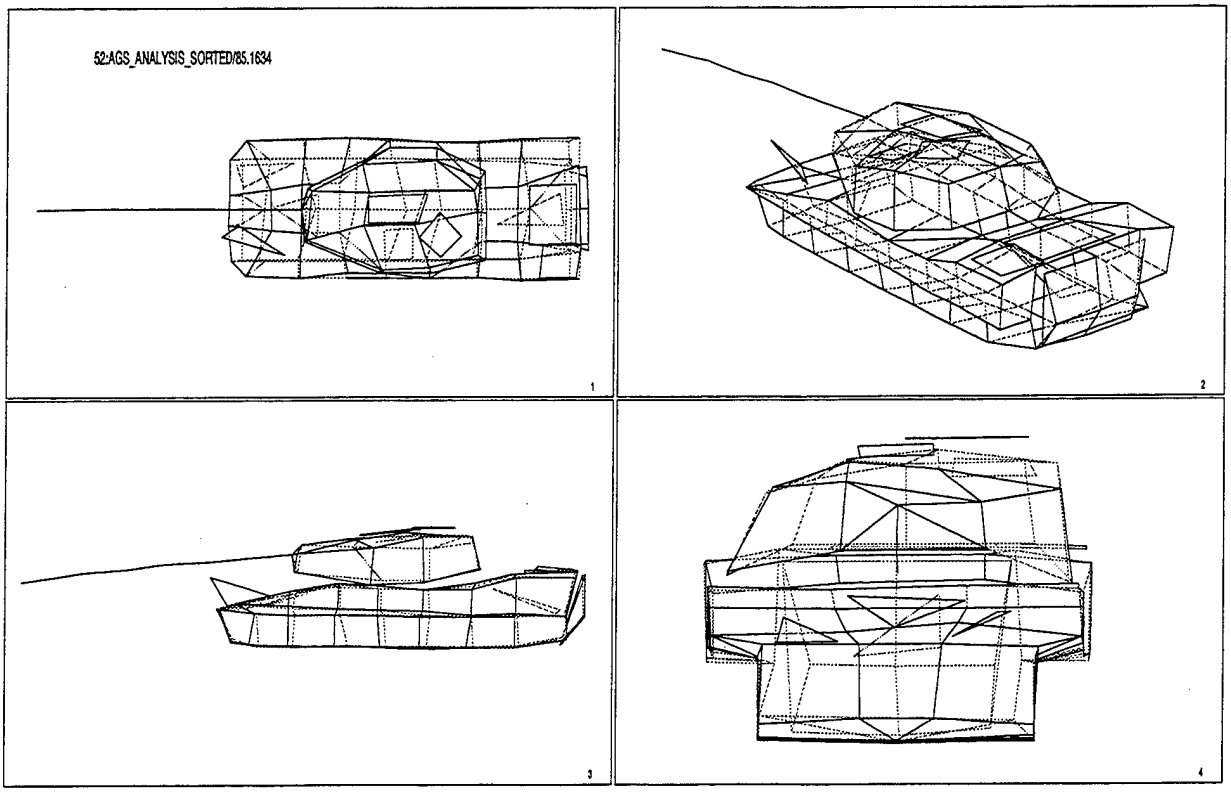
52:AGS_ANALYSIS_SORTED/85.1634
1
2
3
4

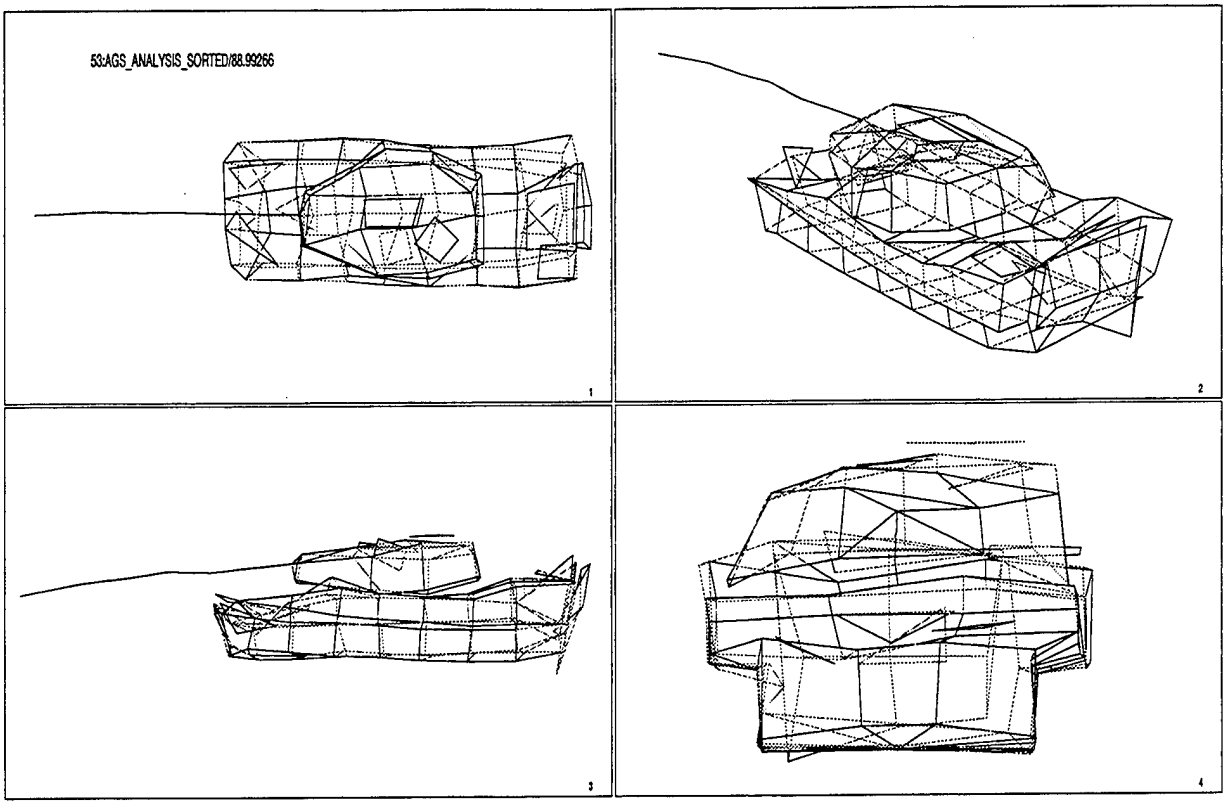
53:AGS_ANALYSIS_SORTED/88.99266
1
2
3
4

INTENTIONALLY LEFT BLANK.

Bibliography

Braun, S. *Mechanical Signature Analysis: Theory and Applications.* London: Harcourt Brace Jovanovich, 1986.

Priebe, R. "Wavelet Applications to Detection and Classification of Impulsive Metallic Transients." Dissertation Submitted to the University of Texas at Austin, 1995.

Priebe, R., and G. Wilson. "Wavelet Applications to Structural Analysis." *Proceedings of the IEEE ICASSP*, 1994.

INTENTIONALLY LEFT BLANK.

NO. OF COPIES ORGANIZATION

2 DEFENSE TECHNICAL INFORMATION CENTER
DTIC DDA
8725 JOHN J KINGMAN RD
STE 0944
FT BELVOIR VA 22060-6218

1 HQDA
DAMO FDQ
D SCHMIDT
400 ARMY PENTAGON
WASHINGTON DC 20310-0460

1 OSD
OUSD(A&T)/ODDDR&E(R)
R J TREW
THE PENTAGON
WASHINGTON DC 20301-7100

1 DPTY CG FOR RDA
US ARMY MATERIEL CMD
AMCRDA
5001 EISENHOWER AVE
ALEXANDRIA VA 22333-0001

1 INST FOR ADVNCD TCHNLGY
THE UNIV OF TEXAS AT AUSTIN
PO BOX 202797
AUSTIN TX 78720-2797

1 DARPA
B KASPAR
3701 N FAIRFAX DR
ARLINGTON VA 22203-1714

1 NAVAL SURFACE WARFARE CTR
CODE B07 J PENNELLA
17320 DAHLGREN RD
BLDG 1470 RM 1101
DAHLGREN VA 22448-5100

1 US MILITARY ACADEMY
MATH SCI CTR OF EXCELLENCE
DEPT OF MATHEMATICAL SCI
MADN MATH
THAYER HALL
WEST POINT NY 10996-1786

NO. OF COPIES ORGANIZATION

1 DIRECTOR
US ARMY RESEARCH LAB
AMSRL DD
2800 POWDER MILL RD
ADELPHI MD 20783-1197

1 DIRECTOR
US ARMY RESEARCH LAB
AMSRL CS AS (RECORDS MGMT)
2800 POWDER MILL RD
ADELPHI MD 20783-1145

3 DIRECTOR
US ARMY RESEARCH LAB
AMSRL CI LL
2800 POWDER MILL RD
ADELPHI MD 20783-1145

ABERDEEN PROVING GROUND

4 DIR USARL
AMSRL CI LP (BLDG 305)

NO. OF COPIES	ORGANIZATION
1	DIRECTOR US ARMY RESEARCH LAB AMSRL CP CA D SNIDER 2800 POWDER MILL RD ADELPHI MD 20783
6	DIRECTOR US ARMY RESEARCH LAB AMSRL WM MB ALC A ABRAHAMIAN M BERMAN A FRYDMAN T LI W MCINTOSH E SZYMANSKI 2800 POWDER MILL RD ADELPHI MD 20783
1	COMMANDER USA ARDEC AMSTA AR FSE T GORA PICATINNY ARSENAL NJ 07806-5000
3	COMMANDER USA ARDEC AMSTA AR TD PICATINNY ARSENAL NJ 07806-5000
5	US ARMY TACOM AMSTA JSK S GOODMAN J FLORENCE AMSTA TR D B RAJU L HINOJOSA D OSTBERG WARREN MI 48397-5000
5	PM SADARM SFAE GCSS SD COL B ELLIS M DEVINE W DEMASSI J PRITCHARD S HROWNAK PICATINNY ARSENAL NJ 07806-5000

NO. OF COPIES	ORGANIZATION
1	COMMANDER USA ARDEC F MCLAUGHLIN PICATINNY ARSENAL NJ 07806-5000
5	COMMANDER USA ARDEC AMSTA AR CCH S MUSALLI R CARR M LUCIANO T LOUCEIRO PICATINNY ARSENAL NJ 07806-5000
2	COMMANDER USA ARDEC AMSTA AR E FENNELL PICATINNY ARSENAL NJ 07806-5000
2	COMMANDER USA ARDEC AMSTA AR PICATINNY ARSENAL NJ 07806-5000
1	COMMANDER USA ARDEC AMSTA AR CCH P J LUTZ PICATINNY ARSENAL NJ 07806-5000
1	COMMANDER USA ARDEC AMSTA AR FSF T C LIVECCHIA PICATINNY ARSENAL NJ 07806-5000
1	COMMANDER USA ARDEC AMSTA AR QAC T/C C PATEL PICATINNY ARSENAL NJ 07806-5000

NO. OF COPIES ORGANIZATION

2 COMMANDER
USA ARDEC
AMSTA AR M
D DEMELLA
F DIORIO
PICATINNY ARSENAL NJ
07806-5000

3 COMMANDER
USA ARDEC
AMSTA AR FSA
A WARNASH
B MACHAK
M CHIEFA
PICATINNY ARSENAL NJ
07806-5000

1 COMMANDER
SMCWV QAE Q B VANINA
BLDG 44 WATERVLIET ARSENAL
WATERVLIET NY 12189-4050

1 COMMANDER
SMCWV SPM T MCCLOSKEY
BLDG 253 WATERVLIET ARSENAL
WATERVLIET NY 12189-4050

8 DIRECTOR
BENET LABORATORIES
AMSTA AR CCB
J KEANE
J BATAGLIA
J VASILAKIS
G FFIAR
V MONTVORI
G DANDREA
R HASENBEIN
R S SOPOK
WATERVLIET NY 12189

1 COMMANDER
WATERVLIET ARSENAL
SMCWV QA QS K INSCO
WATERVLIET NY 12189-4050

NO. OF COPIES ORGANIZATION

1 COMMANDER
PRODUCTION BASE MODERN ACTY
USA ARDEC
AMSMC PBM K
PICATINNY ARSENAL NJ
07806-5000

1 COMMANDER
US ARMY BELVOIR RD&E CTR
STRBE JBC
FT BELVOIR VA 22060-5606

2 COMMANDER
USA ARDEC
AMSTA AR FSP G
M SCHIKSNIS
D CARLUCCI
PICATINNY ARSENAL NJ
07806-5000

1 US ARMY COLD REGIONS RSRCH
AND ENGINEERING LAB
P DUTTA
72 LYME RD
HANOVER NH 03755

1 DIRECTOR
US ARMY RESEARCH LAB
AMSRL WT L D WOODBURY
2800 POWDER MILL RD
ADELPHI MD 20783-1145

3 COMMANDER
US ARMY MISSILE CMD
AMSMI RD W MCCORKLE
AMSMI RD ST P DOYLE
AMSMI RD ST CN T VANDIVER
REDSTONE ARSENAL AL
35898-5247

2 US ARMY RESEARCH OFFICE
A CROWSON
J CHANDRA
PO BOX 12211
RESEARCH TRIANGLE PARK NC
27709-2211

NO. OF COPIES	ORGANIZATION
3	US ARMY RESEARCH OFFICE ENGINEERING SCIENCES DIV R SINGLETON G ANDERSON K IYER PO BOX 12211 RESEARCH TRIANGLE PARK NC 27709-2211
5	PM TMAS SFAE GSSC TMA COL PAWLICKI K KIMKER E KOPACZ R ROESER B DORCY PICATINNY ARSENAL NJ 07806-5000
1	PM TMAS SFAE GSSC TMA SMD R KOWALSKI PICATINNY ARSENAL NJ 07806-5000
2	PEO FIELD ARTILLERY SYS SFAE FAS PM H GOLDMAN T MCWILLIAMS PICATINNY ARSENAL NJ 07806-5000
2	PM CRUSADER G DELCOCO J SHIELDS PICATINNY ARSENAL NJ 07806-5000
2	NASA LANGLEY RESEARCH CTR MS 266 AMSRL VS W ELBER F BARTLETT JR HAMPTON VA 23681-0001

NO. OF COPIES	ORGANIZATION
6	COMMANDER WRIGHT PATTERSON AFB WL FIV A MAYER WL MLBM S DONALDSON T BENSON-TOLLE C BROWNING J MCCOY F ABRAHAMS 2941 P STREET STE 1 DAYTON OH 45433
2	COMMANDER DARPA J KELLY B WILCOX 3701 N FAIRFAX DR ARLINGTON VA 22203-1714
1	NAVAL SURFACE WARFARE CTR DAHLGREN DIV CODE G06 DAHLGREN VA 22448
1	NAVAL SURFACE WARFARE CTR CODE 6383 I WOLOCK WASHINGTON DC 20375-5000
1	OFFICE OF NAVAL RSRCH MECH DIV CODE 1132SM Y RAJAPAKSE ARLINGTON VA 22217
1	NAVAL SURFACE WARFARE CTR CRANE DIV M JOHNSON CODE 20H4 LOUISVILLE KY 40214-5245
1	DAVID TAYLOR RSRCH CTR SHIP STRUCTURES & PROTECTION DEPARTMENT J CORRADO CODE 1702 BETHESDA MD 20084
2	DAVID TAYLOR RSRCH CTR R ROCKWELL W PHYILLAIER BETHESDA MD 20054-5000

NO. OF COPIES	ORGANIZATION
1	DEFENSE NUCLEAR AGENCY INNOVATIVE CONCEPTS DIV R ROHR 6801 TELEGRAPH RD ALEXANDRIA VA 22310-3398
1	EXPEDITIONARY WARFARE DIV N85 F SHOUP 2000 NAVY PENTAGON WASHINGTON DC 20350-2000
1	OFFICE OF NAVAL RSRCH D SIEGEL 351 800 N QUINCY ST ARLINGTON VA 22217-5660
1	NAVAL SURFACE WARFARE CTR J H FRANCIS CODE G30 DAHLGREN VA 22448
2	NAVAL SURFACE WARFARE CTR D WILSON CODE G32 R D COOPER CODE G32 DAHLGREN VA 22448
4	NAVAL SURFACE WARFARE CTR J FRAYSSE E ROWE T DURAN L DE SIMONE CODE G33 DAHLGREN VA 22448
1	COMMANDER NAVAL SEA SYSTEMS CMD D LIESE 2531 JEFFERSON DAVIS HWY ARLINGTON VA 22242-5160
1	NAVAL SURFACE WARFARE M E LACY CODE B02 17320 DAHLGREN RD DAHLGREN VA 22448
1	NAVAL SURFACE WARFARE TECH LIBRARY CODE 323 17320 DAHLGREN RD DAHLGREN VA 22448

NO. OF COPIES	ORGANIZATION
4	DIR LLNL R CHRISTENSEN S DETERESA F MAGNESS M FINGER PO BOX 808 LIVERMORE CA 94550
2	LANL F ADDESSIO MS B216 J REPPA MS F668 PO BOX 1633 LOS ALAMOS NM 87545
1	OAK RIDGE NATIONAL LAB R M DAVIS PO BOX 2008 OAK RIDGE TN 37831-6195
1	PENNSYLVANIA STATE UNIV C BAKIS 227 N HAMMOND UNIVERSITY PARK PA 16802
3	UDLP 4800 EAST RIVER RD P JANKE MS 170 T GIOVANETTI MS 236 B VAN WYK MS 389 MINNEAPOLIS MN 55421-1498
4	DIR SNL APPLIED MECHANICS DEPT DIV 8241 W KAWAHARA K PERANO D DAWSON P NIELAN PO BOX 969 LIVERMORE CA 94550-0096
1	DREXEL UNIVERSITY A S D WANG 32ND AND CHESTNUT ST PHILADELPHIA PA 19104
1	BATTELLE C R HARGREAVES 505 KING AVE COLUMBUS OH 43201-2681

NO. OF COPIES	ORGANIZATION
1	PACIFIC NORTHWEST LAB M SMITH PO BOX 999 RICHLAND WA 99352
1	LLNL M MURPHY PO BOX 808 L 282 LIVERMORE CA 94550
1	NORTH CAROLINA STATE UNIV CIVIL ENGINEERING DEPT W RASDORF PO BOX 7908 RALEIGH NC 27696-7908
1	PENNSYLVANIA STATE UNIV R MCNITT 227 HAMMOND BLDG UNIVERSITY PARK PA 16802
1	PENNSYLVANIA STATE UNIV R S ENGEL 245 HAMMOND BLDG UNIVERSITY PARK PA 16802
1	PURDUE UNIVERSITY SCHOOL OF AERO & ASTRO C T SUN W LAFAYETTE IN 47907-1282
1	STANFORD UNIV DEPT OF AERONAUTICS & AEROBALLISTICS DURANT BLDG S TSAI STANFORD CA 94305
1	UCLA MANE DEPT ENGR IV H T HAHN LOS ANGELES CA 90024-1597
2	U OF DAYTON RSRCH INSTITUTE R Y KIM A K ROY 300 COLLEGE PARK AVE DAYTON OH 45469-0168

NO. OF COPIES	ORGANIZATION
1	UNIV OF DAYTON J M WHITNEY COLLEGE PARK AVE DAYTON OH 45469-0240
2	UNIV OF DELAWARE CTR FOR COMPOSITE MATERIALS J GILLESPIE M SANTARE 201 SPENCER LABORATORY NEWARK DE 19716
1	UNIV OF ILLINOIS AT URBANA CHAMPAIGN NATIONAL CTR FOR COMPOSITE MATERIALS RESEARCH 216 TALBOT LABORATORY J ECONOMY 104 S WRIGHT ST URBANA IL 61801
1	UNIV OF KENTUCKY L PENN 763 ANDERSON HALL LEXINGTON KY 40506-0046
1	UNIV OF UTAH DEPT OF MECH & INDUSTRIAL ENGR S SWANSON SALT LAKE CITY UT 84112
2	THE UNIV OF TEXAS AT AUSTIN CTR FOR ELECTROMECHANICS A WALLS J KITZMILLER 10100 BURNET RD AUSTIN TX 78758-4497
3	VA POLYTECHNICAL INSTITUTE & STATE UNIV DEPT OF ESM M W HYER K REIFSNIDER R JONES BLACKSBURG VA 24061-0219
1	UNIV OF MARYLAND DEPT OF AEROSPACE ENGINEERING A J VIZZINI COLLEGE PARK MD 20742

NO. OF COPIES	ORGANIZATION
1	AAI CORPORATION T G STASTNY PO BOX 126 HUNT VALLEY MD 21030-0126
1	J HEBERT PO BOX 1072 HUNT VALLEY MD 21030-0126
1	ARMTEC DEFENSE PRODUCTS S DYER 85 901 AVE 53 PO BOX 848 COACHELLA CA 92236
2	ADVANCED COMPOSITE MATERIALS CORPORATION P HOOD J RHODES 1525 S BUNCOMBE RD GREER SC 29651-9208
1	SAIC D DAKIN 2200 POWELL ST STE 1090 EMERYVILLE CA 94608
1	SAIC M PALMER 2109 AIR PARK RD S E ALBUQUERQUE NM 87106
1	SAIC R ACEBAL 1225 JOHNSON FERRY RD STE 100 MARIETTA GA 30068
1	SAIC G CHRYSSOMALLIS 3800 W 80TH ST STE 1090 BLOOMINGTON MN 55431
6	ALLIANT TECHSYSTEMS INC C CANDLAND R BECKER L LEE R LONG D KAMDAR G KASSUELKE 600 2ND ST NE HOPKINS MN 55343-8367
1	AMOCO PERFORMANCE PRODUCTS INC M MICHNO JR 4500 MCGINNIS FERRY RD ALPHARETTA GA 30202-3944
1	APPLIED COMPOSITES W GRISCH 333 NORTH SIXTH ST ST CHARLES IL 60174
1	BRUNSWICK DEFENSE T HARRIS STE 410 1745 JEFFERSON DAVIS HWY ARLINGTON VA 22202
1	PROJECTILE TECHNOLOGY INC 515 GILES ST HAVRE DE GRACE MD 21078
1	CUSTOM ANALYTICAL ENGR SYS INC A ALEXANDER 13000 TENSOR LANE NE FLINTSTONE MD 21530
1	NOESIS INC A BOUTZ 1110 N GLEBE RD STE 250 ARLINGTON VA 22201-4795
1	ARROW TECH ASSOC 1233 SHELBURNE RD STE D 8 SOUTH BURLINGTON VT 05403-7700
1	NAVAL SURFACE WARFARE CTR R HUBBARD G33 C DAHLGREN DIV DAHLGREN VA 22448-5000

NO. OF COPIES	ORGANIZATION
5	GEN CORP AEROJET D PILLASCH T COULTER C FLYNN D RUBAREZUL M GREINER 1100 WEST HOLLYVALE ST AZUSA CA 91702-0296
7	CIVIL ENGR RSRCH FOUNDATION H BERNSTEIN C MAGNELL K ALMOND R BELLE M WILLETT E DELO B MATTES 1015 15TH ST NW STE 600 WASHINGTON DC 20005
1	NATIONAL INSTITUTE OF STANDARD AND TECHNOLOGY STRUCTURE & MECHANICS GROUP POLYMER DIV POLYMERS RM A209 G MCKENNA GAITHERSBURG MD 20899
1	DUPONT COMPANY COMPOSITES ARAMID FIBERS S BORLESKE CHESTNUT RUN PLAZA PO BOX 80702 WILMINGTON DE 19880-0702
1	GENERAL DYNAMICS LAND SYSTEMS DIV D BARTLE PO BOX 1901 WARREN MI 48090
3	HERCULES INC R BOE F POLICELLI J POESCH PO BOX 98 MAGNA UT 84044
3	HERCULES INC G KUEBELER J VERMEYCHUK B MANDERVILLE JR HERCULES PLZ WILMINGTON DE 19894
1	HEXCEL M SHELENDICH 11555 DUBLIN BLVD PO BOX 2312 DUBLIN CA 94568-0705
4	INSTITUTE FOR ADVANCED TECH H FAIR P SULLIVAN W REINECKE I MCNAB 4030 2 W BRAKER LN AUSTIN TX 78759
1	INTEGRATED COMPOSITE TECH H PERKINSON JR PO BOX 397 YORK NEW SALEM PA 17371-0397
1	INTERFEROMETRICS INC R LARRIVA 8150 LEESBURG PIKE VIENNA VA 22100
1	AEROSPACE RES & DEV ASRDD CORP D ELDER PO BOX 49472 COLORADO SPRINGS CO 80949-9472
1	PM ADVANCED CONCEPTS LORAL VOUGHT SYSTEMS J TAYLOR PO BOX 650003 MS WT 21 DALLAS TX 76265-0003
2	LORAL VOUGHT SYSTEMS G JACKSON K COOK 1701 W MARSHALL DR GRAND PRAIRIE TX 75051

NO. OF COPIES	ORGANIZATION
1	BRIGS CO J BACKOFEN 2668 PETERBOROUGH ST HERDON VA 22071-2443
1	SOUTHWEST RSRCH INSTITUTE ENGR & MATERIAL SCIENCES DIV J RIEGEL 6220 CULEBRA RD PO DRAWER 28510 SAN ANTONIO TX 78228-0510
1	ZERNOW TECHNICAL SVCS L ZERNOW 425 W BONITA AVE SUITE 208 SAN DIMAS CA 91773
1	R EICHELBERGER CONSULTANT 409 W CATHERINE ST BEL AIR MD 21014-3613
1	DYNA EAST CORPORATION P C CHOU 3201 ARCH ST PHILADELPHIA PA 19104-2711
2	MARTIN MARIETTA CORP P DEWAR L SPONAR 230 EAST GODDARD BLVD KING OF PRUSSIA PA 19406
2	OLIN CORPORATION FLINCHBAUGH DIV E STEINER B STEWART PO BOX 127 RED LION PA 18356
1	OLIN CORPORATION L WHITMORE 10101 9TH ST NORTH ST PETERSBURG FL 33702
1	RENNSAELER POLYTECHNIC INSTITUTE R B PIPES PITTSBURGH BLDG TROY NY 12180-3590

NO. OF COPIES	ORGANIZATION
1	SPARTA INC J GLATZ 9455 TOWNE CTR DRIVE SAN DIEGO CA 92121-1964
2	UNITED DEFENSE LP P PARA G THOMAS 1107 COLEMAN AVE BOX 367 SAN JOSE CA 95103
1	MARINE CORPS SYS CMD PM GROUND WPNS COL R OWEN 2083 BARNETT AVE SUITE 315 QUANTICO VA 22134-5000
1	OFFICE OF NAVAL RES J KELLY 800 NORTH QUINCEY ST ARLINGTON VA 22217-5000
2	NAVAL SURFACE WARFARE CTR CARDEROCK DIV R CRANE CODE 2802 C WILLIAMS CODE 6553 3A LEGGETT CIR ANNAPOLIS MD 21402
5	SIKORSKY H BUTTS T CARSTENSAN B KAY S GARBO J ADELMANN 6900 MAIN ST PO BOX 9729 STRATFORD CT 06601-1381
1	D ADAMS U WYOMING PO BOX 3295 LARAMIE WY 82071
1	MICHIGAN STATE UNIV R AVERILL 3515 EB MSM DEPT EAST LANSING MI 48824-1226

NO. OF COPIES	ORGANIZATION
1	AMOCO POLYMERS J BANISAUKAS 4500 MCGINNIS FERRY RD ALPHARETTA GA 30005
1	HEXCEL T BITZER 11711 DUBLIN BLVD DUBLIN CA 94568
1	BOEING R BOHLMANN PO BOX 516 MC 5021322 ST LOUIS MO 63166-0516
1	NAVSEA OJRI G CAMPONESCHI 2351 JEFFERSON DAVIS HWY ARLINGTON VA 22242-5160
1	LOCKHEED MARTIN R FIELDS 1195 IRWIN CT WINTER SPRINGS FL 32708
1	USAF WL MLS OL A HAKIM 5225 BAILEY LOOP 243E MCCLELLAN AFB CA 55552
1	PRATT & WHITNEY D HAMBRICK 400 MAIN ST MS 114 37 EAST HARTFORD CT 06108
1	BOEING DOUGLAS PRODUCTS DIV L J HART-SMITH 3855 LAKEWOOD BLVD D800 0019 LONG BEACH CA 90846-0001
1	MIT P LAGACE 77 MASS AVE CAMBRIDGE MA 01887

NO. OF COPIES	ORGANIZATION
1	NASA LANGLEY J MASTERS MS 389 HAMPTON VA 23662-5225
1	CYTEC M LIN 1440 N KRAEMER BLVD ANAHEIM CA 92806
2	BOEING ROTORCRAFT P MINGURT P HANDEL 800 B PUTNAM BLVD WALLINGFORD PA 19086
2	FAA TECH CENTER D OPLINGER AAR 431 P SHYPRYKEVICH AAR 431 ATLANTIC CITY NJ 08405
1	NASA LANGLEY RC C C POE MS 188E NEWPORT NEWS VA 23608
1	LOCKHEED MARTIN S REEVE 8650 COBB DR D 73 62 MZ 0648 MARIETTA GA 30063-0648
1	WL MLBC E SHINN 2941 PST STE 1 WRIGHT PATTERSON AFB OH 45433-7750
2	IIT RESEARCH CENTER D ROSE 201 MILL ST ROME NY 13440-6916
1	MATERIALS SCIENCES CORP B W ROSEN 500 OFFICE CENTER DR STE 250 FORT WASHINGTON PA 19034

NO. OF COPIES	ORGANIZATION
1	DOW UT S TIDRICK 15 STERLING DR WALLINGFORD CT 06492
3	TUSKEGEE UNIV MATERIALS RSRCH LAB SCHOOL OF ENGR & ARCH S JEELANI H MAHFUZ U VAIDYA TUSKEGEE AL 36088
4	NIST R PARNAS J DUNKERS M VANLANDINGHAM D HUNSTON POLYMERS DIV GAITHERSBURG MD 20899
2	NORTHROP GRUMMAN ENVIRONMENTAL PROGRAMS R OSTERMAN 8900 E WASHINGTON BLVD PICO RIVERA CA 90660
1	OAK RIDGE NATL LAB A WERESZCZAK BLDG 4515 MS 6069 PO BOX 2008 OAKRIDGE TN 37831-6064
1	COMMANDER USA ARDEC INDUSTRIAL ECOLOGY CTR T SACHAR BLDG 172 PICATINNY ARSENAL NJ 07806-5000
1	COMMANDER USA ATCOM AVIATION APPLIED TECH DIR J SCHUCK FT EUSTIS VA 23604

NO. OF COPIES	ORGANIZATION
1	COMMANDER USA ARDEC AMSTA AR SRE D YEE PICATINNY ARSENAL NJ 07806-5000
1	COMMANDER USA ARDEC AMSTA AR QAC T D RIGOSGLIOSO BLDG 354 M829E3 IPT PICATINNY ARSENAL NJ 07806-5000
7	COMMANDER USA ARDEC AMSTA AR CCH B B KONRAD E RIVERA G EUSTICE S PATEL G WAGNECZ R SAYER F CHANG BLDG 65 PICATINNY ARSENAL NJ 07806-5000
	ABERDEEN PROVING GROUND
66	DIR USARL AMSRL CI AMSRL CI C W STUREK AMSRL CI CB R KASTE AMSRL CI S A MARK AMSRL SL B AMSRL SL BA AMSRL SL BE D BELY AMSRL WM B A HORST E SCHMIDT

NO. OF COPIES ORGANIZATION

ABERDEEN PROVING GROUND (CONT)

AMSRL WM BE
G WREN
C LEVERITT
D KOOKER
AMSRL WM BC
P PLOSTINS
D LYON
J NEWILL
S WILKERSON
AMSRL WM BD
R FIFER
B FORCH
R PESCE-RODRIGUEZ
B RICE
AMSRL WM
D VIECHNICKI
G HAGNAUER
J MCCAULEY
AMSRL WM MA
R SHUFORD
S MCKNIGHT
AMSRL WM MB
W DRYSDALE
J BENDER
T BLANAS
T BOGETTI
R BOSSOLI
L BURTON
S CORNELISON
P DEHMER
R DOOLEY
B FINK
G GAZONAS
S GHIORSE
D GRANVILLE
D HOPKINS
C HOPPEL
D HENRY
R KASTE
R KLINGER
M LEADORE
R LIEB
E RIGAS
D SPAGNUOLO
W SPURGEON
J TZENG

NO. OF COPIES ORGANIZATION

ABERDEEN PROVING GROUND (CONT)

AMSRL WM MC
J BEATTY
AMSRL WM MD
W ROY
AMSRL WM T
B BURNS
AMSRL WM TA
W GILLICH
E RAPACKI
T HAVEL
AMSRL WM TC
R COATES
W DE ROSSET
AMSRL WM TD
D DIETRICH
W BRUCHEY
A DAS GUPTA
AMSRL WM BB
H ROGERS
AMSRL WM BA
F BRANDON
W D AMICO
AMSRL WM BR
J BORNSTEIN
AMSRL WM TE
A NIILER
AMSRL WM BR
J LACETERA

NO. OF COPIES	ORGANIZATION
1	MERL LTD R MARTIN TAMWORTH RD HERTFORD SG13 7DG UNITED KINGDOM
1	SMC SCOTLAND DERA ROSYTH P W LAY ROSYTH ROYAL DOCKYARD DUNFERMLINE FIFE KY 11 2XR UNITED KINGDOM
1	CIVIL AVIATION ADMINISTRATION T GOTTESMAN PO BOX 8 BEN GURION INTERN'L AIRPORT LOD 70160, ISREAL
1	AEROSPATIALE S ANDRE A/BTE/CC/RTE MD 132 316 ROUTE DE BAYONNE TOULOUSE 31060 FRANCE
1	DAIMLER-BENZ AEROSPACE J BAUER D-81663 MUNCHEN MUNICH GERMANY
3	DRA FORT HALSTEAD PETER N JONES DAVID SCOTT MIKE HINTON SEVENOAKS KENT TN 147BP UNITED KINGDOM
1	DEFENSE RESEARCH ESTAB VALCARTIER FRANCOIS LESAGE PO BOX 8800 COURCELETTE QUEBEC COA IRO CANADA

NO. OF COPIES	ORGANIZATION
2	ROYAL MILITARY COLLEGE OF SCIENCE SHRIVENHAM DR DAVID BULMAN DR BRIAN LAWTON SWINDON WILTS SN6 8LA UNITED KINGDOM
1	SWISS FEDERAL ARMAMENTS WKS WALTER LANZ ALLMENDSTRASSE 86 3602 THUN SWITZERLAND
1	ISRAEL INSTITUTE OF TECHNOLOGY FACULTY OF MECHANICAL ENGR PROFESSOR SOL BODNER HAIFA 3200 ISRAEL
1	DSTO MATERIALS RESEARCH LAB PLATFORM VULNERABILTY SHIP STRUCTURES & MATERIALS DIV DR NORBERT BURMAN NAVAL PO BOX 50 ASCOT VALE VICTORIA AUSTRALIA 3032
1	ECOLE ROYAL MILITAIRE PROFESSOR EDWARD CELENS AVE DE LA RENAISSANCE 30 1040 BRUXELLE BELGIQUE
1	DEF RES ESTABLISHMENT VALCARTIER ALAIN DUPUIS 2459 BOULEVARD PIE XI NORTH VALCARTIER QUEBEC CANADA PO BOX 8800 COURCELETTE GOA IRO QUEBEC CANADA
1	INSTITUT FRANCO ALLEMAND DE RECHERCHES DE SANIT LOUIS DE MARC GIRAUD 5 RUE DU GENERAL CASSAGNOU BOITE POSTALE 34 F 68301 SAINT LOUIS CEDEX FRANCE

NO. OF COPIES ORGANIZATION

1 ECOLE POLYTECH
J MANSON
DMX-LTC
CH-1015 LAUSANNE SWITZERLAND

1 TNO PRINS MAURITS LABORATORY
DR ROB IJSSELSTEIN
LANGE KLEIWEG 137
PO BOX 45
2280 AA RIJSWIJK
THE NETHERLANDS

1 FOA NAT L DEFENSE RESEARCH ESTAB
DIR DEPT OF WEAPON & PROTECTION
DR BO JANZON
R HOLMLIN
S 172 90 STOCKHOLM
SWEDEN

2 DEFENSE TECH & PROC AGENCY
GROUND
GERHARD LAUBE
GENERAL HERZOG HAUS
3602 THUN
SWITZERLAND

1 MINISTRY OF DEFENCE
RAFAEL
DR MEIR MAYSELESS
ARMAMENT DEVELOPMENT AUTH
PO BOX 2250
HAIFA 31021 ISRAEL

1 DYNAMEC RESEARCH AB
DR AKE PERSSON
PARADISGRND 7
S 151 36 SODERTALJE
SWEDEN

1 ERNST MACH INSTITUT EMI
DIRECTOR
HAUPTSTRASSE 18
79576 WEIL AM RHEIN
GERMANY

1 ERNST MACH INSTITUT EMI
DR ALOIS STILP
ECKERSTRASSE 4
7800 FREIBURG
GERMANY

NO. OF COPIES ORGANIZATION

1 TNO DEFENSE RESEARCH
DR IR HANS PASMAN
POSTBUS 6006
2600 JA DELFT
THE NETHERLANDS

1 DR BITAN HIRSCH
TACHKEMONY ST 6
NETAMUA 42611
ISRAEL

1 DEUTSCHE AEROSPACE AG
DYNAMICS SYSTEMS
PROF DR MANFRED HELD
PO BOX 1340
D 86523 SCHROBENHAUSEN
GERMANY

REPORT DOCUMENTATION PAGE

Form Approved
OMB No. 0704-0188

1. AGENCY USE ONLY *(Leave blank)*	2. REPORT DATE	3. REPORT TYPE AND DATES COVERED
	December 1999	Final, Aug - Dec 96

4. TITLE AND SUBTITLE
Advanced Gun System (AGS) Dynamic Characterization: Model Test and Analysis, High-Frequency Analysis

5. FUNDING NUMBERS
6WT8D1

6. AUTHOR(S)
Morris Berman, Ting Li, and Abraham Frydman

7. PERFORMING ORGANIZATION NAME(S) AND ADDRESS(ES)
U.S. Army Research Laboratory
ATTN: AMSRL-WM-MB
Aberdeen Proving Ground, MD 21005-5069

8. PERFORMING ORGANIZATION REPORT NUMBER
ARL-TR-2138

9. SPONSORING/MONITORING AGENCY NAMES(S) AND ADDRESS(ES)

10.SPONSORING/MONITORING AGENCY REPORT NUMBER

11. SUPPLEMENTARY NOTES

12a. DISTRIBUTION/AVAILABILITY STATEMENT
Approved for public release; distribution is unlimited.

12b. DISTRIBUTION CODE

13. ABSTRACT *(Maximum 200 words)*

Dynamic characterization tests were performed on the Advanced Gun System (AGS) vehicle. The tests were designed to provide modeling information for high-frequency shock prediction codes, as well as finite element codes. These data obtained were also used to validate the modeling codes. The vehicle was analyzed in a full-up condition with the turret attached. A model analysis was performed to a maximum frequency of 100 Hz. The high-frequency characterization was performed up to 10 kHz.

Methodologies to extract damping estimate up to 10 kHz were developed and implemented. Damping estimates up to 10 kHz were extracted from the structural data obtained during this test.

14. SUBJECT TERMS	15. NUMBER OF PAGES
high frequency, live-fire prediction AGS, modal test, modal analysis, ballistic shock	80
	16. PRICE CODE

17. SECURITY CLASSIFICATION OF REPORT	18. SECURITY CLASSIFICATION OF THIS PAGE	19. SECURITY CLASSIFICATION OF ABSTRACT	20. LIMITATION OF ABSTRACT
UNCLASSIFIED	UNCLASSIFIED	UNCLASSIFIED	UL

INTENTIONALLY LEFT BLANK.

USER EVALUATION SHEET/CHANGE OF ADDRESS

This Laboratory undertakes a continuing effort to improve the quality of the reports it publishes. Your comments/answers to the items/questions below will aid us in our efforts.

1. ARL Report Number/Author ARL-TR-2138 (Berman) Date of Report December 1999

2. Date Report Received _____

3. Does this report satisfy a need? (Comment on purpose, related project, or other area of interest for which the report will be used.) _____

4. Specifically, how is the report being used? (Information source, design data, procedure, source of ideas, etc.) _____

5. Has the information in this report led to any quantitative savings as far as man-hours or dollars saved, operating costs avoided, or efficiencies achieved, etc? If so, please elaborate. _____

6. General Comments. What do you think should be changed to improve future reports? (Indicate changes to organization, technical content, format, etc.) _____

CURRENT ADDRESS

_____
Organization

_____
Name E-mail Name

_____
Street or P.O. Box No.

_____
City, State, Zip Code

7. If indicating a Change of Address or Address Correction, please provide the Current or Correct address above and the Old or Incorrect address below.

OLD ADDRESS

_____
Organization

_____
Name

_____
Street or P.O. Box No.

_____
City, State, Zip Code

(Remove this sheet, fold as indicated, tape closed, and mail.)

(DO NOT STAPLE)

DEPARTMENT OF THE ARMY

OFFICIAL BUSINESS

NO POSTAGE
NECESSARY
IF MAILED
IN THE
UNITED STATES

BUSINESS REPLY MAIL
FIRST CLASS PERMIT NO 0001,APG,MD

POSTAGE WILL BE PAID BY ADDRESSEE

DIRECTOR
US ARMY RESEARCH LABORATORY
ATTN AMSRL WM MB
ABERDEEN PROVING GROUND MD 21005-5069